TALLINN UNIVERSITY OF TECHNOLOGY
SCHOOL OF ENGINEERING

Department of Electrical Power Engineering and Mechatronics

DEVELOPMENT OF GOLDEN SAMPLE FOR HIPOT TESTERS

MASTER THESIS

MECHATRONICS PROGRAM

Student Manoj Karki

Student code 165580MAHM

Supervisor (s) Prof. Mart Tamre

Joonas Karu

Tallinn, 2018

AUTHOR'S DECLARATION

Hereby I declare, that I have written this thesis independently.

No academic degree has been applied for based on this material. All the works, major viewpoints and data of the other authors used in this thesis have been referenced.

"....."……2018

Author: Manoj Karki

.……
/signature/

Thesis is in accordance with terms and requirements.

"....."……2018

Supervisor: Prof. Mart Tamre

…….
/signature/

"....."……2018

Supervisor: Joonas Karu

…….
/signature/

Accepted for defence

"....."……2018

Chairman of theses' defence commission:…….……

/name and signature/

TALLINNA TEHNIKAÜLIKOOL
INSENERITEADUSKOND

Elektroenergeetika ja mehhatroonika instituut

ETALON NÄIDISE ARENDAMINE KÕRGEPINGE TESTRI JAOKS

MAGISTRITÖÖ

MEHATROONIKA ÕPPEKAVA

Üliõpilane Manoj Karki

Üliõpilaskood 165580MAHM

Juhendaja Prof. Mart Tamre

Joonas Karu

Tallinn, 2018

AUTORIDEKLARATSIOON

Olen koostanud lõputöö iseseisvalt.
Lõputöö alusel ei ole varem kutse- või teaduskraadi või inseneridiplomit taotletud. Kõik töö koostamisel kasutatud teiste autorite tööd, olulised seisukohad, kirjandusallikatest ja mujalt pärinevad andmed on viidatud.

"....."……2018

Töö autor: Manoj Karki

……..
/ allkiri /

Töö vastab lõputööle esitatavatele nõutele

"....."……2018

Juhendaja: Prof. Mart Tamre

……..
/ allkiri /

"....."……2018

Juhendaja: Joonas Karu

……..
/ allkiri /

Kaitsmisele lubatud

"....."…….....2018

Kaitsmiskomisjoni esimees …….....

/ nimi ja allkiri /

School of Engineering

MSc THESIS TASK

Student:	Manoj Karki, 165580MAHM
Study program	MAHM02/13
Specialty:	Mechatronics
Supervisors:	Professor Mart Tamre, Tallinn University of Technology
	PCBA Quality Engineer, Joonas Karu, ABB
Consultant:	Paul Taklaja, Senior Lecturer, Tallinn University of Technology

THESIS TOPIC:
(in English) Development of Golden Sample for Hipot Testers
(in Estonian) Etalon näidise arendamine kõrgepinge testri jaoks

Assignments to be completed and the timeline

No.	Description of the assignment	Completion date
1.	Understanding the task and research on similar works	09.02.2018
2.	Selection of resistors and ordering	13.02.2018
3.	Modeling of the system	02.03.2018
4.	Experiments for selecting Golden sample	06.04.2018
5.	Selection of components	20.04.2018
6.	CAD designs	10.05.2018
7.	Simulating the system in MATLAB-SIMULINK	14.05.2018
8.	Compiling thesis	18.05.2018

Design and Engineering problems to be solved:

1. Select golden sample.
2. Design system for temperature and humidity control.
3. Developing golden sample for Hipot testing.

Language of the thesis: English

Deadline for submission of the application for defense: 14.05.2018

Deadline for submission of the thesis: 25.05.2018

Student: Manoj Karki	Signature:…… …	"....."……2018
Supervisor: Prof. Mart Tamre	Signature:…… …	"....."……2018
Supervisor: Joonas Karu	Signature:…… …	"....."……2018
Consultant: Paul Taklaja	Signature:…… …	"....."……2018

CONTENTS

PREFACE

This thesis focuses on developing the golden sample for Hipot tester. The inspiration for the thesis comes from the time when I was participating as a long-term trainee at ABB Drives and Renewables factory, Jüri, Estonia. Most of the experiments and developments were carried out jointly in ABB Drives and Renewables factory, Jüri, Estonia and Department of Electrical Power Engineering and Mechatronics, Tallinn University of Technology, Tallinn, Estonia for the Masters level education (MSc. in Mechatronics).

I would like to extend gratitude towards the supervisors Prof. Mart Tamre and Joonas Karu for providing immense support and guidance during the work. I would like to thank senior lecturer Paul Taklaja from Department of Electrical Power Engineering and Mechatronics, TTU for providing equipment's, consultation on the thesis work and senior researcher Oliver Järvik from Department of Energy Technology for his assistance throughout the project.

Also, I would like to thank Mr. Illo Joe (Project Manager) from ABB for giving me an opportunity and encouragement to work on this project. A special thanks to Mr. Vasily Krupin from ABB for continuous support on testing procedures and guidance throughout the thesis work as well as Mr. Urmo Tuul from ABB for his assistance throughout the project.

Manoj Karki

Tallinn, 2018

EESSÕNA

Käesolev lõputöö keskendub etalon näidise arendamisele kõrgepinge testri rakenduseks. Lõputöö teema valik tulenes ABB Drives and Renewables tehase pikaajalisest praktikaprogrammis osalemisest. Enamik eksperimente ja uurimustööd viidi läbi ABB Drives and Renewables tehases, Jüris, Eestis ja Elektriajamire ja mehhatroonika instituudis, Tallinna tehnikaülikoolis, Tallinnas, Eestis, magistrikraadi hariduse omandamise käigus.

Ma tahaksin tänada oma juhendaiajd, Professor Mart Tamre ja Joonas Karu-t, abistamise eest ja toetuse eest töö vältel. Tänan vanem lector Paul Taklajat Elektriajamite ja jõuelektroonika instituudist, TTÜ-st, aitamaks seadmetega,pakkudes konsultatsiooni võimalust lõputööga seoses ja vanem uurijat Oliver Järvikut, Energiahalduse instituudist tema abi puhul kogu projekti vältel.

Tahaksin tänada Illo Jõe-d(projektijuht) ABB-st, andmaks mulle võimaluse ja julgustades mind töötama selle projektiga. Suur tänu Vasily Krupinile ABB-st pideva toe ouhul tootmise protsessidega seoses töö vältel ja Urmo Tuule-le ABB-st aitamaks projekti vältel.

Manoj Karki

Tallinn, 2018

LIST OF SYMBOLS

A_{lm}	Area of the insulated box (m^2)
$c_{p,air}$	Specific heat of air (J/(kg·K))
$c_{p,w}$	Specific heat of water (J/(kg·K))
c_v	Specific heat for mixed mass inside box (J/(kg·K))
h_{water}	Enthalpy of water (J/kg)
I_{heater}	Heater current (A)
K	Thermal resistance (W/(m·K))
$\dot{m}_{dry,air,in}$	Mass flow rate of dry air towards inlet (kg/s)
$\dot{m}_{dry,air,out}$	Mass flow rate of dry air towards outlet (kg/s)
$\dot{m}_{in}$	Mass flow rate at inlet (kg/s)
$\dot{m}_{out}$	Mass flow rate at outlet (kg/s)
$\dot{m}_{water,in}$	Mass flow rate of water towards inlet (kg/s)
$\dot{m}_{water,out}$	Mass flow rate of water towards outlet (kg/s)
P_{heater}	Power due to heater (W)
PowerRating	Power rating of resistor (W)
P_r	Power to the resistor (W)
$\bar{Q}_{air,out}$	Heat flow rate of air from outlet to the inlet (J/s)
$\bar{Q}_{in}$	Heat flow rate at inlet (J/s)
$\bar{Q}_{loss}$	Rate of heat loss (J/s)
$\bar{Q}_{out}$	Heat flow rate at outlet (J/s)
$\bar{Q}_{water}$	Heat flow rate of water to the inlet (J/s)
R_0	Original resistance (Ω)
ΔR_{TC}	Change in the resistance due to temperature coefficient (Ω)
ΔR_{VC}	Change in resistance due to voltage coefficient (Ω)
$T_{\theta 1}$	Time at 63 % of θ_m (s)
$T_{\theta 2}$	Time at 37 % of θ_m (s)

T_1	Temperature of surface 1 (^{0}C)
T_2	Temperature of surface 2 (^{0}C)
TC	Temperature coefficient of the given resistor (ppm/^{0}C)
T_c	Change in temperature due to cooling (^{o}C)
$T_{c,v}$	Change of temperature inside the box (^{0}C)
T_h	Change in temperature due to heating (^{o}C)
T_{in}	Temperature at inlet of box (^{0}C)
T_{max}	Maximum temperature with 100 % power (^{o}C)
$T_{MAX\_PWR\_100}$	Temperature where power ratings starts to fall (^{o}C)
T_{mix}	Temperature of mixed air inside box (^{0}C)
T_{out}	Outside temperature (^{0}C)
ΔT_{SH}	Change in temperature due to power dissipation (^{o}C)
T_{water}	Temperature of water (^{0}C)
VC	Voltage coefficient of the given resistor (ppm/^{0}C)
V_{heater}	Voltage across heater (V)
$\omega_{c.v.}$	Rate of change of humidity ratio (kg $_{water}$/ kg $_{dry\ air}$)
ω_{in}	Humidity ratio flowing inside (kg $_{water}$/ kg $_{dry\ air}$)
ω_{mix}	Humidity ratio inside box (kg $_{water}$/ kg $_{dry\ air}$)
ω_{out}	Outside humidity ratio (kg $_{water}$/ kg $_{dry\ air}$)
θ	Change in current and initial temperature values (^{o}C)
θ_m	Change in initial and final temperature values (^{o}C)
θ_{SH}	Thermal resistance due to self-heating (^{o}C/W)
δ	Thickness of the isolated box (m)

LIST OF ABBREVIATIONS

AHU	Air Handling Unit
CAD	Computer-Aided Design
C.C.	Cooling Coil
EA	Exhaust Air
EPS	Expanded PolyStyrene
H.C.	Heating Coil
H.D.	Humidifier
Hipot	High Potential
HMI	Human Machine Interface
MA	Mixed Air
N.A.	Not Available
OA	Outdoor Air
PID	Proportional Integral Derivative
PLC	Programmable Logic Controller
RA	Return Air
RH	Relative Humidity
SA	Stabilized Air
SP	Set Point
SQL	Structured Query Language
TCR	Temperature Coefficient of Resistor
VCR	Voltage Coefficient of Resistor

1 INTRODUCTION

1.1 Problem statement

ABB is one of the largest producers of frequency converters, classified as high, medium and low voltage drives. All of these products are subject to Hipot testing (to determine the insulation level of electrical devices) after the end of the assembly for safety reasons to prevent the leakage current or electric shocks that might occur from the manufactured device. It is a high-voltage test that is applied to all devices for a specific time to ensure that the insulation is strong to prevent such hazard.

Due to seasonal changes in temperature and humidity, the tested drives have variation in results when subjected to Hipot testing. In ABB, there are different types of Hipot testers and it is likely that they suffer from deviations due to temperature and humidity which results in test failure. The root cause of the failures comes from a faulty drive, Hipot tester station or changes induced by atmospheric conditions.

1.2 Overview

Over time, with the widespread use of electricity, the issue of leakage current (current which flows from protective ground conductor towards the ground) has come to the forefront since 1960's [1]. In the absence of ground connection, the leakage current might smoothly flow through any conductive part like human body or surface of the non-conductive section towards the ground when available. The fault in design or other factors might break down the insulation resulting in an excessive leakage current flow. This current if flows through the human body might even lead to the death of the victim [2]. Therefore, electrical safety testing for measuring and verifying the electrical insulation in electronic and electric devices (like Printed Circuit Board, transformers, drives, motors, etc.) are must for minimizing hazards to operators and the surrounding environment and equipment. It is referred to the term Hipot and is abbreviated as the high potential [3].

Hipot test quantifies the electrical insulation properties of a product or component. During the Hipot test, the higher voltage is applied between the metallic shield or frame and product current carrying conductors. This test helps in determining braided shielding errors, terminal spacing problems, crushed insulation, conductive or corrosive contaminants around the conductors and tolerance errors in cables [4]. Hipot test is done with the help of Hipot tester, an electronic device which verifies electrical insulation, or another wired assembly. This test focuses on voltage withstand test (specified voltage is applied to the device under test and leakage current flow is monitored during) and Insulation resistance test (specified voltage is applied to the device under test and value of resistance is measured) [5].

Hipot testing is affected by humidity. The insulation of a device is changed by the change in humidity. In humid conditions, insulation will absorb the humidity in the environment and can cause insulation resistance variation, which leads to test failures. When wire insulation absorbs water or water vapor, electricity begins to flow from conductors to lower potential parts which can cause insulation resistance test failures. Different materials respond differently to the same humidity [6].

Temperature is another factor which affects the Hipot testing. As the temperature of the insulator increases, the resistance offered by the insulator decreases. The primary cause of an increase in temperature of the device under test is the higher supply voltage. As the voltage supplied to the device increases, the temperature of the device under test also increases. This increase in temperature decreases the resistance offered by the insulator. Furthermore, continuous high voltage testing is degrading the insulation properties of the insulating material [3].

Due to the seasonal change, temperature and humidity are also changing. This change affects the Hipot test as it is dependent on the temperature and humidity. The results in leakage current and voltage withstand test obtained during summer season varies from that of the winter season. Therefore, it is sometimes difficult to determine the main reason for the failure of the device under test during Hipot test is whether due to the actual insulation breakdown or if it is due to the change in the temperature and humidity. Such change is one of the challenges in Hipot testing.

The above discussion creates an inevitable need for producing a measurement device that gives comparable results and abides by the following specifications. The device under test must not be affected by any external temperature and humidity. The temperature and humidity within the model can be adjustable. It should have higher insulation resistance (in MΩ) with the fixed value. There should be a control unit with display for adjustable temperature and humidity. Furthermore, it should produce similar results during the Hipot testing and negligible deviations between different Hipot testers, when measuring the same sample.

1.3 Objectives of the research

The primary objective of this research is the development of the golden sample for Hipot tester with stabilized temperature and humidity for ABB Drives and Renewables Factory in Juri, Estonia and to design a controller to control the temperature and humidity inside the insulated box. Components for designing such box are to be selected and verified before design through simulation. The measurement sample developed should not be affected by the seasonal changes and changes in temperature and humidity. The sample needs to produce similar results during the Hipot testing and negligible deviation between different Hipot testers when measuring the same sample. For better control of the heating and humidifying properties inside the box, PID control is currently planned for the system. The aim is to design a universal sample robust enough for testing in the different Hipot tester in ABB.

1.4 Scope of the thesis

The thesis focuses on selecting a suitable resistor to act as a golden sample and observing key properties of the sample i.e., self-heating, nominal resistance, stability, leakage current and short-term and long-term tests. Also, the mathematical modeling regarding these changes needs to be formulated and predicted for different conditions based on the observed properties.

For the selection of the golden sample, various resistors are tested with the different voltage source (i.e. 2,7 kV AC and 1 kV DC), its self-heating properties, short-term test and long-term test. Various properties like the change in the resistance, leakage current, loss of resistance at various voltages were observed during these

tests. It helped in selecting a perfect golden sample required for the development of the measuring sample. Furthermore, the obtained results were used for predicting the self-heating properties of the resistor during real time testing.

For the thermally insulated box, simulation and mathematical modeling have to be created where the temperature and humidity inside the box can be controlled. To control the system being considered, PID control was selected for better control of temperature and humidity inside the box. Various approaches for designing such box has been recommended by few authors to improve the heating and humidifying features inside the box [7] [8].

In this research, a simulation is created to design a thermally insulated box which offers a fixed temperature and humidity. Temperature and humidity are adjustable and the user is able to set the desired setpoint for temperature and humidity for the system. Furthermore, the simulation environment helps in observing the time at which the temperature and humidity reach the desired set point. For simulating the system, Simulink – MATLAB is used [9].

1.5 Overview of the thesis

Chapter 2 gives an overview of existing models for control strategies regarding heating ventilation and air conditioning systems. It also gives an overview of insulation tester calibration box available. The requirements mentioned by ABB for selection of golden sample and controlled temperature and humidity is also mentioned.

Chapter 3 describes the basic theory regarding the temperature and humidity control and its mathematical modeling. General theory regarding golden sample and loss of resistance from the resistor is also described in this chapter.

Chapter 4 focuses on the selection of golden sample and the results obtained from testing various resistors and its comparison. A golden sample is selected at the end of the chapter for using it in the final design.

Chapter 5 explains the components selected for prototyping of the final device. The method of placing the component for the real design is shown with the help of assembly drawings. A discussion is made on how it is going to be used for testing in the Hipot testers.

Chapter 6 aims at implementing the model from chapter 3 using the parameters of selected components from chapter 5 for obtaining the desired temperature and humidity. The implementation is done by creating a simulation in MATLAB and the results from the simulations are illustrated.

2 BACKGROUND OF THE APPLICATION AND RELATED WORK

2.1 Overview

The background work has been divided into two sections:

- Temperature and humidity control
- Insulation tester

Various works have been done separately for temperature and humidity control and insulation tester but the work describing both sections combined has not been addressed so far. Hence, two separate sections are taken into consideration for the literature review.

There is a number of works done for maintaining the stable temperature and humidity. It serves as a diverse array of applications across a wide range of industries like pharmaceutical, automotive, drives and cosmetic industries to test the resilience of product samples under controlled temperature and humidity. At the beginning, modeling of stable temperature and humidity control device, currently available applications like HVAC, heating systems and air conditioning systems were thoroughly studied. In interest in particular has been centered on mathematical derivation, modeling and control strategies of controlling temperature and humidity parameters from the beforehand mentioned applications [7] [8] [10].

Selection of golden sample (offering fixed resistance) depends on various parameters like type of material, temperature, humidity and long term test. Tests have been conducted to predict the performance and aging of resistor. Various devices are available in the market for insulation test with fixed resistance but it only provides resistance at the normal testing temperature (i.e. room temperature). The temperature and humidity of the resistor cannot be controlled. For the literature review section, calibration box that is available in the market for testing the Insulation tester is considered and is described in detail in the later chapter 2.3 [11] [12] [13].

2.2 Background work regarding temperature and humidity control

- **Dynamic model of an HVAC system for control analysis**

Paper [10] focuses on steps required for deriving a dynamic model of HVAC system which includes a zone, humidifier, dehumidifier, heating coil, cooling coil, ductwork, fan and mixing box. The modeled equations are balanced using energy and mass balance equation for heating and cooling processes. The temperature and humidity is maintained at a set point using PID control action for the indoor application. The PID parameters have to be tuned carefully such that it produces less oscillatory responses and is done using Ziegler-Nicholas rule [14]. The overall modeling is simulated using MATLAB.

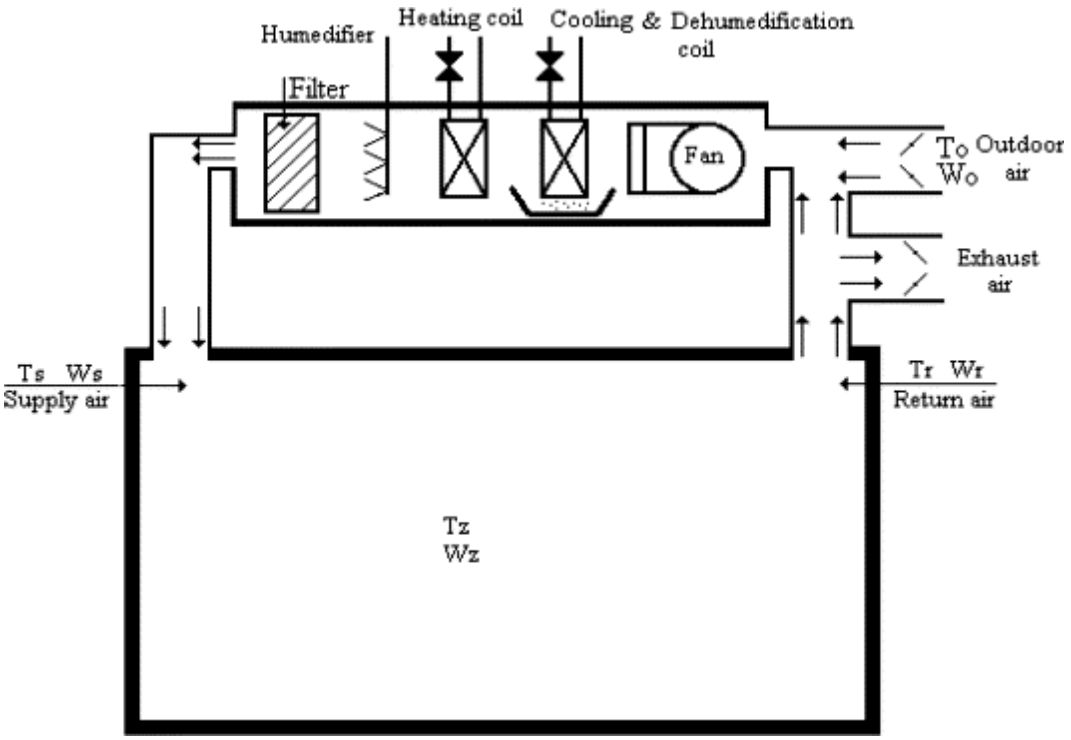

Figure 2.1 Schematic Diagram of general HVAC system [10]

The system is modeled to work at two different operational seasons namely summer and winter seasons. During summer operation season, hot and humid air passes through cooling and dehumidification coil which decreases air temperature, condenses water moisture and results in decreased relative humidity. So, the control unit signals for passing decreased water temperature to cooling coil in case of higher temperature. Also for dehumidification, a signal is given for reducing the water temperature such that the humidity ratio in the zone is reduced as the water vapor in the supplied humid air is condensed.

During winter operation season, cold and dry air passes air handling unit. A signal is sent to the controller by sensing the temperature in the zone using the thermostat. The signal sent is used to control the input temperature of the water that flows through the heating coil. The temperature inside the zone is increased and also vapor is generated through humidifier to control humidity ratio of the air.

The simulation result shows the open and closed loop responses of the indoor temperature and humidity ratios were reliable. The transient behavior of the system was improved by the use of PID controllers. The gains for proportional, integral and differential were obtained using Ziegler-Nicholas method. Set point setting was met using fine tuning by trial and error method after the previous step. The results obtained showed that the system is capable of rejecting disturbances effectively with an error up to 2,3 % and reaching the temperature and humidity set point in 1200 s during the summer season and that for the winter season is 800 s.

- **Modeling Validation and Control Analysis for controlled temperature and humidity of Air Conditioning system**

Paper [7] focuses on the construction of energy based model of a thermal system for controlled temperature and humidity air conditioning systems. It describes the influence of the mass flow rate, heater and humidifier for proposed control criteria to achieve the controllable temperature and humidity of air conditioning system. MATLAB dynamic simulation is used to validate the reliability of the proposed thermal system. PID control strategy is applied for controlling air mass flow rate, heating capacity and humidifying capacity.

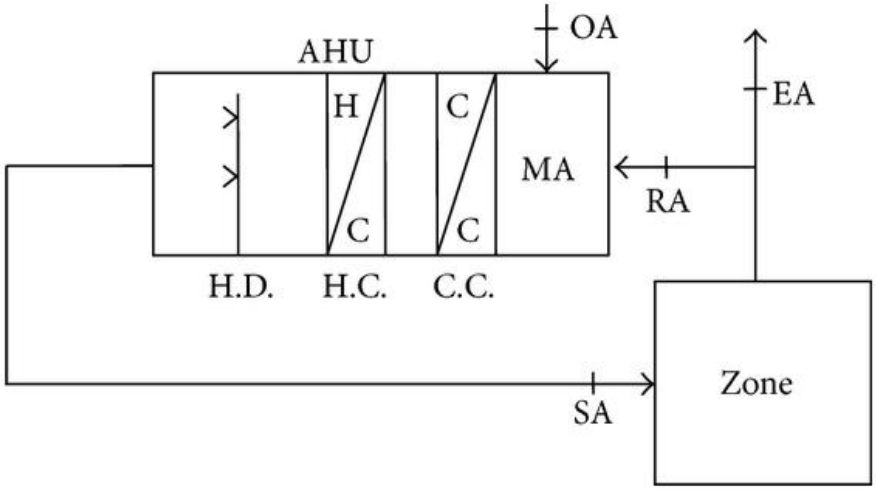

Figure 2.2 Air conditioning system thermal model diagram [7]

The system is modeled to make temperature and humidity within the zone to be constant in order to meet different industrial requirements, such as chemical laboratory, a process of high- tech industry, measuring and testing laboratory and electronic machine room.

Initially, the difference between measured values and target values is obtained through detection of indoor state and flow of return air is controlled by exhaust air, then the outdoor air is introduced for generation of mixed air in air-handling unit. The mixed air is then processed through cooling, dehumidifying and cooling coil. Also, heating is done by heating coil, humidifying is done by humidifier to mix the desired state for air conditioned zone gradually.

The maximum error between room temperature simulation and literature is 1 ^{o}C and 2,4 % humidity ratio as the wall heat transfer and disregarded in this research. PID control was used to control the system and Ziegler-Nicholas empirical rule was used for controlling mass- flow rate, heater output power and humidifier output power. The PID stabilization was at 541 s at high temperature and humidity. The maximum temperature disturbance obtained was 0,14 ^{o}C and 7,5 % humidity ratio error. In general, the goal for constant temperature and humidity attained was obtained effectively.

- **Analysis of control strategies and simulation of heating systems using SIMULINK/MATLAB potential**

In this research, [8] Simulink/MATLAB is used for simulating the dynamic model of a forced air type heating system. It emphasizes on the analysis of control strategies to improve the thermal parameter on system performance and energy efficiency. It shows a comparative analysis of On-OFF and PID control strategies for controlling the indoor temperature in terms of power consumption. The effects regarding thermal capacity, equivalent thermal resistance and set point settings were investigated.

The system consists of the outdoor environment, heating coil, thermal characteristics of the house and control system. Initially, the cold air enters the heater and is heated up and sent to the air conditioned space. There is two modes of operation On-Off control and PID control. During On-Off control, the heater is turned on and off after sensing the difference between the indoor temperature and the set point through thermostat limiting the fluctuations around the set point. During PID control, the error signal (difference in the desired temperature and actual temperature) modulates the actuator used to modify an output of the heater.

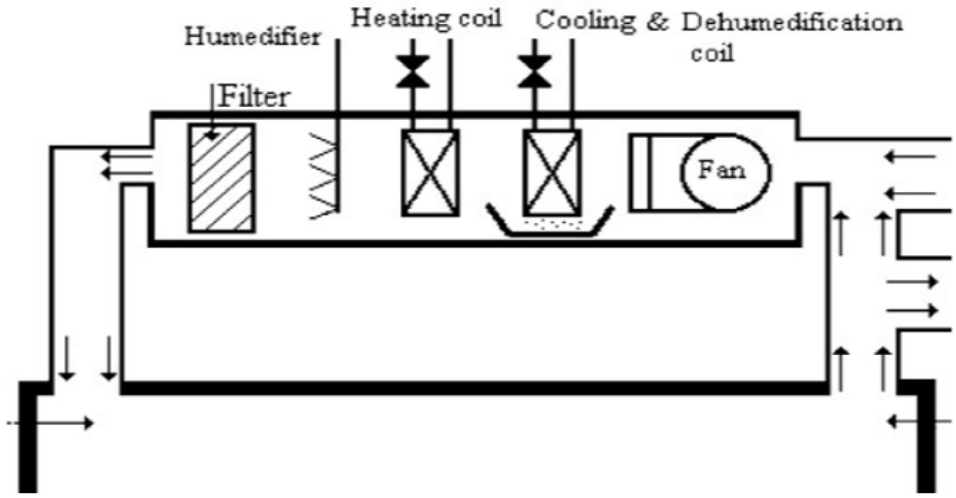

Figure 2.3 Schematic Diagram of the system [8]

The temperature set points were traced more effectively using PID controller rejecting the outdoor disturbances. The fluctuations caused by On-Off controller influences the temperature significantly while the fluctuations with PID control were less significant. If the thermal capacity of the system controlled by the On-off algorithm is increased then it led to a decrease in frequency of fluctuations while that for the PID algorithm led to an increase in overshoot percentage and settling time. The energy consumption was same for On-Off controllers and PID controller but set point value played an important role in reducing energy consumption.

2.3 Background work regarding insulation tester calibration device

There are various calibrators available for checking the calibration of the tester which offers settings such as insulation testing, voltage and frequency, low resistance and continuity testing. The regular calibration of the device allows the test equipment to be regulated and within desired boundaries. These calibrators offer higher resistance of ranges from kΩ to GΩ and the quality depends upon the price of the calibrator. Since, this research is focused on insulation resistance test so focus is on insulation resistance in the calibrators as follows [11] [12][13] .

- **NICEIC CalCard Calibration checkbox**

These calibrators are shaped like credit cards and are used to check the accuracy of the insulation testers. It is a portable device and can be carried easily in a purse. They have durable contact points made of nickel, copper and gold. It is easy to check the accuracy of insulation and continuity resistance testers. Specifications of NICEIC CalCard calibration checkbox are in table 2.1 [12].

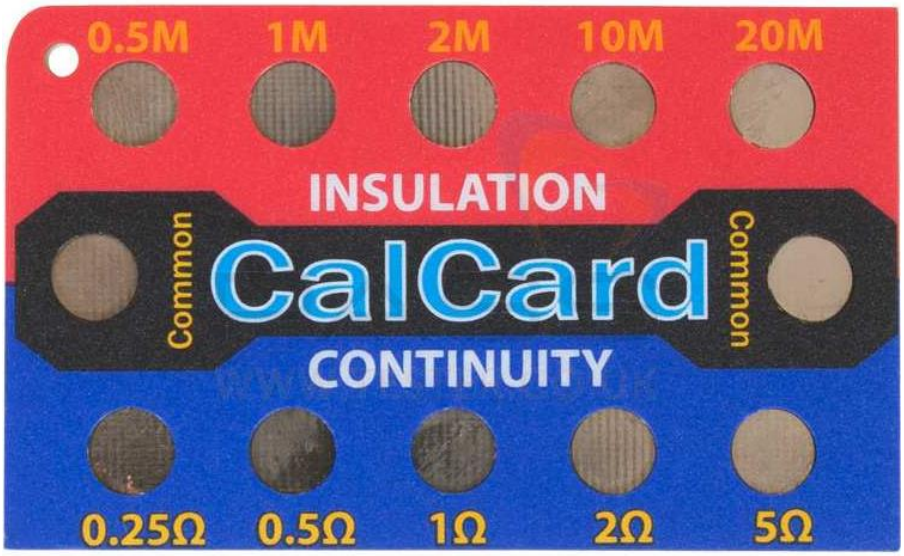

Figure 2.4 Image of NICEIC CalCard calibration checkbox [12].

Table 2.1 Specification of NICEIC CalCard calibration checkbox

Parameters	**Parameters values**
Insulation resistance range	0,5 MΩ, 1 MΩ, 2 MΩ, 10 MΩ, 20 MΩ fixed values
Test voltage for insulation resistance	1500 V
Resistance tolerance	-
Voltage coefficient	-
Temperature coefficient	-
Price	Around $ 35
Dimensions	86 mm × 54 mm x 1 mm

- **Megger CB101 5KV Calibration Box**

The CB101 calibration box is used for checking the accuracy of insulation testers. It offers four fixed resistances range from MΩ to GΩ. It consists of high-quality resistors with calibration certificate provided such that the actual value of resistance for each checkpoint is provided itself in the box. The connections are made easily to the four difference resistors that are offered by the calibration box. The resistors are suitable for checking the values of the resistance with the test voltage of 5kV. All the resistors have a common ground connection which can be seen in the figure 2.5. Specifications of Megger CB101 5kV calibration box are in table 2.2 [13].

Figure 2.5 Image of Megger CB101 5kV calibration box [13]

Table 2.2 Specification of Megger CB101 5kV calibration box

Parameters	**Parameters values**
Insulation resistance range	10 MΩ, 100 MΩ, 1 GΩ, 10 GΩ fixed values
Test voltage for insulation resistance	5000 V
Resistance tolerance	2 %
Voltage coefficient	1 ppm/V
Temperature coefficient	250 ppm/^{0}C
Price	Around $ 600
Dimensions	130 mm x 68 mm x 68mm

- **5069 INSCAL Insulation Tester Calibration System**

The precision instrument is suitable for calibrating and testing insulator resistors with various test voltages. The construction is done with high strength co-polymer plastic case and powered with a rechargeable battery which prevents stray current. The insulation resistance provides a precision four dial decade resistance bank which can be set to a maximum of 99,99 GΩ and can be seen in the figure 2.6. Furthermore, a display is present for showing the calibration results. It is a rugged and portable device suitable for site calibration work [11].

a) 3D view b) Top view of the control section

Figure 2.6 Image of 5069 INSCAL insulation tester calibration system [11]

Table 2.3 Specifications of 5069 INSCAL insulation tester

Parameters	**Parameters values**
Insulation resistance range	5 MΩ, 2 MΩ, 1 MΩ, 500 kΩ, 200 kΩ, 100 kΩ fixed values and 10 GΩ, 1 GΩ, 100 MΩ, 10 MΩ decade ranges
Test voltage for insulation resistance	10000 V
Resistance tolerance	1 % up to 10 GΩ and 5 % for 10 to 100 GΩ
Voltage coefficient	1 ppm/V
Temperature coefficient	< 250 ppm/^{0}C
Price	Around $ 4500
Dimensions	406 mm x 175 mm x 330 mm

2.4 Comparison of available tester calibration devices

NICEIC CalCard, Megger CB101 and 5069 INSCAL insulation tester are compared regarding the specifications in a single table in the table 2.4.

Table 2.4 Comparison of NICEIC CalCard, Megger CB101 and 5069 INSCAL insulation tester

Basis	**NICEIC CalCard**	**Megger CB101**	**5069 INSCAL Insulation Tester**
Insulation resistance range	0,5 MΩ, 1 MΩ, 2 MΩ, 10 MΩ, 20 MΩ fixed values	10 MΩ, 100 MΩ, 1 GΩ, 10 GΩ fixed values	5 MΩ, 2 MΩ, 1 MΩ, 500 kΩ, 200 kΩ, 100 kΩ fixed values and 10 GΩ, 1 GΩ, 100 MΩ, 10 MΩ decade ranges
Test voltage for Insulation resistance	1500 V	5000 V	10000 V
Resistance tolerance	N.A.	2 %	1 % up to 10 GΩ and 5 % for 10 to 100 GΩ
Voltage coefficient	N.A.	1 ppm/V	N.A.
Temperature coefficient	N.A.	250 ppm/C	< 250 ppm/C
Price	Around $ 35	Around $ 600	Around $ 4500
Dimensions	86 mm × 54 mm x 1 mm	130 mm x 68mm x 68 mm	406 mm x 175 mm x 330 mm

The above table 2.4 illustrates that NICEIC is the cheapest device but the resistance tolerance, voltage coefficient and temperature coefficient are not provided. Megger CB101 has four different fixed resistors 10 MΩ, 100 MΩ, 1 GΩ or 10 GΩ but the user can not vary the results. 5069 INSXAL insulation Tester has greater tolerance and provides variable resistances up to GΩ but the price is quite expensive.

2.5 System requirements for insulation tester calibration device

The tester calibration device has to selected based on the criteria and parameters required in the testing of leaking current and voltage withstand test for Hipot stations used in ABB Drives and Renewables Factory in Juri, Estonia. The list of parameters to be considered while selecting a resistor is as follows:

1. Leakage current reading during the test should be greater than 0,1 mA due to the limitation in precision with the available device. The available device is Kikusui TOS5050a and the readings are to be obtained with AC test voltage of 2700 V and DC test voltage of 1000 V.
2. Change in resistance over time has to be slow i.e. the temperature of resistor should not rise exponentially (more than 5 ^{o}C) within 2 to 3 s. This is the self-heating property and is not desired because the loss of resistance increases with increase in temperature.
3. Leakage current should not be affected over time with multiple tests i.e. the value of leakage current should not raise rapidly after each test of 2 to 3 s. Moreover, it should produce results with the equivalent value after each test such that it can be compared.
4. The resistance of the resistor should not be changing over time after every test which lasts for 2 to 3 s. The resistor needs to have long term stability and negligible degradation in the material over time.

5. The geometry of the wiring connection should not affect the readings from the leakage current and resistance of the resistor. There should be negligible capacitive and inductive component effects on the resistance property if possible.
6. The temperature and humidity of the tester calibration device should not be affected by the ambient conditions. Moreover, there should be the possibility to control these parameters for the tester calibration device.

The specification for the insulation tester calibration device to meet the above requirements is in table 2.5. Explanation for each parameter and the parameter values are also explained below.

Table 2.5 Specification for the requirement of proposed insulation tester calibration device

Parameters	**Parameters values**
Insulation resistance range	1 to 50 MΩ fixed Value
Test Voltage	1000 V DC (for insulation resistance), 2700 V AC (for leakage current)
Resistance Tolerance	Up to 1 %
Voltage Coefficient	Up to 4 ppm/V
Temperature Coefficient	Should not make loss in resistance more than 1 % of the original value
Test Time	2 to 3 s for each test voltage

- The Insulation resistance of range 1 to 50 MΩ fixed value is currently the desired range because the voltage withstands tester device Kikusui TOS5050a present in ABB is able to measure the current within the limits 0,01 mA to 110 mA AC. Selecting the resistance of higher values limits the accuracy of the device.
- Test Voltage of 1000 V DC is selected for insulation resistance test and 2700 V AC for leakage current test according to CSN EN 50178 standard [15] describing electronic equipment for use in power installations.
- The replacement of the tester calibration device is done after it starts to degrade and higher tolerance produces results which are not comparable with the previous device. Therefore, tolerance not greater than 1 % is selected for obtaining comparable results.
- Voltage coefficient and temperature coefficients make a loss in the value of resistance to the tester calibration device so they are selected to the given range such that it does not changes more than 1 % of the original value of the resistance.
- The testing time lasts for 2 to 3 s each for insulation resistance test and leakage current test.

2.6 System requirements for temperature and humidity control

The insulation Tester calibration device must be maintained at stable temperature and humidity while the test is carried out. Temperature and humidity control has to be selected based on the parameters defined for Hipot stations testing used in ABB, Juri, Estonia. The lists of parameters are:

1. The tester calibration device is subject to stable temperature and humidity before the test is carried out. The test is carried out only when it is maintained at the stable temperature and humidity.
2. The temperature and humidity should be controllable and must be stable with a tolerance of ± 1 ºC after time not more than 15 min.

3. Loss of heat and humidity should be negligible for maintaining stable temperature and humidity to the tester calibration device.
4. The set point temperature for the tester calibration device is always greater than the ambient temperature.

The specification for the controlled temperature and humidity to meet the above requirements is in table 2.6.

Table 2.6 Specification for controlled temperature and humidity

Parameters	**Parameters values**
Temperature set point range	15 to 40 °C
Humidity set point range	10 to 75 % Relative Humidity
Time for controlled temperature and humidity	Up to 15 min
Tolerance for temperature	± 1 °C
Tolerance for humidity	± 4 % relative humidity

The set point for temperature and humidity are selected based on the testing requirements for Hipot test stations at ABB. Moreover, the maximum limit for the temperature of 40 °C is chosen based on the maximum temperature which might be possible in the summer time. The testing needs to be done at the same set point for obtaining comparable results. The total wait time for obtaining controlled temperature and humidity is 15 min at maximum. The lesser the time, better the performance of the system.

2.7 Conclusion

The insulation tester calibration device available in the market does not meet the requirements for tester calibration device listed by ABB. Furthermore, the tester calibration device must have temperature and humidity control. Currently, there are no products available in the market which consists of tester calibration device along with temperature and humidity control. Thus, it calls for the development of the device that meets the requirements and specifications for carrying out the Hipot testing defined by ABB.

For the construction of temperature and humidity control device literature from chapter 2.2 is considered. It is used for understanding the mathematical modeling and design steps which is discussed in detail in chapter 3. For the selection of golden sample, various properties are to be understood and various tests are to be done which is discussed in next chapter 3 and chapter 4. The overall dimension of the developed device should not exceed the dimension 540 mm x 400 mm x 460 mm which is obtained from the measurement of all the Hipot testers at ABB.

3 SYSTEM DESCRIPTION OF PROPOSED MODEL

3.1 Proposed model description

The model consists of subsystems such as outdoor environment, heater, humidifier and control system. Inlets and outlets are present for passing the air and humidification. During operation, air enters from the outdoor environment and is heated up to the desired temperature with the help of heating coil. Furthermore, the temperature of the liquid that is to be used for the humidification is also set to the desired temperature before humidifying it. A fan is present in the system which helps in passing the warm and humid air inside the box. No cooler is used in this system because the set point for the temperature are higher than the outdoor environment.

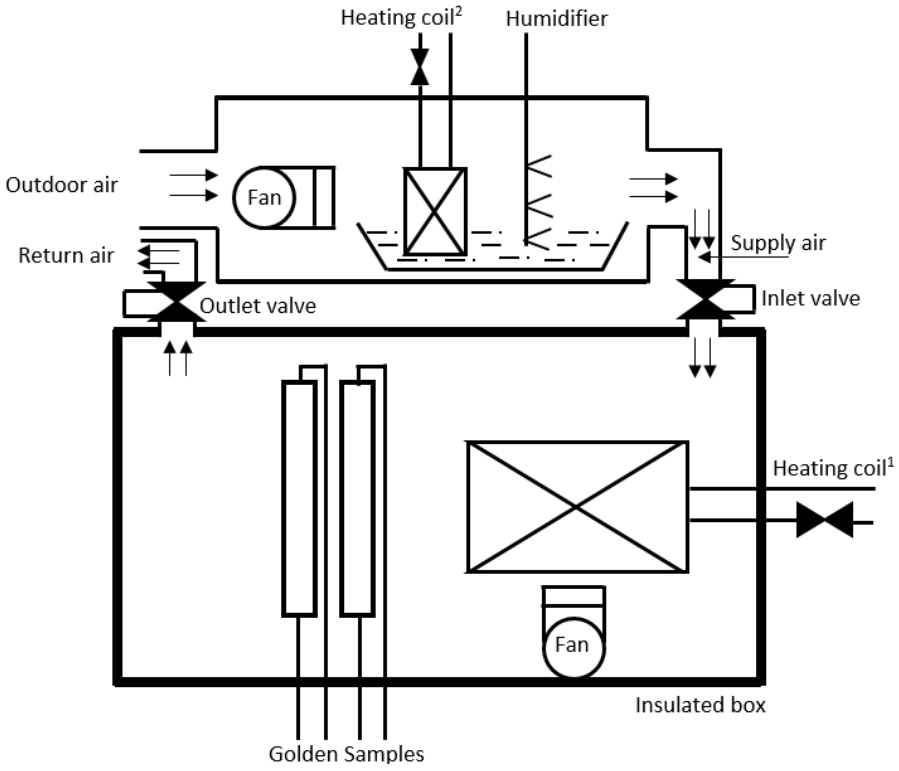

Figure 3.1 Schematic diagram of the proposed system

There are two solenoid valves present at the inlet and outlet. They are used to limit the flow of supply air and the return air to the insulated box. The temperature inside the box is maintained with the help of the heating coil present inside the box. There is a fan present inside the insulated box to maintain same temperature and humidity inside the box. The desired humidity is passed through supply air. Furthermore, for the dehumidification process, the humidity inside the box is emptied out by passing air to the inlet and letting it out from the outlet with the help of a fan and outdoor air. As the environment inside the insulated box attains desired temperature and humidity, then the sample is subject to Hipot testing. Two golden samples of same resistance and materials are used because in the real device under test two separate test are done for main circuit and auxiliary circuit with different voltages (1 kV DC, 2,7 kV AC for main circuit and 1 kV DC, 2 kV AC for the auxiliary circuit).

The process flow diagram of the system that has been described can be easily understood from the figure 3.2.

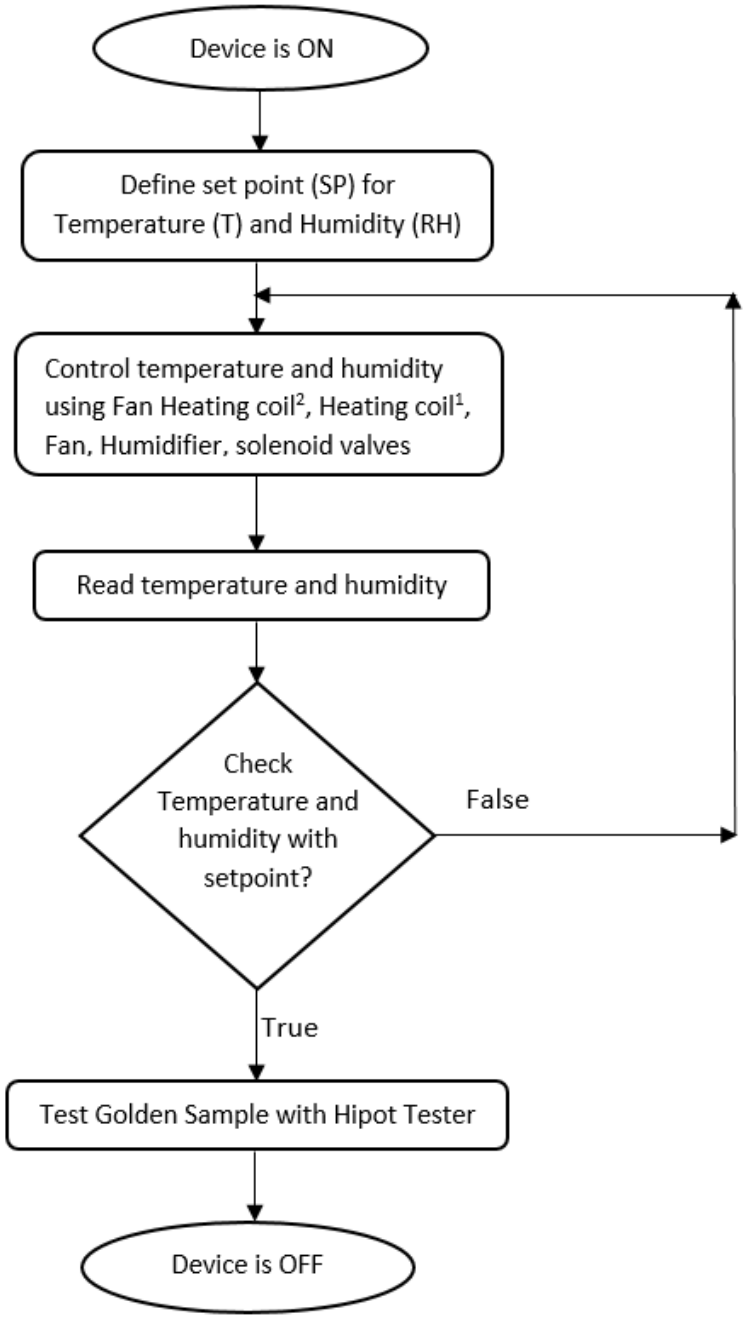

Figure 3.2 Working Principle of the proposed system

3.2 Properties of golden sample

3.2.1 Overview

In this thesis, golden sample refers to a device which has fixed resistance. A resistor is being used for providing fixed resistance within range 1 to 50 MΩ. Here, a resistor is a passive electronic component having fixed electrical resistance limiting the flow of electrons in the circuit. The resistance is subject to insulation resistance test and leakage current test. If the resistor meets the desired requirements, produces same results over multiple tests and has high-quality standard for multiple statistical comparison then it is named as a golden sample in this thesis work. The golden sample is to be used a large number of times for calibrating the insulation tester before starting to test the original product.

The resistor has various properties which affect its resistance during the test. For instance, some of the properties are material core properties like self-heating, time for self-heating, temperature coefficient and voltage coefficient, etc. of the resistor. Higher deviation in the resistance of the resistor due to these properties might lead to a non-consistent resistor value which is not desired. Furthermore, these properties help in predicting the lifetime, degradation properties and time for replacing the resistor. Some of these properties which influence the resistor are described in detail as follows.

3.2.2 Material used for manufacturing the resistor

Thick film resistor is mainly focused on understanding the material used for manufacturing the resistor because they are the most widely used resistors in electrical and electronic devices. Furthermore, thick film resistors are applicable for high voltage supplies and offer a wide range of stable resistance [16].

The material which offers resistance is composed of paste with the mixture of a carrier, binder and the metal oxides to be deposited. The carrier is of organic solvent systems and plasticizers while the binder is of glassy frit. Furthermore, the resistor pastes are usually ruthenium oxide, iridium oxide or rhenium oxide. A Substrate such as alumina (Al_2O_3) is printed onto the resistive layer at 850 °C and forms a film. The film becomes glasslike after firing the paste on the carrier, providing protection against moisture [17]. The anatomy of resistor can be seen in the figure 3.3 with detail description of each part.

- Substrate like alumina is used as the core material for making the resistor because it is a hard compound which possesses strong ionic interatomic bonding and resists any type of wear. Alpha phase alumina is considered to be the stiffest and strongest of the oxide ceramics. Its high hardness, refractoriness, excellent dielectric properties and good thermal properties make it the material of choice for electronic substrates. Some of the electrical properties of 96 % alumina material commonly used in making resistor are in table 3.1 [18] [19].

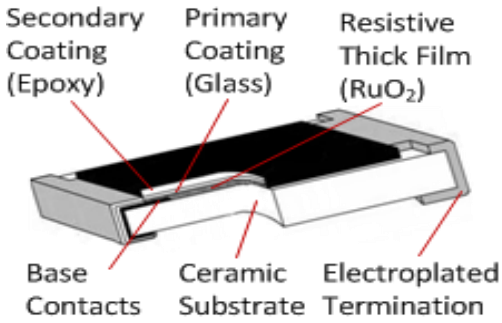

Figure 3.3 Anatomy of a thick film resistor [17]

Table 3.1 Electrical properties of 96 % Alumina Material

Electrical Properties	**Units of measure**	**SI/Metric**
Dielectric Strength	AC-kV/mm	14,6
Dielectric Constant (at 1 MHz)		9,0
Dissipation Factor (at 1 kHz)		0,0011
Dielectric loss angle (at 1 MHz)		$4x10^{-4}$
Volume Resistivity	Ω·cm	$> 10^{14}$
Loss Factor		38

It is clear from above table 3.1 that it can withstand higher electric field as it has a higher dielectric strength of 14,6 AC-kV/mm. The dielectric constant for alumina at 1 MHz is around nine which allow it to the large quantity of charge for a longer period of time. From the factors like dissipation factor, loss factor it is clear that the loss of energy due to various reasons like dissipation, oscillation, conduction are low. Higher volume resistivity greater than 10^{14} Ω·cm signifies that this material can highly oppose the flow of electric current. Due to these characteristics alumina is widely used substrate for designing resistors.

- Ruthenium oxide is electrically conducting crystalline solid with black color and rutile structure. Doping technique, when introduced to ruthenium oxide, leads to better reproducibility, better control over resistivity and temperature coefficient. Because temperature coefficient of resistance is positive and ruthenium oxide is metallic the introduction of non-conducting oxide like aluminum oxide exerts a negative influence which helps to control temperature coefficient. The thickness of this material is adjusted for better power dissipation while designing the resistor giving a feature of the higher power dissipations. Therefore, these materials are widely used for designing of thick film resistors [20].
- Two different layers of protective coating of glass and epoxy are used. Glass coating offers protection against moisture while the epoxy coating is a strong and hard material which protects the inner composition of the material for making the thick film resistor.
- Electroplated termination is present at the ends of the resistor. It provides protection against crack formation due to heat, solder joint stress, mechanical flexure and resulting leakage current conduction when subject to power supply [17].
- Base contacts help in separating the resistor region and the primary and secondary coatings.

3.2.3 Self-heating property of resistor

The temperature of the resistor increases when the dissipation of power in a resistor increases therefore leads to a change in the resistance. The error introduced in the measurement by resistor self-heating can be calculated from the derating curve of rated power (%) vs. ambient temperature commonly shown in resistor specifications [21].

The resistor will heat up due to self-heating and changes its temperature which is represented by ΔT_{SH}. The actual temperature of the resistor is the sum of ambient temperature and ΔT_{SH}. ΔT_{SH} can be calculated from the graph shown in figure 3.4.

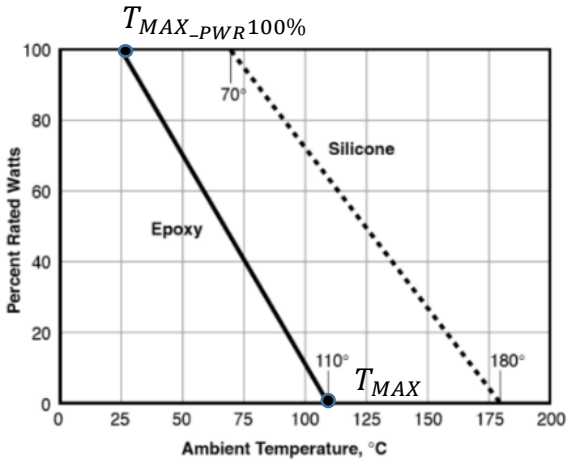

Figure 3.4 Derating curve for resistor [22]

The thermal resistance (θ_{SH}) is therefore equal to the absolute value of the slope between T_{MAX} and $T_{MAX\_PWR}100\%$ points in the derating curve and is given by equation below [21]

$$\theta_{SH} = \frac{T_{MAX} - T_{MAX\_PWR}100\%}{PowerRating}. \quad (3.1)$$

Where T_{max} denotes maximum temperature with 100 % power, $T_{MAX\_PWR\_100}$ denotes temperature where power ratings start to fall and PowerRating refers to the resistor rating of the power.

If P_r is the power to the resistor and ΔT_{SH} gives the change in temperature due to power dissipation then the following equation gives the change in temperature of the resistor [21]

$$\Delta T_{SH} = \theta_{SH} * P_r \, . \quad (3.2)$$

3.2.4 Time for self-heating of resistor

When power is supplied to the resistor, self-heating property indicates that the resistance increases as hyperbolical curve (in form $y = C(1 - e^{-kt}), k > 0$) over time initially. Then it increases slowly until it increases with the temperature of ΔT_{SH}. The temperature of the resistor decays exponentially over time once the supply is off. The stages of the heating property in the resistor can be seen in the figure 3.5 [23].

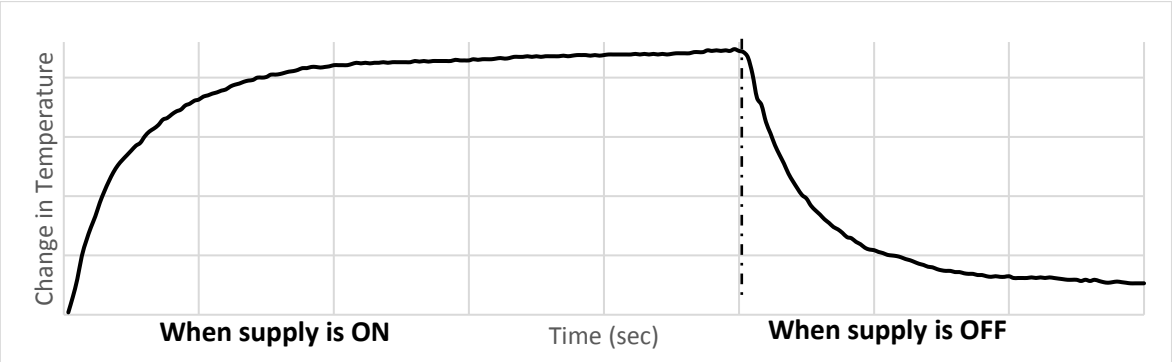

Figure 3.5 Self-heating property of resistor when supply is ON and OFF [23]

The equation for the hyperbolic curve and exponential decay can be described by the graph and equations as follows [23].

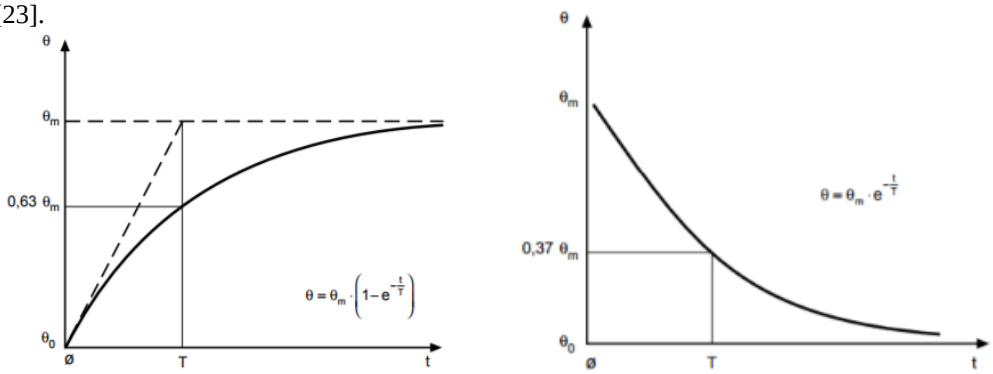

Figure 3.6 Response when heating is ON (left) and when heating is OFF (right) [23]

Let θ_m be the change in temperature between final value and initial temperature of the resistor. Let θ be the change between current value and initial temperature. Let $T_{\theta 1}$ be the time at 0,63 * θ_m, t is the time at the instant then the increase in temperature of resistor over time so θ is given by [23]

$$\theta = \theta_m \left(1 - e^{-\frac{t}{T}}\right). \tag{3.3}$$

Let T_h replace θ and ΔT_{SH} replace θ_m. If T is replaced by $T_{\theta 2}$ then the equation (3.3) becomes

$$T_h = \Delta T_{SH} \left(1 - e^{-\frac{t}{T_{\theta 1}}}\right). \tag{3.4}$$

Let θ_m be the change in temperature between final value and initial temperature of the resistor. Let θ the change between current value and initial temperature. Let $T_{\theta 2}$ be the time at 0,37 * θ_m, t is the time at the instant then the decrease in temperature of resistor θ over time is given by [23]

$$\theta = \theta_m . e^{-\frac{t}{T}}. \tag{3.5}$$

Let T_c replace θ and ΔT_{SH} replace θ_m. If T is replaced by T_θ then the equation (3.5) becomes

$$T_c = \Delta T_{SH} . e^{-\frac{t}{T_{\theta 2}}} . \tag{3.6}$$

3.2.5 Loss from resistor

Loss of resistance from Resistor occurs due to various reasons. Some of the major reasons are listed below [24].

1. Tolerance
2. Solder heat stability
3. TCR error at T_{min} / T_{max}
4. VCR error at V_{max}
5. Environmental stability
6. Material degradation

- Tolerance is considered as the percentage of error in the resistor's resistance which varies the actual measured resistance from its stated resistance. Tolerance leads to change of resistance which changes the actual value.
- During soldering of resistor, there is a certain amount of loss of resistance due to the presence of thermal stress. Furthermore, the flux residue and fabrication residue can be another reason affecting the resistance.
- Environmental stability is the limits of non-reversible resistance change under given loading and environmental conditions. Humidity and moisture can be some of the reasons which might affect the resistance of the resistor
- The materials used for making resistors degrade over time so they also have some effect in long term. During Insulation resistance test the insulation of the material gets degraded slowly over time.
- Loss due to temperature coefficient

  The temperature of the resistor increases when the dissipation of power in a resistor increases and leads to a change in the resistance value. The formula for calculating the change in the resistance due to temperature coefficient ΔR_{TC} are as follows [25]

$$\Delta R_{TC} = R_0 \left(\frac{\Delta T_{SH} * TC}{1000000\ ppm}\right). \quad (3.7)$$

  Where R_0 is the initial resistance, ΔT_{SH} is the change in temperature due to self-heating and TC is the temperature coefficient of the given resistor.

- Loss due to voltage coefficient

  The supplied voltage to the resistor depends on the change in the value of the resistor. The resistor value is inversely proportional to the supplied voltage and the formula for calculating the change in the resistance due to voltage coefficient is as follows [26]

$$VC = \frac{\Delta R_{VC}}{(R_0 * V)}$$

$$\Delta R_{VC} = R_0 * V * VC. \quad (3.8)$$

  Where $R_0$is the resistance, V is the supplied voltage and VC is the voltage coefficient.

3.3 Modeling of temperature and humidity control

3.3.1 Assumptions for modeling of temperature and humidity control

The golden sample needs to be measured at constant temperature and humidity so the main function of controlled temperature and humidity is to provide these constraints at a constant rate for the effective measurement. The outdoor temperature and humidity are likely to effect the measurement reading of the golden sample. Similarly, the mass of humidity and air at the inlet and outlet, heat generated needs to be understood for better modeling of the system. Set points for reaching the desired temperature and humidity required for the measurement are the main goal that needs to be obtained while modeling the system. The assumptions for designing the controlled temperature and humidity device for the simulation are as follows [7] [10].

1. There is no leakage inside the box consisting of the golden sample.
2. The boundary needs to be insulated for the box.
3. The specific heat and density of the air are assumed to be constant.
4. A negligible amount of pressure is considered to be lost
5. There is uniform distribution of air temperature and humidity inside the box.

The description for the mathematical modeling is based on the inlet, inside the box and at the outlet.

3.3.2 At inlet

Heating coil, humidifier and fan are used for producing the supply air by making the use of outdoor air. This supply air is passed to the inlet valve which is further passed to the insulated box. Initially, the liquid for humidification is heated up to the desired temperature with the help of heating coil which is placed inside the liquid. A thermostat is used to sense the temperature of the liquid. After that, the humidifier is turned ON to generate the humidification from the liquid which is set according to set point. In this way, the desired humidity of required temperature is passed to the inlet of the box with the help of a fan.

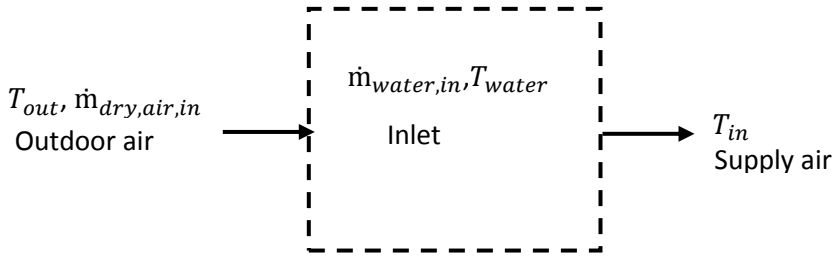

Figure 3.7 Schematic of the inlet

If T_{out} be the environmental temperature, $\dot{m}_{dry,air,in}$ be the mass flow rate of air towards inlet, $\dot{m}_{water,in}$ be the mass flow rate of water towards inlet, T_{water} be the temperature of water, T_{in} be the temperature at inlet of box, $c_{p,air}$ be the specific heat of air and $c_{p,w}$ be the specific heat of water then the heat flow rate in the inlet from air and water are given by following equations

$$\bar{Q}_{air,out} = \dot{m}_{dry,air,in} * c_{p,air}(T_{in} - T_{out}), \quad (3.9)$$

$$\bar{Q}_{water} = \dot{m}_{water,in} * c_{p,w}(T_{water} - T_{out}). \quad (3.10)$$

Furthermore, the equation for the mass is given by

$$\dot{m}_{dry,air,in} * \omega_{in} = \dot{m}_{dry,air,in} * \omega_{out} + \dot{m}_{water}. \quad (3.11)$$

Where $\dot{m}_{dry,air,in}$the mass flow rate of dry air from the outside environment, ω_{in} the humidity ratio flowing inside and ω_{out} the outside humidity ratio.

3.3.3 Inside box

The insulated box consists of a fan and heating coil. The heating coil inside the box maintains the temperature inside the box according to the value defined by the setpoint. The fan is used for mixing the air inside the box. Through the inlet, the supply air is sent into the box. Humidification inside the box is maintained by the supply air. In the presence of excess humidification or higher temperature than the desired set point, there is an outlet valve which is opened to let out the air and humidity mixture. The valves in the inlet and outlet are said to be inlet valve and outlet valve and they control the supply air and return air. They help in maintaining stable temperature and humidity inside the box.

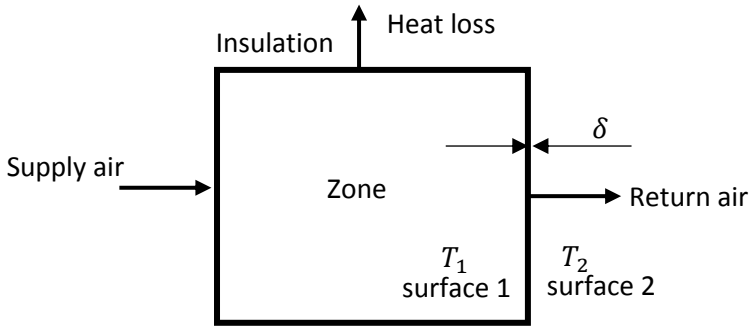

Figure 3.8 Schematic of the temperature and humidity controlled zone

Heating coil is present inside the box for setting up the temperature up to the desire set point. The heat generated by the heater (P_{heater}) inside the box is given by product of current I_{heater} and voltage V_{heater} across the heater as

$$P_{heater} = I_{heater} * V_{heater}. \quad (3.12)$$

Heat dissipated from the box that causes energy loss and is dependent upon the type of material, the thickness of the isolated box (δ), an area of the material used in isolate box (A_{lm}) and thermal resistance (K) is given as

$$\bar{Q}_{loss} = A_{lm}\frac{K}{\delta}(T_1 - T_2). \quad (3.13)$$

Where T_1, T_2 are the temperature of surface 1 and 2 respectively.

3.3.4 At outlet

The outlet is present at one of the side of the insulated box. At the outlet, the air and humidification leave from the insulated box and there is a presence of outlet valve at this end.

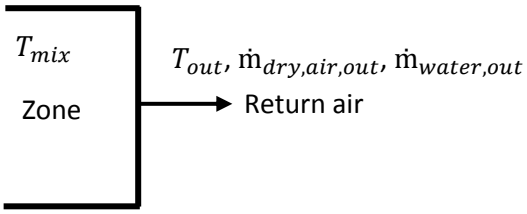

Figure 3.9 Schematic of the outlet

If T_{out} is the environmental temperature, $\dot{m}_{dry,air,out}$ is the mass flow rate of air towards outlet, $\dot{m}_{water,out}$ the mass flow rate of water towards outlet, T_{mix} is the temperature at mixed air inside box, $c_{p,air}$ is the specific heat of air and h_{water} is the enthalpy of water at that temperature then the energy at the outlet is given by the equation as follows

$$\bar{Q}_{out} = \dot{m}_{dry,air,out} * c_{p,air}(T_{mix} - T_{out}) + \dot{m}_{water,out} * h_{water}. \quad (3.14)$$

The equation for the mass conversion is given by

$$\dot{m}_{out} = \dot{m}_{dry,air,out} * \omega_{mix} + \dot{m}_{water,out}. \quad (3.15)$$

Conservation of energy states that 'the total energy of an isolated system remains constant, it is said to be conserved over time' [27]. If there is no kinetic energy and potential energy then from the energy balance equation the rate of change of temperature inside the box is obtained. Using equation (3.9), equation (3.10), equation (3.12), equation (3.13) and equation (3.14) the energy balance equation is as follows

$$\bar{Q}_{c.v.} = \Sigma\bar{Q}_{in} - \Sigma\bar{Q}_{out} - \Sigma\bar{Q}_{loss}$$

$$m * c_v * \frac{dT_{c,v}}{dt} = \dot{m}_{dry,air,in} * c_{p,air}(T_{in} - T_{out}) + \dot{m}_{water,in} * c_{p,w}(T_{water} - T_{out}) + I_{heater}V_{heater} - -\mathrm{A}_{lm}\frac{K}{\delta}(\mathrm{T}_1 - \mathrm{T}_2) - \dot{m}_{dry,air,out} * c_{p,air}(T_{mix} - T_{out}) - \dot{m}_{water,out} * h_{water}. \quad (3.16)$$

Where m is mass of mixed air and water flowing inside the box, c_v is specific heat for mixed mass inside the box and $T_{c,v}$ the change of temperature. If Laplace transform [28] is applied to equation (3.16) where $T_{c,v}$ is replaced by T_{mix} then,

$$T_{mix}(s) = \frac{1}{s} * \frac{1}{m*c_v}\Big[\dot{m}_{dry,air,in} * c_{p,air}\big(T_{in}(s) - T_{out}(s)\big) + \dot{m}_{water,in} * c_{p,w}\big(T_{water}(s) - T_{out}(s)\big) + I_{heater}V_{heater} - \mathrm{A}_{lm}\frac{K}{\delta}(\mathrm{T}_1(s) - \mathrm{T}_2(s)) - \dot{m}_{dry,air,out} * c_{p,air}(T_{mix}(s) - T_{out}(s)) - \dot{m}_{water,out} * h_{water}\Big]. \quad (3.17)$$

At steady state,

$$\bar{Q}_{out} = \bar{Q}_{in} \text{ and} \tag{3.18}$$

$$\bar{Q}_{heater} = \bar{Q}_{loss}. \tag{3.19}$$

Conservation of mass states that 'For any system closed to all transfer of matter and energy, the mass of the system must remain constant over time, as system's mass cannot change, so quantity cannot be added nor removed' [27]. Using equation (3.11) and equation (3.15), mass flow equation is given by

$$m\frac{d\omega_{c.v.}}{dt} = \dot{m}_{in} - \dot{m}_{out}$$
$$m\frac{d\omega_{c.v.}}{dt} = \dot{m}_{dry,air,in} * \omega_{out} + \dot{m}_{water,in} - \left[\dot{m}_{dry,air,out} * \omega_{mix} + \dot{m}_{water,out}\right]. \tag{3.20}$$

Where $\omega_{c.v.}$ is the rate of change of humidity ratio inside the box which is replaced by ω_{mix} and m is the mass of mixed air and water inside the box. If Laplace transform is applied to equation (3.20) then,

$$\omega_{mix}(s) = \frac{1}{s} * \frac{1}{m}\left[\dot{m}_{dry,air,in} * \omega_{out}(s) + \dot{m}_{water,in} - \left[\dot{m}_{dry,air,out} * \omega_{mix}(s) + \dot{m}_{water,out}\right]\right]. \tag{3.21}$$

3.4 Conclusion

Resistor's properties are to be observed and the selected resistor is subject to controlled temperature and humidity according to the requirements mentioned in chapter 2.5 and 2.6 so a new system is proposed. Various properties of the resistors are to be considered for selecting it as a golden sample. The material used for manufacturing of the resistor, self-heating property, time for self-heating and loss from resistor is considered for proving that the resistor is suitable for use as the golden sample.

For stable temperature and humidity control, heat generated at the inlet, inside the box and outside the box is considered. Energy and mass balance equations were used to obtain equilibrium in the system. The losses that occur in the box are dependent on thickness, area and type of material used. Other losses that might incur are assumed to be negligible. At steady state, the heat in the inlet $\bar{Q}_{in}$ is same as the heat generated at the outlet $\bar{Q}_{out}$. Also, the loss in the system $\bar{Q}_{loss}$ is equal to the heat generated by the heater $\bar{Q}_{heater}$.

The actual device under test has two circuits named main circuit and an auxiliary circuit. They are subject to test with different voltages (i.e. 1 kV DC, 2,7 kV AC to the main circuit and i.e. 1 kV DC, 2 kV AC to the main circuit) with the same testing procedure (discussed in chapter 4.5.4). So, there are two golden sample in the proposed schematic diagram. One of the samples is to be used for producing test results similar to the main circuit and the other for producing results similar to the auxiliary circuit. Both the golden samples have same resistance and material.

4 SELECTION OF GOLDEN SAMPLE

4.1 Overview

For the selection of the golden sample, various resistors are subject to test. Measurement of heating properties of the resistors was obtained using thermal cameras FLIR T440 [29] and FLIR E40 [30]. The main specifications for these cameras are discussed in appendix A. AC voltage is supplied with device Kikusui TOS5050A [31] and DC voltage is supplied with C.A 6547 [32]. The same device is capable of measuring the insulation resistance and leakage current. Detailed description of these devices are discussed in the appendix A. These devices were setup in the ABB drives and renewables factory, Juri and Tallinn University of Technology, Mechatronics department for carrying out the test with a resistor. The selection of cameras and image setup are discussed in detail in the appendix B.

4.2 Measurement errors and Uncertainty

- **Accuracy**

The closeness of agreement in between the true quantity value of measurand and measured quantity value and is mathematically represented as follows [33]

$$\text{Accuracy Error}_{\text{given value}} = \text{Measurement} * \frac{\text{Accuracy}}{100}. \quad (4.1)$$

- **Reading error**

It is the error due to the resolution of the measuring device and is obtained while reading the measurements and is mathematically represented as follows [33]

$$\text{Reading Error} = \text{Units Reading Error} * \text{Lowest Unit on Display}. \quad (4.2)$$

- **Absolute Error**

If the error limit is determined for a given measurand x having the confidence level 1-α, then the result can be presented as [33]

$$x_t = \text{x} \pm \Delta x_{1-\alpha},$$

Where absolute error is given by

$$\Delta x_{1-\alpha} = \text{Accuracy error} + \text{Reading Error}. \quad (4.3)$$

And x_t gives the measurement value with measurement errors.

- **Measurement error for FLIR E40 and T440 thermal camera**

Both devices have accuracy of ± (2 % ± 2 ^{0}C) and lowest unit of display as 0,1 [29] [30]. The calculation is obtained using the equations (4.1), (4.2) and (4.3).

Table 4.1 Calculation of measurement error in temperature measurement for FLIR E40 and T440

Accuracy Error	**Reading Error**	**Absolute Error**
Error at 30 ^{0}C = 0,6 ^{0}C	Error at 30 ^{0}C = 0,2 ^{0}C	Error at 30 ^{0}C = 0,8 ^{0}C
Error at 40 ^{0}C = 0,8 ^{0}C	Error at 40 ^{0}C = 0,2 ^{0}C	Error at 40 ^{0}C = 1,0 ^{0}C
Error at 70 ^{0}C = 1,4 ^{0}C	Error at 70 ^{0}C = 0,2 ^{0}C	Error at 70 ^{0}C = 1,6 ^{0}C
Error at 120 ^{0}C = 2,4 ^{0}C	Error at 120 ^{0}C = 0,2 ^{0}C	Error at 120 ^{0}C = 2,6 ^{0}C

The measurement error for measuring temperature increases with the increase in temperature.

- **Measurement error for TOS5050a**

The accuracy for TOS5050a is ± (5 % ± 20 µA) and lowest unit of display is 0,01 [31]. The calculation is obtained using the equations (4.1), (4.2) and (4.3).

Table 4.2 Calculation of measurement error in current measurement for TOS5050a

Accuracy Error	**Reading Error**	**Absolute Error**
Error at 1,00 mA = 50 µA	Error at 1,00 mA = 0,2 µA	Error at 1,00 mA = 50,2 µA
Error at 2,70 mA = 135 µA	Error at 2,70 mA = 0,2 µA	Error at 2,70 mA = 135,2 µA

This device is used to measure leakage current for AC test and the error in the measurements are 50,2 µA and 135,2 µA for 1 mA and 2,7 mA measurements respectively.

- **Measurement error for C.A 6547**

The accuracy for C.A 6547 is ± (5 %) for resistance measurement and lowest unit of display is 0,001 [32]. The calculation is obtained using the equations (4.1), (4.2) and (4.3).

Table 4.3 Calculation of measurement error in resistance measurement for C.A 6547

Accuracy Error	**Reading Error**	**Absolute Error**
Error at 1,00 MΩ = 50 kΩ	Error at 1,00 MΩ = 1 kΩ	Error at 1,00 MΩ = 51 kΩ
Error at 10,00 MΩ = 500 kΩ	Error at 10,00 MΩ = 10 kΩ	Error at 10,00 MΩ = 510 kΩ

The measurement error for the measurement of 10 MΩ resistors is quite higher in this case.

The accuracy for C.A 6547 is ± (10 %) for current measurement and lowest unit of display is 0,001 [32]. The calculation is obtained using the equations (4.1), (4.2) and (4.3) for both resistors.

Table 4.4 Calculation of measurement error in current measurement for C.A 6547

Accuracy Error	**Reading Error**	**Absolute Error**
Error at 1,00 mA = 100 µA	Error at 1,00 mA = 1 µA	Error at 1,00 mA = 101 µA
Error at 2,70 mA = 270 µA	Error at 2,70 mA = 1 µA	Error at 2,70 mA = 271 µA

The measurement errors are 101 µA and 271 µA for 1,00 mA and 2,7 mA respectively and this is more than 10 % of error.

- **Uncertainty**

They are composed of Type-A and Type-B components. Type-A is determined using statistical methods or multiple measurements for same device and is reduced by increasing the frequency of measurements. Type-B is obtained from sources like accuracy, absolute error, precision, etc. [33]. Mathematically,

$$u_C = \sqrt{{u_A}^2 + {u_B}^2} \tag{4.4}$$

Where u_A is uncertainty due to type-A and u_B is the uncertainty in type-B.

For this thesis work uncertainty due to environment and uncertainty due to method of doing test, uncertainty due to repeatability are negligible so they are neglected in this case.

4.3 Selection of resistor of 1 to 50 MΩ

Initially few resistors were chosen from the range of 1 MΩ to 50 MΩ. An AC 2,7 kV tests were applied to the resistor without monitoring the self-heating properties of the resistor. This test was done to be sure if a more detailed test could be carried out on selected resistor. The list of the resistor and the corresponding comments regarding the tests are shown in table 4.5 [16] [22].

Table 4.5 Property of various resistors

Basis	**SM102031004FE**	**MOX97021004FVE**	**SM102031005FE**	**SM102034005FE**	**SM102035005FE**
Resistance	1 MΩ	1 MΩ	10 MΩ	40 MΩ	50 MΩ
Power	1,5 W	19,4 W	1,5 W	1,5 W	1,5 W
Tolerance	1 %	1 %	1 %	1 %	1 %
Voltage ratings	5 kV	90 kV	5 kV	5 kV	5 kV
Power dissipated by resistor at 2,7 kV	$=V^2/R$ $= 2,7^2/1$ = 7,29 W	$=V^2/R$ $= 2,7^2/1$ = 7,29 W	$=V^2/R$ $= 2,7^2/10$ = 0,729 W	$=V^2/R$ $= 2,7^2/40$ = 0,18 W	$=V^2/R$ $= 2,7^2/50$ = 0,145 W
Leakage current from 2,7 kV AC Test	-	2,7 mA	0,27 mA	0,07 mA	0,05 mA
Remarks	Did not support the power rating itself	Could be proceeded with later tests	Could be proceeded with later tests	Has less reading precision than desired (i.e. 0,1 mA)	Has less reading precision than desired (i.e. 0,1 mA)
Suitable for later tests	✗	✓	✓	✗	✗

The above table 4.5 illustrates that the resistors SM102034005FE and SM102035005FE which has resistance of 40 MΩ and 50 MΩ shows leakage current of 0,07 mA and 0,05 mA respectively when it is supplied with 2,7 kV AC. The reading that was required by the company was in the range of 0,1 mA so it was rejected for further tests. Resistor SM102031004FE did not have sufficient power ratings to support the supply voltage so it was rejected. However, MOX97021004FVE and SM102031005FE showed better leakage current readings so they are subject to further test.

4.4 Properties of the selected resistor

4.4.1 Properties of resistor SM102031005FE

The specification of this resistor is as follows in table 4.6 [22].

Table 4.6 Specification for resistor SM102031005FE

Parameters	Parameters Values
Resistance	10 MΩ
Voltage Rating	5 kV
Resistor Element Type	Thick-film
Power Rating	1,5 W
Resistance Tolerance	± 1 %
Temperature coefficient	± 25 ppm/^{0}C
Voltage Coefficient	± 2 ppm/^{0}C
Dimensions	14,73 mm x 2,54 mm

Figure 4.1 Image of the resistorSM102031005FE

If the derating curve of the resistor SM102031005FE is seen in figure 4.2 following values are obtained [22].

Derating temperature start = 25 ^{0}C
Derating temperature end = 110 ^{0}C

The thermal resistance (θ_{SH}) is therefore equal to the absolute value of the slope between the 25 °C and the 110 °C points in the derating curve [21] [22]. The values of θ_{SH} can be calculated using equation (3.1) as follows.

$$\theta_{SH} = \frac{(110 - 25)}{1{,}5}$$

$$\theta_{SH} = 56{,}67\ ^0\text{C /W}$$

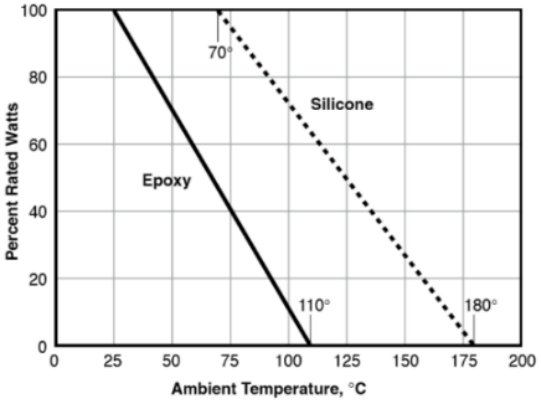

Figure 4.2 Derating curve of the resistor SM102031005FE [22].

4.4.2 Properties of resistor MOX97021004FVE

The specification of this resistor MOX97021004FVE are in table 4.7 [16].

Table 4.7 Specification for resistor MOX97021004FVE

Parameters	Parameters Values
Resistance	1 MΩ
Voltage Rating	90 kV
Resistor Element Type	Thick-film
Power Rating	19,4 W
Resistance Tolerance	± 1 %
Temperature coefficient	± 50 ppm/^{0}C
Voltage Coefficient	± 0,04 ppm/^{0}C
Dimensions	153,7 mm x 8,2 mm

Figure 4.3 Image of the resistor MOX97021004FVE

If the derating curve of resistor MOX97021004FVE is seen in figure 4.4 following values are obtained [16].

Derating temperature start = 25 ^{0}C

Derating temperature end = 225 ^{0}C

The thermal resistance (θ_{SH}) is therefore equal to the absolute value of the slope between the 25 °C and the 225 °C points in the derating curve [16] [21]. The values of θ_{SH} can be calculated using equation (3.1) as follows.

$$\theta_{SH} = \frac{(225 - 25)}{19{,}4}$$

$\theta_{SH} = 10{,}3\ ^0$C /W

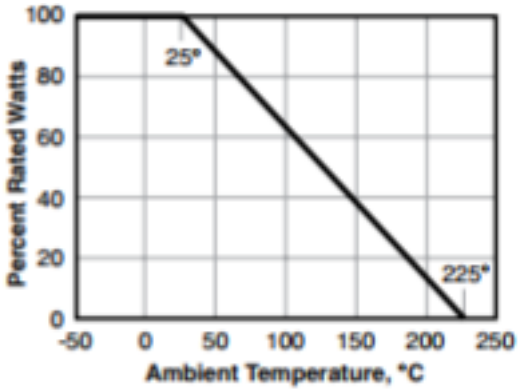

Figure 4.4 Derating curve of the resistor MOX97021004FVE [16]

4.5 Comparison of SM102031005FE and MOX97021004FVE resistor

4.5.1 Comparison of self-heating property

For observing the self-heating property of the two resistors over time following parameters and devices were selected for both resistors listed in table 4.8.

Table 4.8 Parameters and devices for studying self-heating property

Parameters	**Parameters values**
Tester Device Info	C.A 6547 for DC test Kikusui 5050a for AC test
Measurement of Temperature	FLIR E50 for DC test FLIR T440 for AC test
Room Temperature	23 to 25 ^{o}C
Number of samples	378
Frequency of sample	Once every 5 s
DC test voltage	1000 V
AC test voltage	2700 V
Uncertainty	For 10 MΩ: ± 0,8 ^{0}C (1 kV DC), ± 1,6 ^{0}C (2,7 kV AC) For 1 MΩ: ± 1,0 ^{0}C (1 kV DC), ± 2,6 ^{0}C (2,7 kV AC)

If the resistor SM102031005FE (10 MΩ) and MOX97021004FVE (1 MΩ) are compared regarding the temperature change then it can be seen in more detail in the figure 4.5.

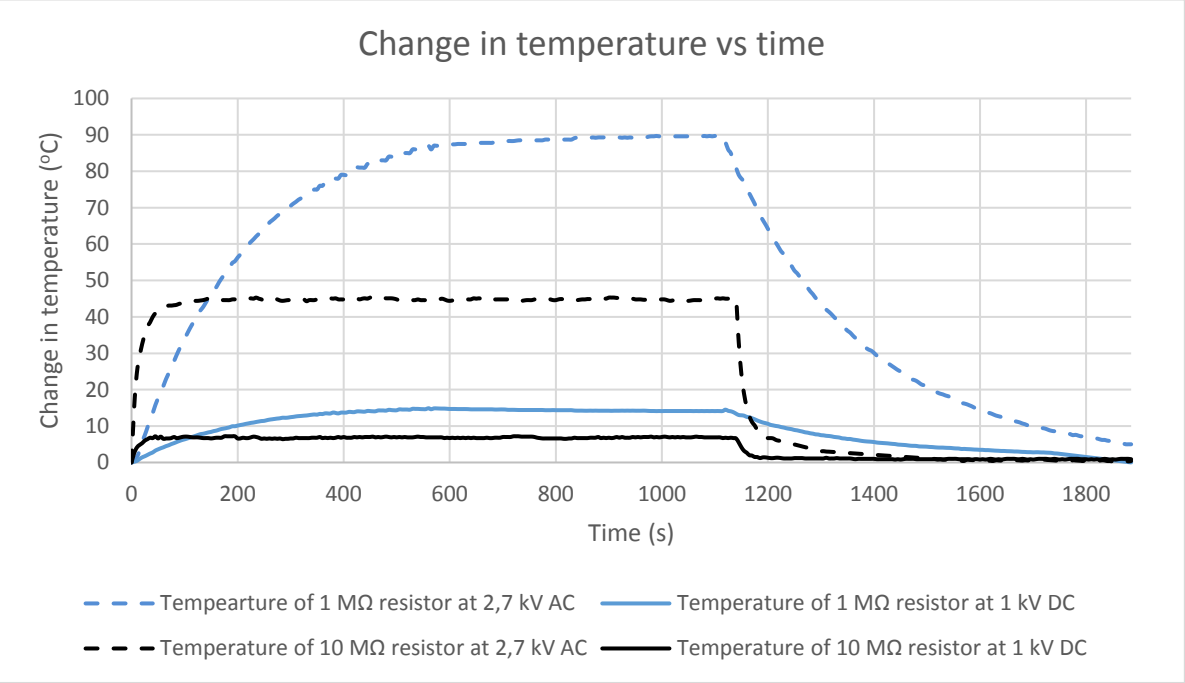

Figure 4.5 Comparative graph of self-heating of resistors

Some of the other results are calculated in table 4.9 using equation (3.2) for ΔT_{SH}, equation (3.7) for ΔR_{TC} and equation (3.8) for ΔR_{VC}.

Table 4.9 Results observed from self-heating property of resistor

Cases	Power (V^2/R) (W)	ΔT_{SH} calculated (^0C)	ΔT_{SH} observed (^0C)	ΔR_{TC} (kΩ)	ΔR_{VC} (kΩ)	Sum (kΩ)	Observed ΔR (kΩ)	Observed R (MΩ)
Case 1 (2,7 kV AC,1MΩ)	$2,7^2/1$ = 7,29	10,31 * 7,29 = 75,16	89,7	1 * 89,7 * 50 = 4,48	0,11	4,59	3	0,997
Case 2 (1 kV DC,1MΩ)	$1^2/1$ = 1	10,31 * 1 = 10,31	14,9	1 * 14,9 * 50 = 0,75	0,04	0,79	1	0,999
Case 3(2,7 kV AC,10MΩ)	$2,7^2/10$ = 0,729	56,67 * 0,729 = 41,31	45,3	10 * 45,31* 25 = 11,33	54	65,33	90	9,910
Case 4 (1 kV DC,10MΩ)	$1^2/10$ = 0,1	56,67 * 0,1 = 5,67	7,2	10* 7,2 * 25 = 1,8	20	21,8	20	9,980

The temperature coefficient calculations for resistor MOX97021004FVE (1MΩ) are different from the measured ones because maybe the resistor is slightly different from the mentioned characteristics in the datasheet. Or maybe the datasheet consists of specifications at different testing conditions. However, the total loss observed due to this reason is negligible and the total loss from the resistor that is calculated is same as that of the loss that has been observed.

The value of the resistor is not as rated due to the tolerance of the resistor i.e. 1 % for the selected resistors. Also, the precision and accuracy of the measuring device play an important role in the error.

4.5.2 Comparison of long-term Test

For the measurement of the long-term testing of both the resistors, the initial conditions are in table 4.10.

Table 4.10 Parameters and devices for studying long term test

Parameters	Parameters values
Tester Device Info	C.A 6547
Measurement of Temperature	FLIR E50
Room Temperature	23 to 25 ^oC
Number of samples	37
Frequency of sample	Once every 5 min
DC test voltage	1000 V

AC and DC test with same voltage produced same results so DC test was chosen for long term-test because of the limitation in Kikusui 5050a tester device that it can test up to the total time of 999 s [31] but C.A 6547 can continuously tests for 1 hour (i.e. 3600 s) [32]. Therefore, AC test was not carried out for the long-term test.

The plot of resistance change with respect to original resistance vs time can be seen for two different resistors in the figure 4.6.

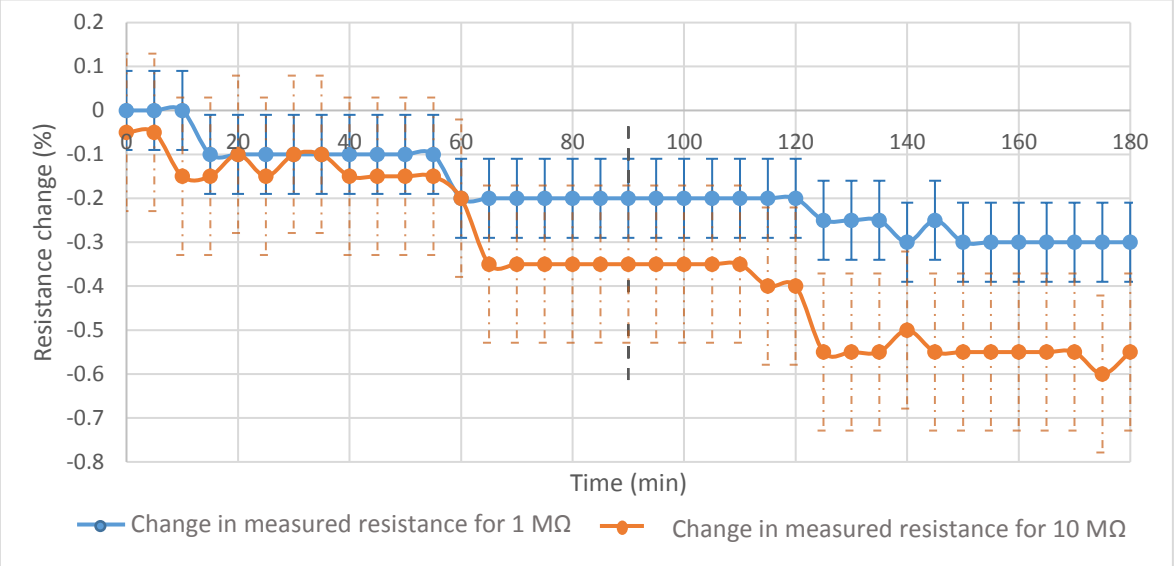

Figure 4.6 Comparative graph of change in resistance (%) during long- term test

The loss of resistance is negative and higher for 10 MΩ resistor with higher uncertainty. The final value of change at the end of 3 hours shows that the change is two times more for 10 MΩ resistor.

The figure 4.7 illustrates the value of the leakage current during the 3 hour as follows.

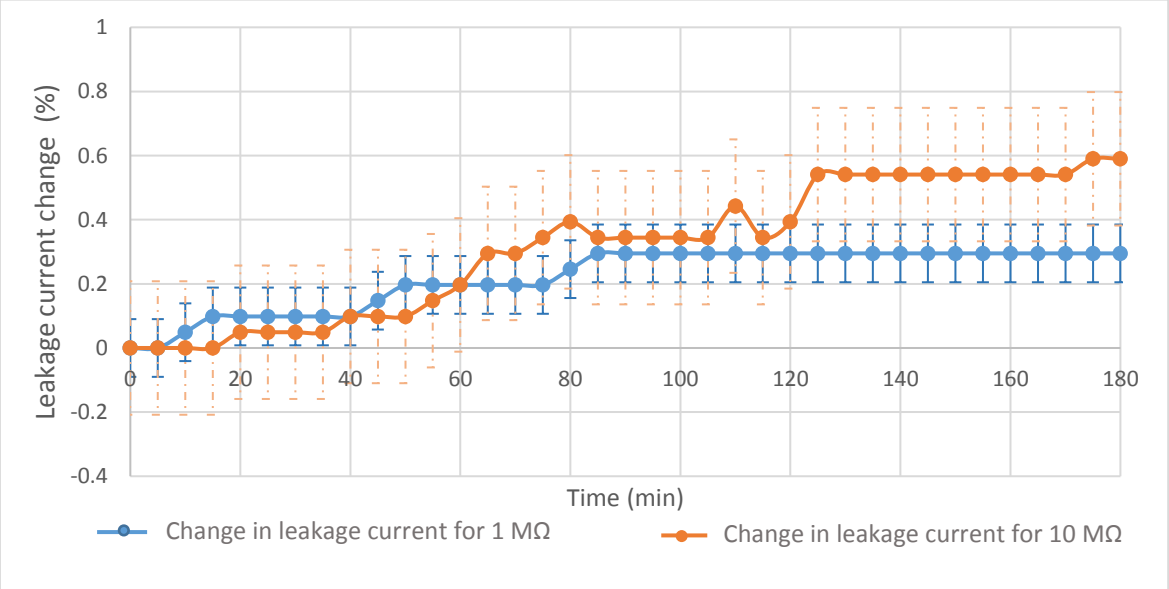

Figure 4.7 Comparative graph of change in leakage current (%) during long-term test

The change in the leakage current is twice more for 10 MΩ at the end of the test than that for the 1 MΩ resistor. The change in the values are positive for the change of leakage current.

The graph regarding the temperature of the resistor over time while making the reading of the current and resistance can be seen from the figure 4.8.

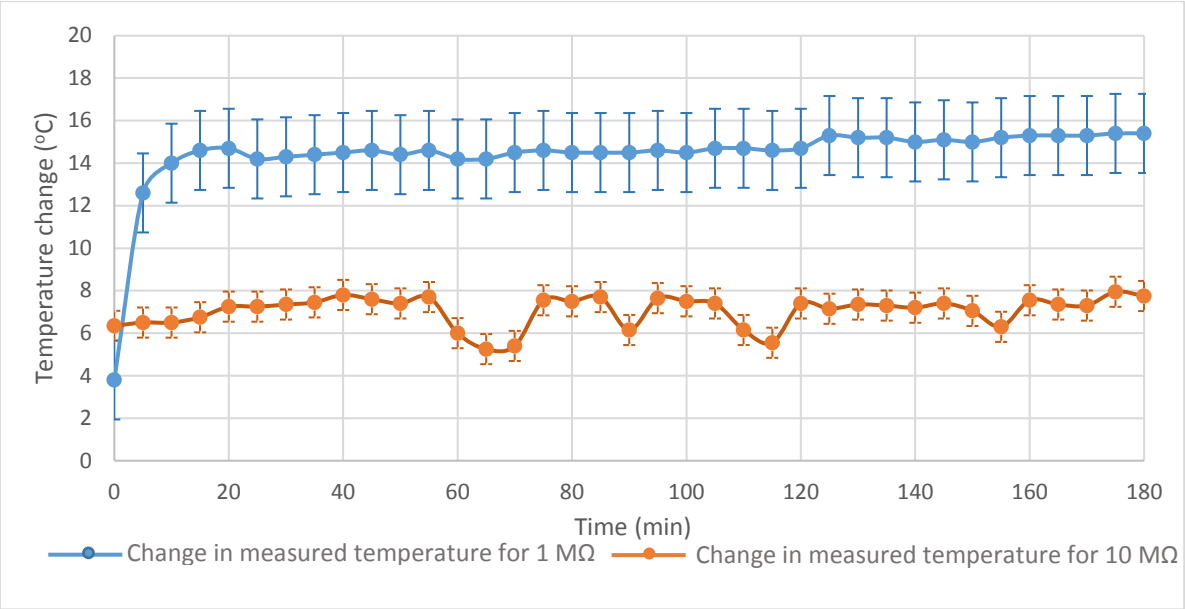

Figure 4.8 Comparative graph of change in temperature (°C) during long-term test

Temperature is more stable for 1 MΩ resistor. The instability seen in temperature change for 1 MΩ resistor is due to the use of the camera having lower precision and accuracy.

4.5.3 Comparison of short-term test

For the measurement of the short-term testing of both the resistors, the testing conditions are in table 4.11.

Table 4.11 Parameters and devices for studying long-term test

Parameters	Parameters values
Tester device info	Kikusui 5050a
Measurement of temperature	FLIR T440
Room temperature	23 to 25 °C
Number of samples	100
Time for each test	3 s
AC test voltage	2800 V

If the results of the test supply with 2,8 kV with 100 tests and each test lasting 3 s for two resistors are compared then the graph can be seen from figure 4.9.

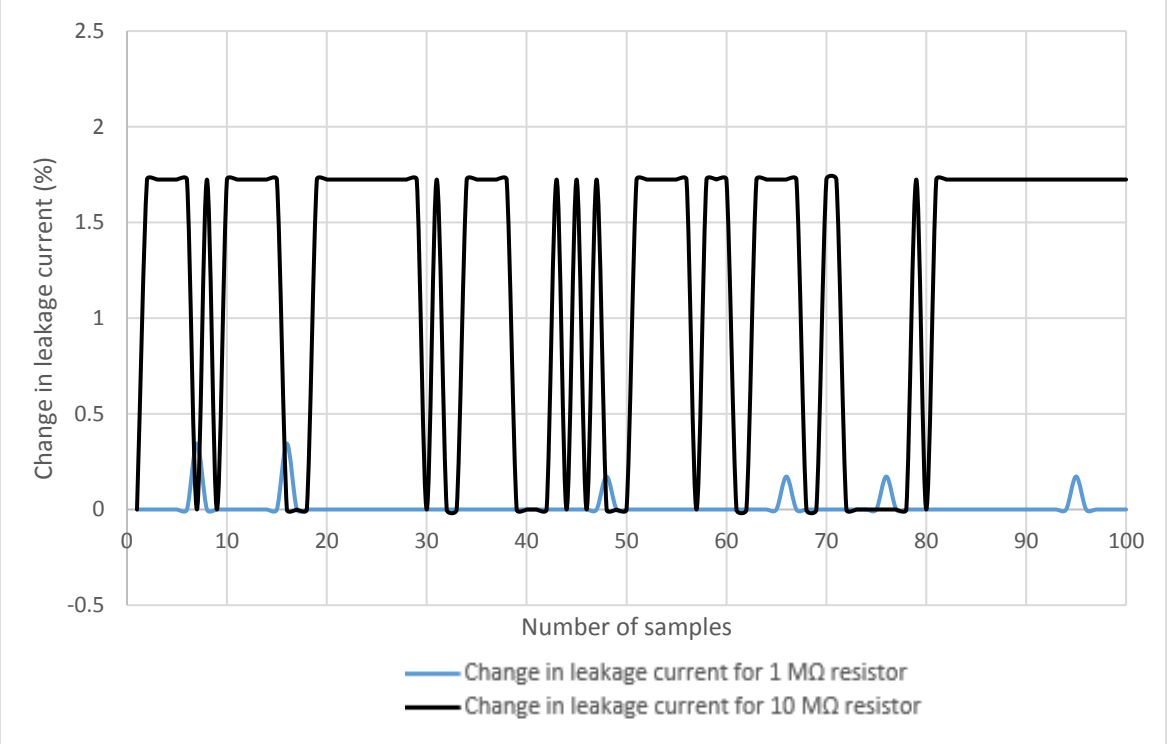

Figure 4.9 Comparative graph of change in leakage current (%) for short-term test

One of the reasons for the change in leakage current is because the voltage applied changed automatically for Kikusui 5050a. It can be observed that the change in leakage current is 6 times more in 10 MΩ resistor.

4.5.4 Assumptions of self-heating for Hipot device under test

The method for testing modules in ABB for the Hipot tester consists of series of steps. The test sequence suggested by ABB in regard to Hipot testing is as follows. These steps are for the main circuit whilethe steps for the auxiliary circuit are not shown here because the test is done with lower voltage i.e. 1 kV DC and 2 kV AC to the auxiliary circuits but with higher voltage i.e. 1 kV DC and 2,7 kV AC to main circuit. In a current case, two golden samples having same resistance and material replaces the main and auxiliary circuits. The test sequence is same (except voltage applied) for both circuit so assumptions for the main circuit is only considered.

1. 1000V DC is applied, insulation resistance is measured for 1 to 3 s.
2. Approximately 5 to 15 s pause.
3. 2700V AC is applied, leakage current is measured for 1 to 3 s.
4. Approximately 5 to 15 s pause.
5. 1000V DC is applied, insulation resistance is measured for 1 to 3 s.

Assumptions:

Few assumptions are made to the testing sequence that is mentioned by ABB for predicting the nature of self-heating of the resistors. The assumptions are made to provide a fixed value of testing time and are as follows.

Step 1. No supply is given to 4 seconds.
Step 2. 1000V DC is applied after 4 s, insulation resistance is measured for 3 s .
Step 3. 15 s pause.
Step 4. 2700V AC is applied, the leakage current is measured for 3 s.
Step 5. 15 s pause.
Step 6. 1000V AC is applied, insulation resistance is measured for 3 s.

The self- heating of the resistor is calculated using equation (3.2) and the rate at which it heats up and cools is calculated using equation (3.4) and equation (3.6). The following case in figure 4.10 is considered for an ideal case when there is no temperature fluctuations during the measurements. The value of T_θ is obtained from figure 4.5. The value of t is obtained from the individual steps mentioned above. The table 4.12 shows the rate at which heats up and cools for the above steps.

Table 4.12 Test sequence and a corresponding change in temperature for two resistors

Test sequence	ΔT_{SH} **for MOX97021004FVE (1 MΩ)**	ΔT_{SH} **for SM102031005FE (10 MΩ)**	**Remarks**
Step 1	0	0	No voltage is applied
Step 2	$14{,}9\left(1-e^{-\frac{t}{201}}\right)$	$7{,}2\left(1-e^{-\frac{t}{14}}\right)$	14,9 and 7,2 are obtained from equation (3.2).
Step 3	$0{,}29\left(e^{-\frac{t}{258}}\right)$	$1{,}8\left(e^{-\frac{t}{43}}\right)$	0,29 and 1,8 are the ΔT_{SH} at end of step 2.
Step 4	$89{,}7\left(1-e^{-\frac{t}{201}}\right)$ $+\Delta T_{SH\ from\ step\ 3}$	$45{,}3\left(1-e^{-\frac{t}{14}}\right)$ $+\Delta T_{SH\ from\ step\ 3}$	89,7 and 45,3 are obtained from equation (3.2) and $\Delta T_{SH\ from\ step\ 3}$ is the ΔT_{SH} change at end of step 3.
Step 5	$1{,}6\left(e^{-\frac{t}{258}}\right)$	$10\left(e^{-\frac{t}{43}}\right)$	1,6 and 10 are the ΔT_{SH} at end of step 5.
Step 6	$14{,}9\left(1-e^{-\frac{t}{201}}\right)$ $+\Delta T_{SH\ from\ step\ 5}$	$7{,}2\left(1-e^{-\frac{t}{14}}\right)$ $+\Delta T_{SH\ from\ step\ 5}$	14,9 and 7,2 are obtained from equation (3.2) and $\Delta T_{SH\ from\ step\ 5}$ is the ΔT_{SH}change at end of step 5.
Afterward	$1{,}73\left(e^{-\frac{t}{258}}\right)$	$8{,}46\left(e^{-\frac{t}{43}}\right)$	1,73 and 8,46 are the ΔT_{SH} at end of step 6.

As per the results obtained from the previous test the predicted graph for self-heating is in figure 4.10.

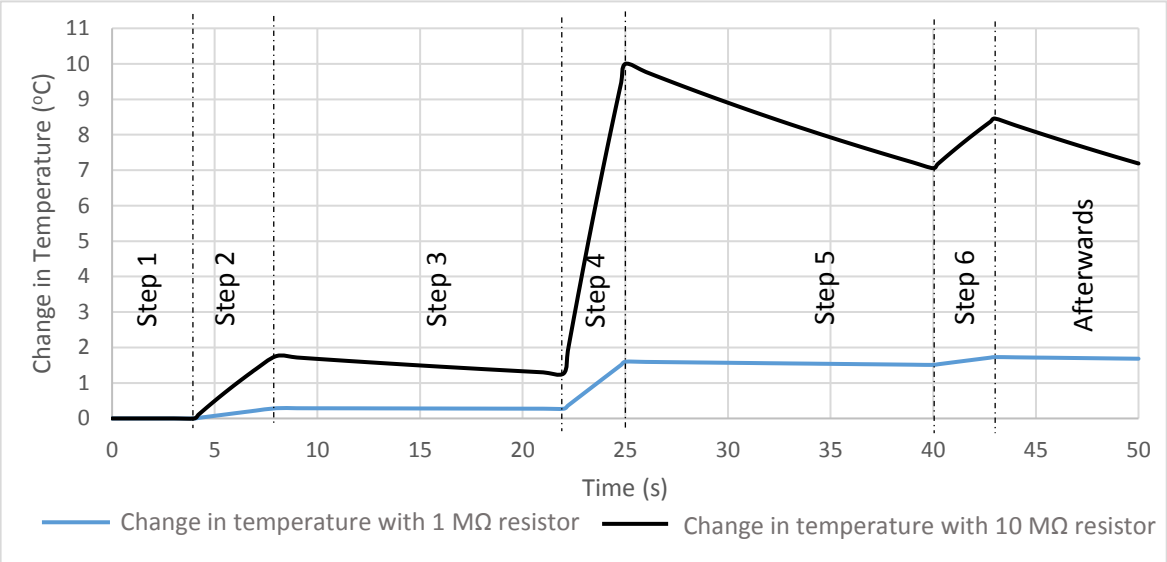

Figure 4.10 Comparative graph for prediction of self-heating for resistors

It is evident from the figure 4.10 that if the resistor SM102031005FE (10 MΩ) heats quite faster as compared to the resistor MOX97021004FVE (1 MΩ) but in this case, it is desired that the resistor heats more slowly. It is clear from this test that resistor MOX97021004FVE (1 MΩ) is more favorable for this application.

4.5.5 Test of resistors with humidity

As described in chapter 3.2.2 regarding the coating of thick film resistor, there are two layers of protective coatings: glass and epoxy. Glass coating offers protection against moisture while the epoxy coating is a strong and hard material which protects the inner composition of the material for making the thick film resistor. This property of the thick film resistor does not allow it to be affected by the humidity. Although these coatings were present, it was subject to a test at different percentage of relative humidity to check if the resistor might be affected by humidity. The test with humidity was done using the normal room humidifier.

Table 4.13 Parameters and devices for studying test with humidity

Parameters	**Parameters values**
Tester Device Info	C.A 6547
Measurement of Temperature	FLIR E50
Room Temperature	23 to 25 ^{0}C
DC test voltage	1000 V

Table 4.14 Test with various level of humidity to resistor MOX97021004FVE and SM102031005FE

Relative Humidity (%)	**ΔR for MOX97021004FVE (1 MΩ)**	**ΔR for SM102031005FE (10 MΩ)**
50	No change	No change
75	No change	No change
100	No change	No change

The results from table 4.14 indicates that humidity does not affect the resistance of the selected resistor.

4.5.6 Comparative analysis for selection of golden sample

The two different resistors MOX97021004FVE (1 MΩ) and SM102031005FE (10 MΩ) are compared based on the previous tests and the comparison table is made in table 4.15.

Table 4.15 Comparative analysis of MOX97021004FVE and SM102031005FE

Basis	**MOX97021004FVE**	**SM102031005FE**	**Remarks**
Self–heating if voltage is continuously supplied	15 ^{0}C for 1 kV DC and 90,2 ^{0}C for 2,7 kV AC	5,7 ^{0}C for 1 kV DC and 44,3 ^{0}C for 2,7 kV AC	More heating for MOX97021004FVE resistor
Loss in resistance at 1KV DC	1/1000 * 100 = 0,1 %	20/10000*100 = 0,2 %	2 times more for SM102031005FE
Loss in resistance at 2,7 KV AC	3/1000 * 100 = 0,3 %	90/10000*100 = 0,9 %	3 times more change for SM102031005FE
Change in Resistance in long term test	0,3 %	0,6 %	2 times more changing in SM102031005FE
Change in leakage current in long term test	0,3 %	0,6 %	2 times more changing in SM102031005FE
Rate of Temperature rise at 1 min*	ΔT_{SH} * 0,26	ΔT_{SH} * 0,99	MOX97021004FVE changes 3,8 ΔT_{SH} times more
Change with 100 test at 2,8 kV test	Up to 0,3 %	Up to1,8 %	6 times more for SM102031005FE
Voltage Coefficient	0,04 ppm/V	2 ppm/V	50 times more affected by voltage for SM102031005FE leading to more loss

For the calculation of the rate of temperature rise at 1 min equation (3.4) is used and following value of T and t are used.

For 1 MΩ resistor, $T_{\theta 1}$=197 s so at t=60 s so $T_h = \Delta T_{SH} * 0{,}26$

For 10 MΩ resistor, $T_{\theta 1}$=13 s so at t=60 s so $T_h = \Delta T_{SH} * 0{,}99$

The resistor MOX97021004FVE (1 MΩ) is selected because it heats up quite slowly, has less loss in resistance, better results from short-term test, long-term tests and voltage coefficient. This resistor is the golden sample of this project.

4.6 Geometry of wiring for golden sample

The geometry of wire plays an important role in the measurement of insulation resistance [34]. During AC supply, the current density is large on the surface of the conductor due to skin effect [35]. The geometrical cross-section is different from the effective cross-section for the current flowing path. Due to this reason, inductance and capacitance are generated as the wires are more bent which increases the resistance of the wire [35]. The wires described are the ones coming from the Hipot tester device that is connected to the golden samples. The figure 4.11 to 4.15 represents the connection in various setup. For each case, the golden sample was disconnected with the wire, connected afterward and the test was done.

Figure 4.11 Measurement of golden sample at setup 1

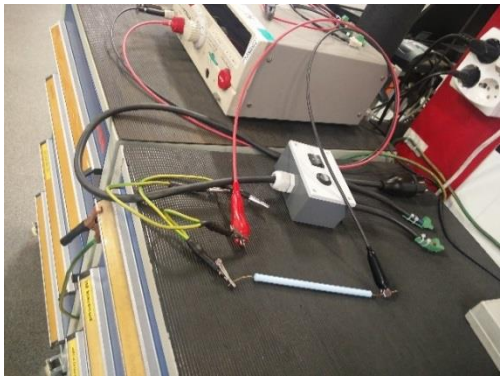

Figure 4.12 Measurement of golden sample at setup 2

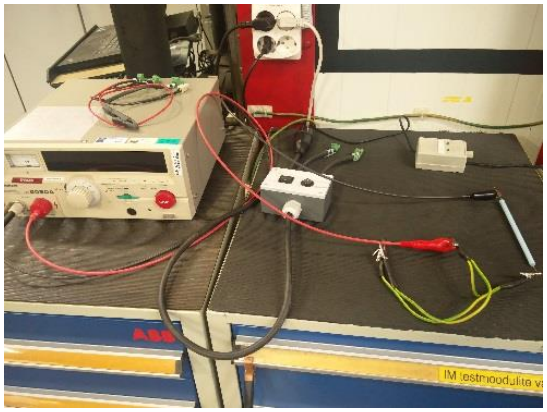

Figure 4.13 Measurement of golden sample at setup 3

Figure 4.14 Measurement of golden sample at setup 4

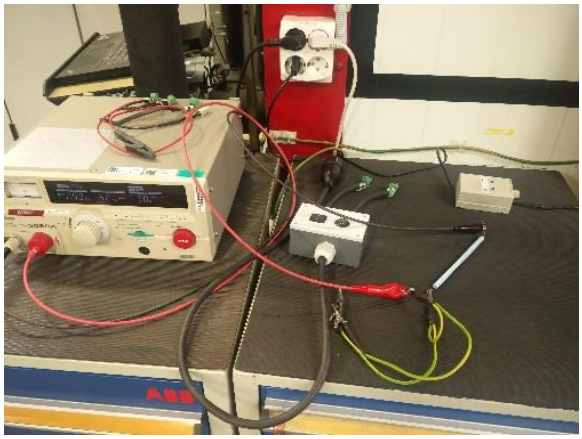

Figure 4.15 Measurement of the golden sample at setup 5

For all of 5 cases same measurement results were seen.

Table 4.16 Measurement results for different geometry

Parameters	**Parameters values**
Supply voltage	1000 V AC
Measurement device	Kikusui 5050a
Measured resistance	994 kΩ
Measured current	1,01 mA

The selected resistor is not affected by the geometry of the wiring setup. For all the test it showed the same value of resistance. It is because the current was big enough to balance out all the parasitic parts i.e. parasitic inductance and capacitance which gives variation in micro and nano-ampere region. The same test was performed with DC supply out of curiosity as there is no skin effect in DC supply [35] but the results showed that it has no effect on the geometry of the wiring setup.

4.7 Conclusion

Resistor temperature always changes with the self-heating properties. The actual temperature of resistor is obtained by the sum of ambient temperature and temperature due to self-heating of resistor ΔT_{SH}. The self-heating property remained same for both AC and DC test measurements and the resistor's temperature changed in the same nature. Self-heating of the resistor is also dependent on the voltage supplied to the resistor. Loss of resistor is dependent on the voltage coefficient of the resistor. Higher voltages have more effect on the loss of resistance than the lower voltages.

The temperature of the resistor raised hyperbolically when the voltage is supplied and decayed exponentially when supply was turned off. The changes in temperature that occurred inside the room were neglected. However, the accuracy of the measurement device altered the results. It was observed that the temperature of the resistor remained same if tested with the same power supply for the same resistor. It gets heated as per the calculations from equation (3.2), (3.4) and (3.6) over time and does not exceed once it reaches the calculated temperature.

The resistance was different if the test was done for a long time and if it the measurements were started again making new connections. It can be seen from the figure 4.16 for the resistor SM102031005FE.

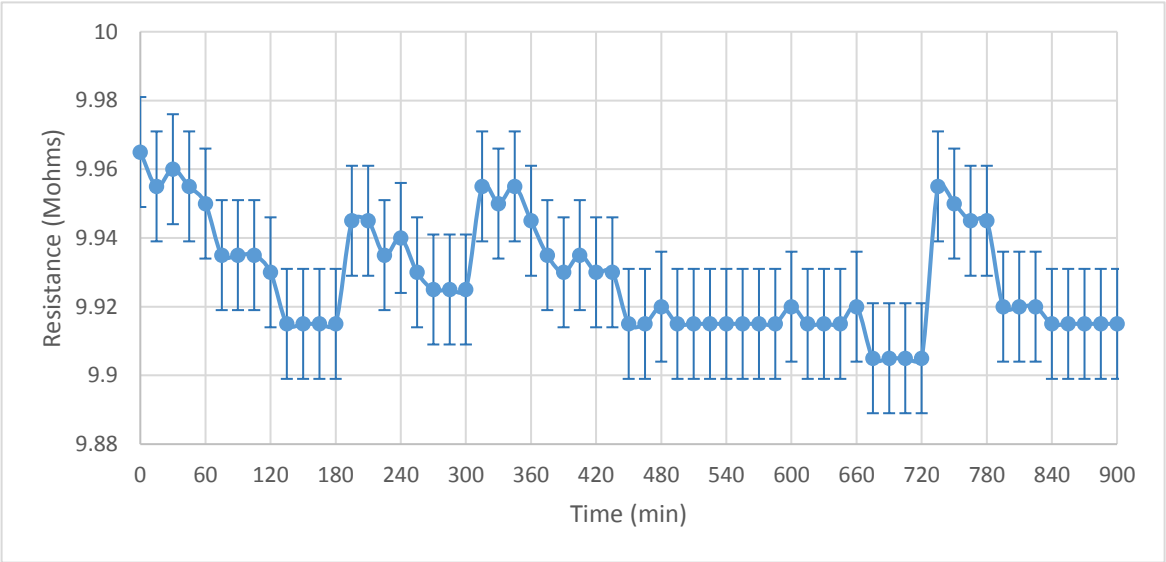

Figure 4.16 Measured resistance when rewired during long term test

For longer tests, the resistance decreased linearly from 9,960 MΩ to 9,905 MΩ from time 0 to 180 min but if a new long-term test is made then the resistor regains its lost resistance. It can be seen after the new connection and test is made at 180 min, 300 min and 720 min. This could be due to the uncertainty from the measurement and absolute error of the measurement device. The test was made with 1000 kV DC supply using C.A 6547 and E40 devices. But observing this property does not lie on the scope of this project as the test in the factory is carried out for 2 to 3 s and the resistor does not lose any resistance during this period of time.

According to Ohm's law, as the resistance keeps on decreasing the current increases and the graph for leakage current for the test described in the previous step is in figure 4.17.

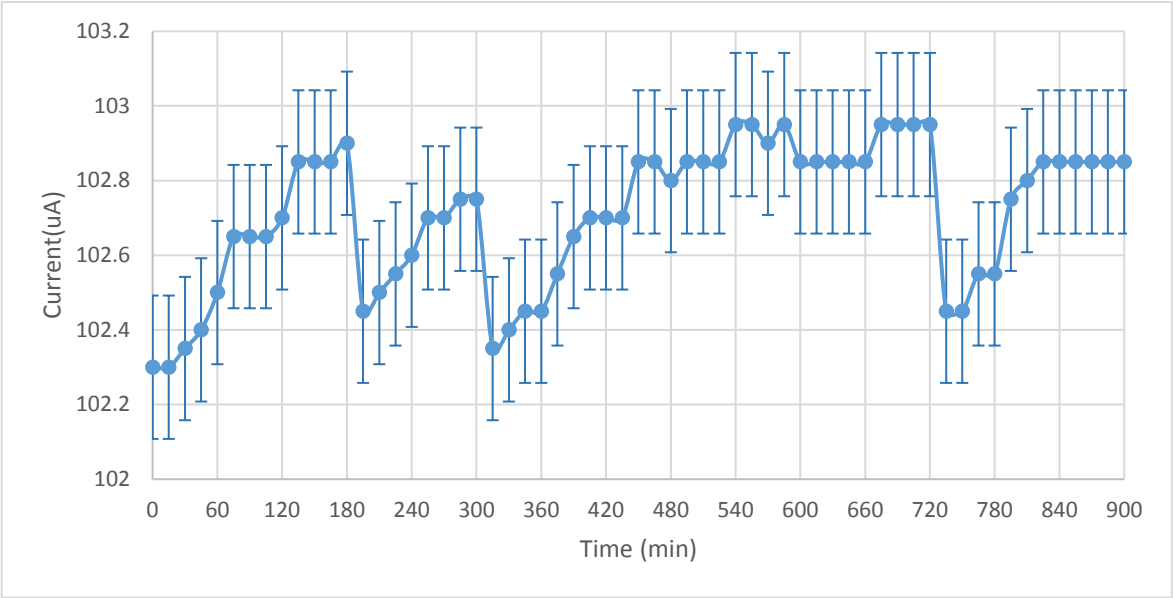

Figure 4.17 Measured resistance when rewired during long-term test

The leakage current increased linearly until it was rewired. During the long-term test for measurement of leakage current, it behaved exactly opposite to the long-term test for measured resistance. The measured changes might be due to the uncertainty in the measurement.

MOX97021004FVE (1 MΩ) is selected over SM102031005FE (10 MΩ) because it has a lower temperature rise over time and the resistance, leakage current change is 2 times less over time. Apart from this, it gives more precision and accuracy to the measuring device so, 1 MΩ resistor is selected over 10 MΩ resistor. The geometry of wiring did not affect MOX97021004FVE (1 MΩ) during the voltage withstand test and leakage current test. The golden sample for this project is MOX97021004FVE (1 MΩ) resistor and is not affected by the humidity.

5 PROTOTYPE AND TESTING

5.1 Requirement analysis

The prototyping needs to be done considering all the requirements specified by the ABB in chapter 2.5 and 2.6. Selection of golden sample is of primary importance. The selected golden sample is subject to controlled temperature and humidity. After selecting the golden sample it must be kept at the temperature and humidity which is defined by the setpoint. For maintaining a controllable temperature and humidity for the golden sample, it is important to place the sample in an insulated box which produces negligible heat loss.

Temperature and humidity control needs to be provided by a control system. PLC is considered for the control system. Various components like the heating coil, fan, solenoid valves and humidifier are connected to the PLC. It is a better approach to place all these components inside a box which provides protection to these devices. The temperature and humidity sensors provide the data regarding the temperature and humidity inside the box regularly. The PLC controls the humidifier, heating coil, solenoid valves and fan based on the information received from the sensor. The set point for the PLC is controlled by adding a control display panel having HMI.

There is a requirement for two boxes, one for storing the golden sample and the other for a control system. Since, there is a requirement of external air supply, supplying into the inlet and releasing from the outlet, so use of a single box was not considered to prevent heat loss from the box consisting of the golden sample. By taking in all of the requirement and possible solutions, following conceptual design in figure 5.1 is prepared.

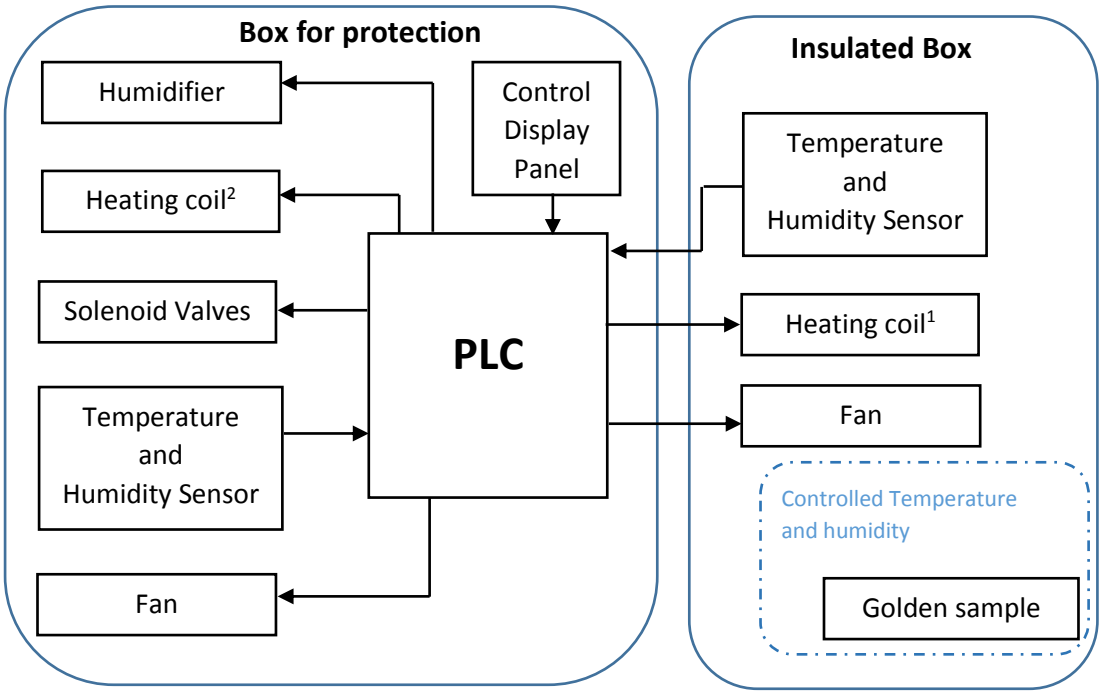

Figure 5.1 System conceptual design diagram

5.2 Components selection

The list of devices selected for the design and the reason for selection of the particular device is explained below.

1. PLC based solution is chosen for control system because they are reliable controller for automation of industrial electromechanical processes. Some of the features that were observed while selecting the PLC are as follows.

- Availability of IO modules
- Programming software license cost
- Price of the product
- Support for EtherCAT fieldbus modules
- Works with DC supply
- Programming experiences in past and service support

  Initially, few PLC from Beckhoff, Schneider Electric, Omron and Mitsubishi were considered as they fulfilled the specification. But PLC from ABB was selected because of easier availability and ABB encourages on using its own products. After thorough investigation PM564 [36] from ABB was selected as a control system. An additional IO module DA501 [37] was also selected because PM564 had limited number of the analog input port (i.e. two) but it is required to have at least four in this application which is provided by DA501. In case the digital input and output are not sufficient then it can provide a connection.

2. A control display panel for HMI has to be selected which has the following specification.
    - Communication protocol to PLC
    - Touch screen features
    - Smaller dimension of 7 to 8 inches to fit in box
    - Support DC power supply

   After considering the above specification control display panel from ABB, SIMENS, Schneider Electric and Higgstec were investigated, but panel CP607 from ABB was selected because it supports all the above features and is more suitable for ABB PLC products [38].

3. The insulator box for placing the golden sample was designed by using CAD software SOLIDWORKS. The dimensions are explained in detail in the appendix C. It consists of 3 different layers. The inner and outer layers are made of acrylic material because it is strong material (protection device from external damages) and good insulator for electricity. The central layer consists of expanded polystyrene which is a good insulator of heat. The primary function of this box is to protect the golden samples from external damages and prevent heat loss during testing. The box consists of lid with box buckle so it is easily opened and closed for replacing the golden samples if needed. The structure of the insulator box can be seen from the figure 5.2.

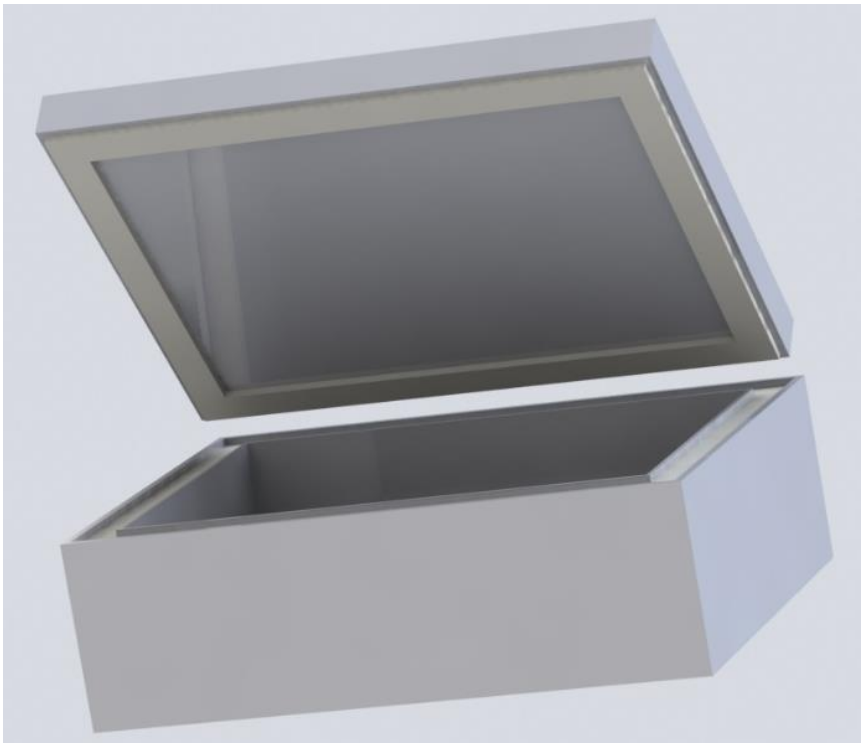

Figure 5.2 Insulator Box for placement of golden sample

4. Golden sample MOX97021004FVE [16] is selected based on the results obtained from chapter 4.
5. Humidification is created with the help of mist makers. One disc mist maker is used for creating the desired humidity. Since it has misting disc size of 20 mm which has the output of 500 ml per hour with average droplet size of 3 to 5 microns so it was selected [39].
6. Axial fan 614NGH was chosen because it operates with DC supply of 24 V. Furthermore, it has dimensions of 60 mm x 60 mm x 25 mm, draws less current 103 mA and has a flow rate of 0,76 m^3/min which is suitable for this design [40].
7. Touch Safe PTC heaters STEGO 06030.0-00 is used to heat the insulator box because it is touch safe, supports DC power source and has dimensions of 98 mm x 38 mm x 75 mm [41]. It is selected because it is touch safe and does not damage the components of the insulator box.
8. LC-R127R2PG, 12 V rechargeable battery is used to provide DC supply. It provides supply for all the electrical devices. Since it has battery capacity of 7,2 Ah, has a mass of 2,47 kg and dimension 94 mm x 64,5 mm x 151 mm which is better than other available battery so it is selected [42]. Two of this battery are used in series for 24 V supply because some devices like PLC, fan, heater, etc. require 24 V for operation.
9. T9602-3-D-1 - humidity/ temperature sensor is selected for monitoring temperature and humidity because it is capable of providing digital and analog sensor output with the accuracy of ± 2 % relative humidity and
   ± 0,3 °C for temperature [43]. Furthermore, it operates with DC power supply so it was selected.

10. A box PJ14126RTW for placing all the components like heater, humidifier, PLC, battery and beaker is selected because it is made up of polyester, has the dimension of 399,44 mm x 211,11 mm x 351,84 mm (same in length and breadth with insulator box) and can hold all other components [44].
11. Panel heater HP05-1/10-24 is used for heating the water in PJ14126RTW box as it operates with DC power supply of 24 V, has the power rating of 50 W and lower dimensions of 35 mm x 40 mm x 8,3 mm [45].
12. AQT15SC solenoid valve is selected because it can transmit air, water and gas, with more than 20,000 times of lifespan, has a thread size of 1/2 inch and works with DC voltage source meeting all the specification required for this system [46].

To summarize the list of selected components and the quantity required it is presented in the table 5.1.

Table 5.1 List of selected components

Item No	Product name	Quantity	Description	Supplier
1	PM564	1	PLC	ABB
2	DA501	1	IO module for PLC	ABB
3	CP607	1	Control display panel for PLC	ABB
4	Insulator Box	1	Insulated box for golden sample	-
5	MOX97021004FVE	2	Resistor (golden sample)	Farnell
6	1 disc mist maker	1	Humidifier	House of Hydro
7	614NGH	2	Axial fan	Farnell
8	HP05-1/10-24	1	Panel Heater	Farnell
9	STEGO 06030.0-00	1	Touch safe heater	Farnell
9	LC-R127R2PG	2	12 V rechargeable battery	Farnell
10	T9602-3-D-1	3	Temperature and humidity sensor	Farnell
11	PJ14126RTW	1	Junction Box for other component	Farnell
12	AQT15SC	2	Solenoid valves	Farnell

Some of the other components like distilled water, beaker (for holding water), tubes and pipes are not mentioned because they are locally available and are subject to change for getting the desired results.

5.3 Placement of components

The final device to be built can be seen in the figure 5.3. It consists of two boxes named box 1 and box 2. Box 1 is used for placement of control unit and all other components like: solenoid valves, heating coil, vessel for holding liquid, humidifier, PLC while box 2 is an insulated box which consists or golden samples and is designed to maintain negligible humidity and heat loss.

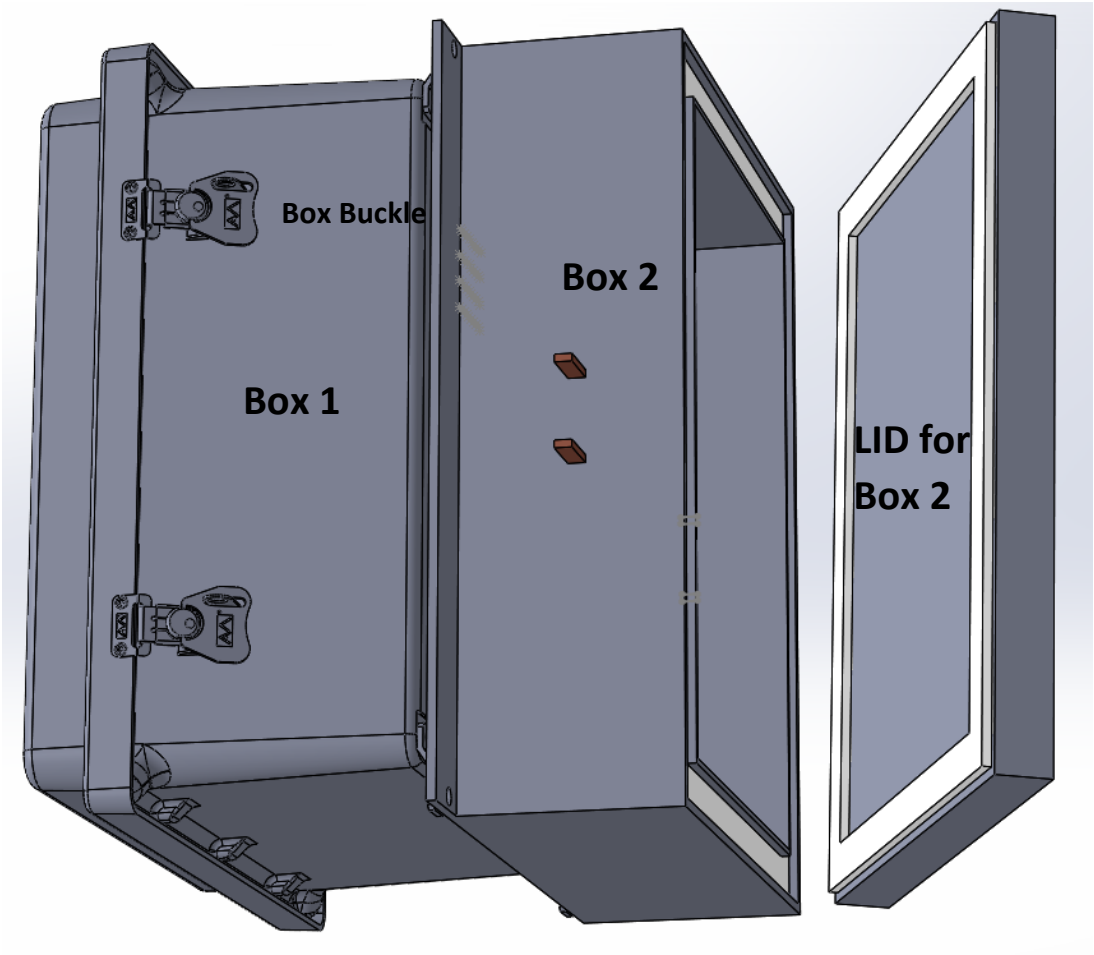

Figure 5.3 Bottom view of the proposed system

The lid for both box can be opened from the bottom part. Lid is kept in box 2 because it helps in replacement of the golden sample. Moreover, it leaves an option for cooling the whole box in case the temperature rises to the level that is two to three times more than desired range. Box buckle is present on both of the box for opening and closing lid of the box easily.

The front view of box 1 can be seen in the figure 5.4. A humidifier is placed on the bottom of the beaker. A heating coil is also dipped inside the distilled water. Distilled water is used because it will prevent golden sample and bus bar to mix with the impurities. The water is heated to the desired temperature with the help of the heating coil. Once it reaches to the desired setpoint it is humidified with the help of humidifier. The moisture is passed towards the inlet. A fan is placed perpendicular to the valve which works as a blower to pass the moisture inside the insulated box. The construction of pipe (with tempearture and humidity sensor) is used to pass the moisture to the inlet and from outlet without allowing it to flow on the whole box is not described in this figure 5.4. It is beacuse this design is used to give overview of how the major components are placed inside the box. Also, these pipes are connected directly to the lid of the box so the air and humidity is passed to and from the outer environment. The lid of the box consists of a control display panel parallel to PLC and is not shown to have better front view.

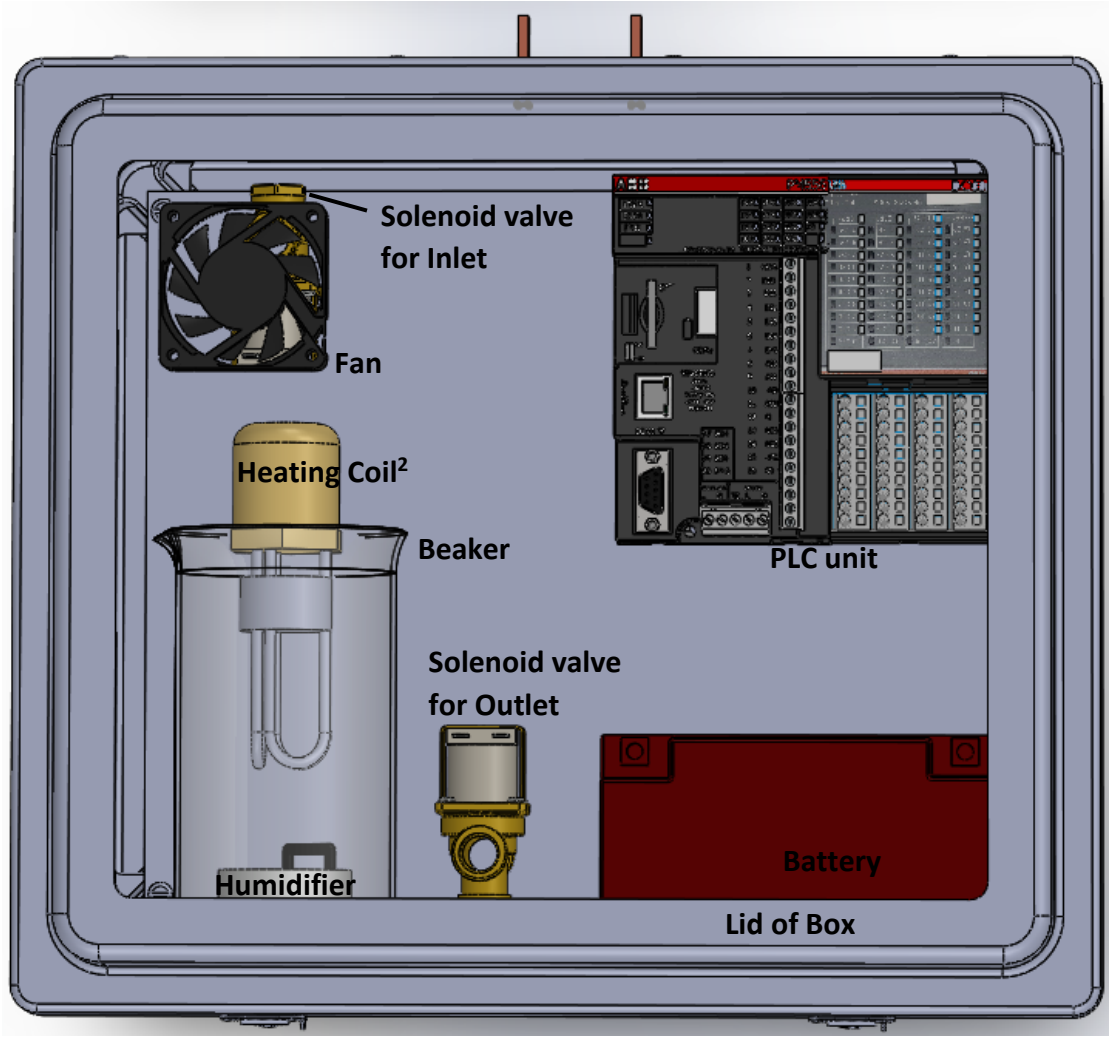

Figure 5.4 Front view of Box 1

PLC which is used to control the whole system is also placed inside this box. Battery which gives power to the whole electrical components is placed in the bottom of the right side.

The front view of box 2 can be seen in the figure 5.5. This figure shows the components which are placed inside the box. It consists of a heating coil which is used to set the temperature inside the box according to the set point. A fan is placed perpendicular to the inlet which acts as a mixer for the box. It is used to mix the heat generated by the heating coil with the moisture inside the box. An oulet is also present in the middle on the lower section to pass the moisture and air. Temperature and humidity sensor are placed inside the box 2 for providing feedback to the PLC and checking with the set point.

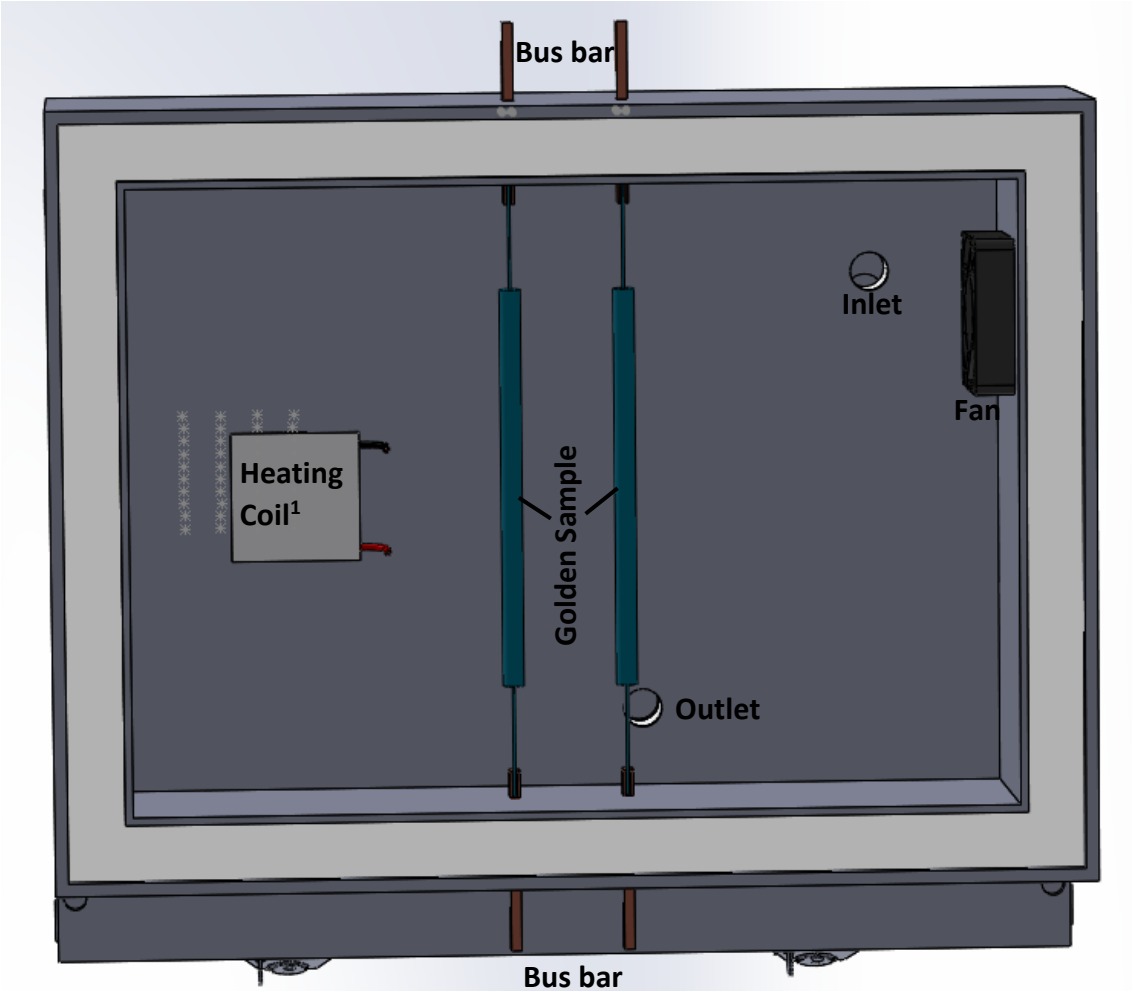

Figure 5.5 Front View of Box 2

There are two golden samples placed inside the box. Both of the samples are composed of same material and have same resistance. One of the sample is used for carrying out test similar to the test with auxiliary curcuit (DC test voltage is 1kV and AC test voltage is 2 kV) while the other one is used for carrying out the test similar to the main circuit (DC test voltage: 1 kV and AC test voltage: 2,7 kV). The golden samples are further connected to the outer section of the box with bus bar. Bus bar is further connected with crocodile wires and the test voltages are applied during real test. The whole box is designed with arcyl (for inner and outer cover) and expanded polystyrene(in between the arcyl material) so it is a better insulator of heat and is not affected by the voltage source during test.

5.4 Software development

The development of software is divided into two segments as user interface and device control. Various softwares are used for this application. The user interface for HMI is developed in different platform and PLC program in a different one. The control display panel has the HMI for easier inerface between human and machine. It sends the input from the user to the PLC. The PLC is the main control system which control the whole system and electrical components. The software programs used can be seen in the figure 5.6.

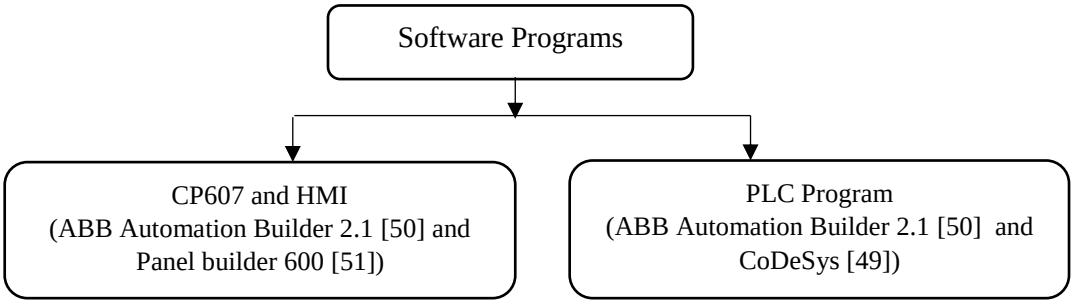

Figure 5.6 Structure of software development

The program can be divided into three parts. One for maintaining controlled temperature, other for maintaining controlled humidity and the main program. The control algorithm takes place in the PLC PM564. The PLC controls the heater, humidifier, solenoid valves and fan based on the signal received from the temperature and humidity sensor. The display panel CP607 is used to input the value of temperature and humidity for the insulated box.

- **Main program**

The control display panel is used initially to provide input from the user. The user is able to provide temperature and humidity input required to carry out the test. The information regarding the temperature and humidity inside the box is obtained with the help of the temperature and humidity sensor that is placed inside the insulted box. If the correct temperature and humidity is sensed by the device, then it is indicated back to the display that it is ready for test. Then, the device is subject to test with the golden sample. If the readings differ from the desired setpoints then it checks the temperature initially. Secondly, it checks the humidity of the device for maintaining the controlled temperature and humidity. Once it is ready for test it is subject to Hipot test.

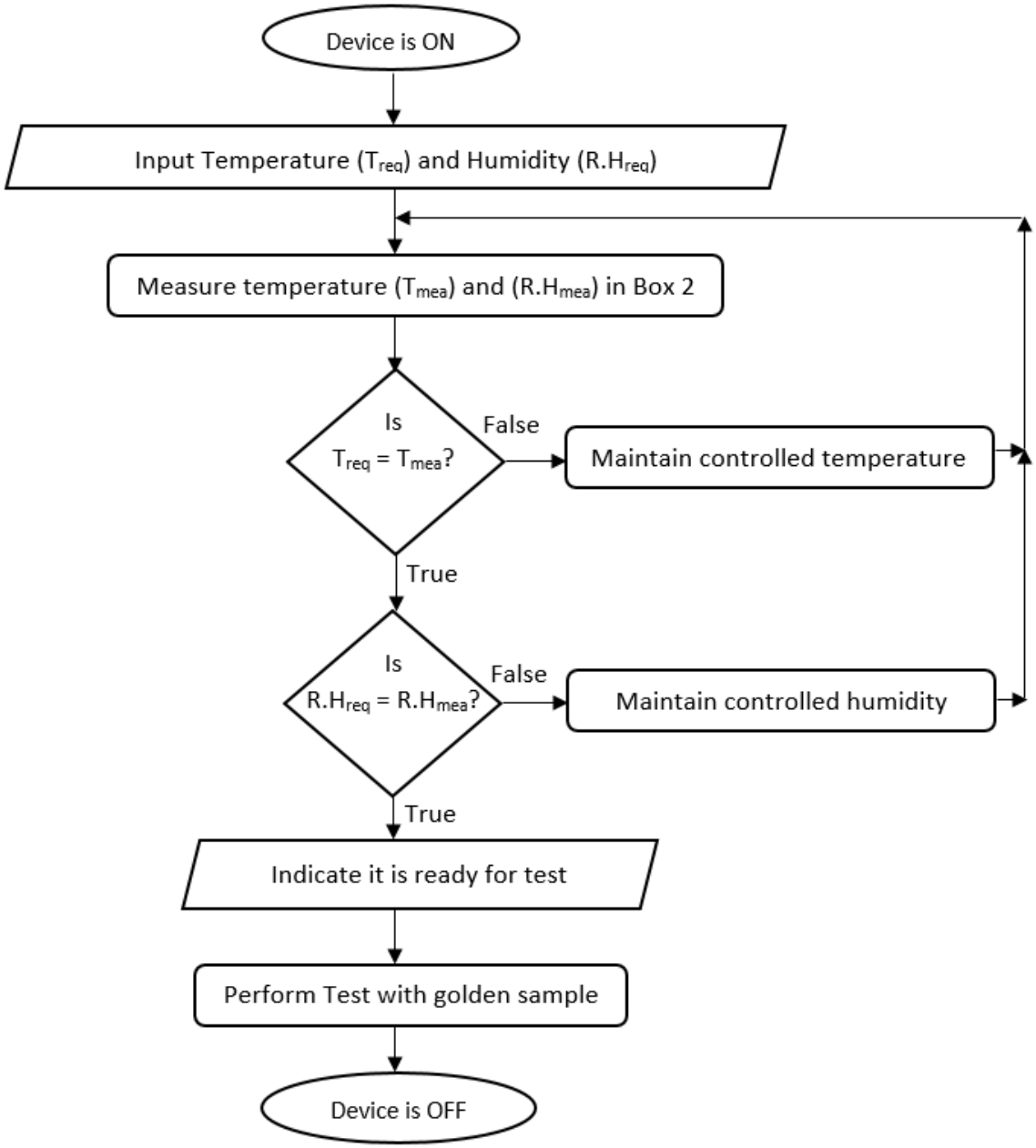

Figure 5.7 Flowchart for the main program

- **Maintaining controlled temperature**

The algorithm for maintaining the controlled temperature is shown in figure 5.8.

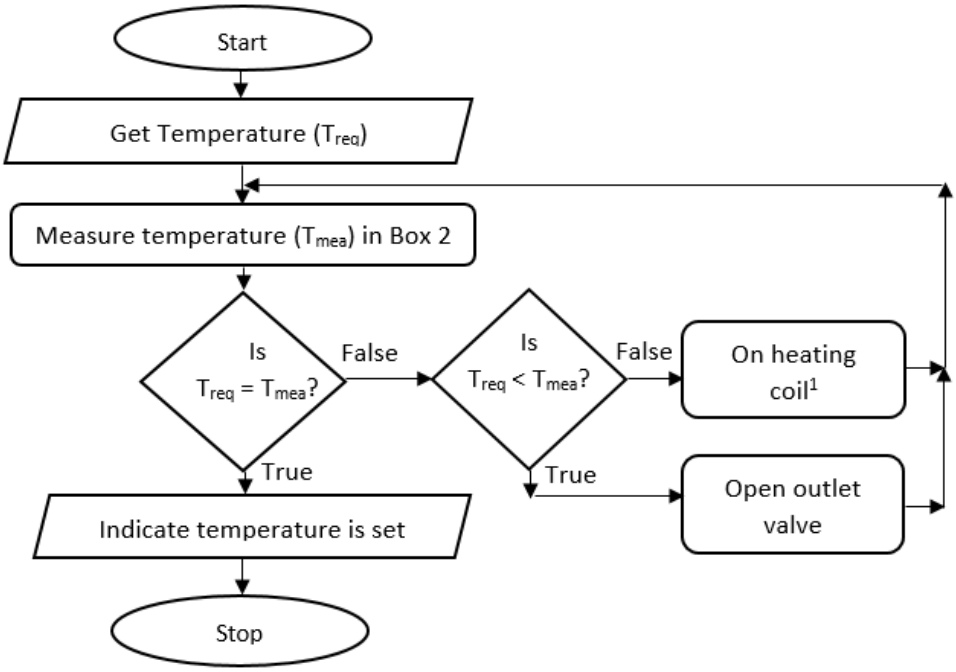

Figure 5.8 Flowchart to maintain controlled temperature

- **Maintaining controlled temperature**

The algorithm for maintaining the controlled humidity is shown in figure 5.9.

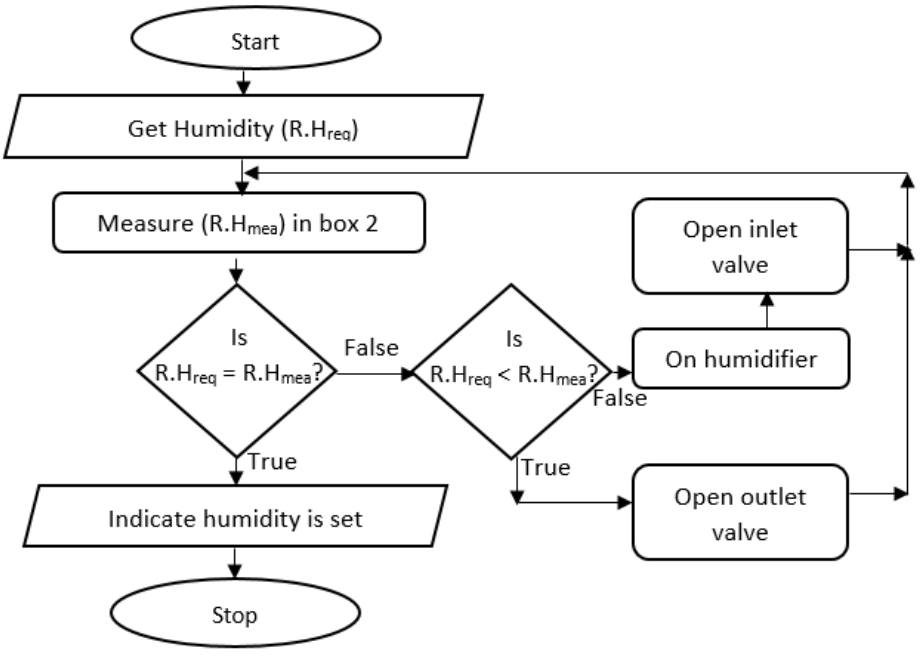

Figure 5.9 Flowchart to maintain controlled humidity

5.5 Testing procedures

The assembled product consisting of golden sample is kept in a four wheel trolley for easier movement. Initially, the temperature and humidity are set up to the desired set point. Once the golden sample is maintained at the desired temperature and humidity it is placed inside the Hipot testers. It is further connected to the Hipot testers with the help of crocodile wires. The connection is made in between the bus bar and the Hipot tester device. Once the connection has made and the golden sample is at desired temperature and humidity, it is subject to Hipot testing. There are two main reasons for carrying out with the golden sample in the factory i.e. one for the daily testing and other is special cause testing.

- **Daily testing**: 1st test every day is made with golden unit. Temperature and humidity are set and then test is made with special golden unit Hipot test sequence, which is based on standard Hipot sequence (general description is explained in chapter 4.5.4. Results are saved to SQL database for each Hipot tester separately. Based on the results, statistical process control graphs are built in automatic mode. Automatic notification is given, if the measurement point is out of control limits or strange behaviour of process is being observed. If everything is OK, then product testing can be started for this day.

If some failure occurs due to some special cause, then testing team is sent to investigate the reason. Testing is stopped, until the root cause is verified and permission from the testing team is given to continue tests.

- **Special cause testing:** If the Hipot-related error occurs during product testing and final control cannot quickly determine the root cause (failure is not common), test with golden unit is being made. If the test is successful, then the test system can be used for further tests with different products. Final control starts to search for the root cause in failed product and/or check factory ambient conditions. If golden unit test is not successful, then testing is stopped and testing team is sent to investigate the reason. Testing is stopped, until the root cause is verified and permission from the testing team is given to continue tests.

5.6 Conclusion

The requirement analysis was done from the requirements given by ABB mentioned in chapter 2. The components were selected for the fulfillment of the requirement made by ABB. The final view of the prototype was designed in SOLIDWORKS and it was observed that the overall dimension for the device was 400 mm x 362 mm x 351 mm which is smaller than the mentioned dimensions of 540 mm x 400 mm x 460 mm. Furthermore, the insulated box is designed with material having higher insulation properties so the overall heat loss from the box is negligible.

The flowchart for maintaining stable temperature and humidity consists of two different steps. Initially, the temperature is set to the defined setpoint then the humidity is set to the desired setpoint. Also, the values for the setpoint and the measured temperature and humidity are equal if it lies within some tolerance that is mentioned in chapter 2.6. The selected components should give results which fulfills the requirement of ABB and must work based on the modeling of the system. A simulation is explained in chapter 6 for this purpose.

6 SIMULATION AND RESULTS

6.1 Overview

A simulation is created to observe if the features from the selected components give desired results or not. During the simulation, the main focus is centered on obtaining controlled temperature and controlled humidity. Two separate simulations are designed to obtain controlled temperture and controlled humidity. The simulation is prepared using MATLAB (matrix laboratory) tool [9].

The simulation was run by without PID and using PID control strategies. PID is widely used control process for industrial applications and a basis for advanced control algorithms as it is closed loop control. The input - output relationship for PID control consists of three different elements and the transfer function can be defined as follows

$$G_c(s) = K_p + \frac{K_i}{s} + K_d * s. \tag{6.1}$$

Where K_p, K_i and K_d are known as proportional , integral and derivative gain. These three adjustments needs to be tuned for better interaction with each other. The tuning of these gain values are done manually in the MATLAB for obtaining best performance according to design specification of the system [47].

6.2 Simulated system for temperature control

The temperature has to be set based on the setpoint that has been defined. The system for obtaining controlled temperature can be seen in the figure 6.1 which is based on equation (3.17).

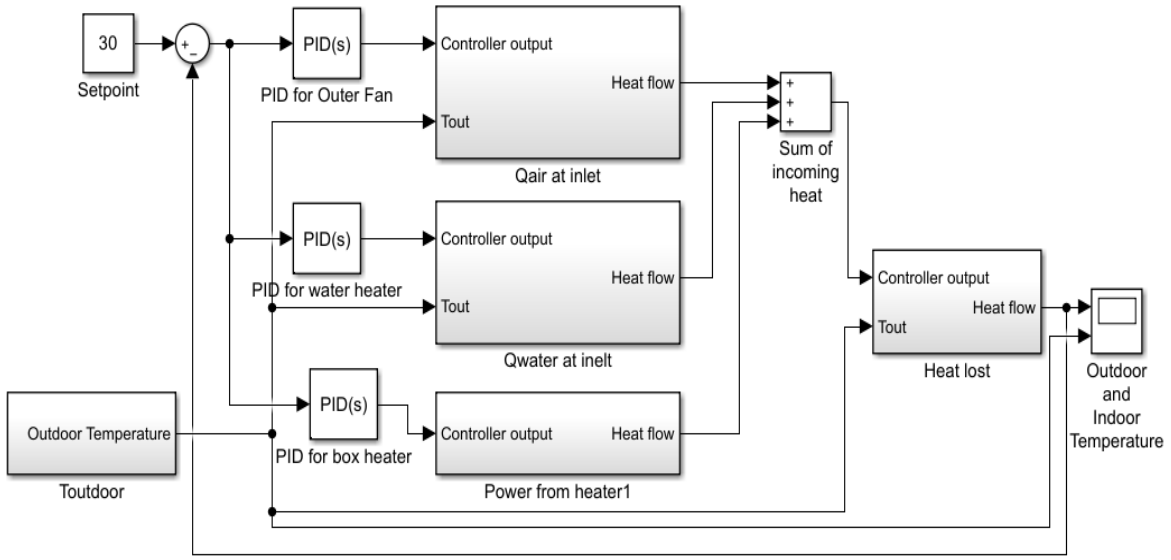

Figure 6.1 Simulated system for temperature control

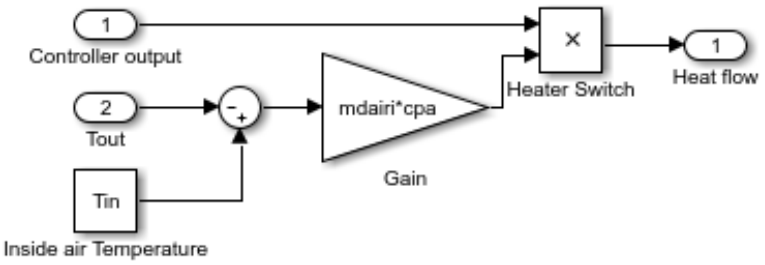

Figure 6.2 Inside subsystem Qair at inlet

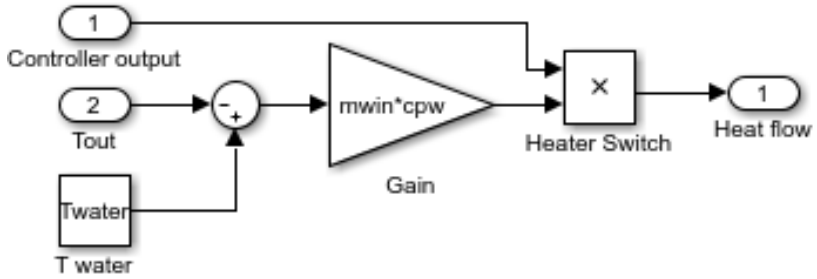

Figure 6.3 Inside subsystem Qwater at inlet

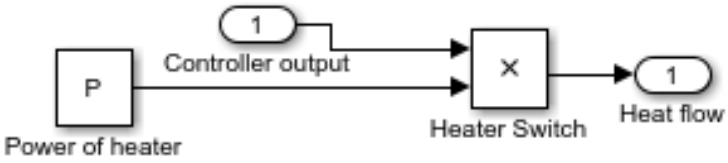

Figure 6.4 Inside subsystem Power for heater1

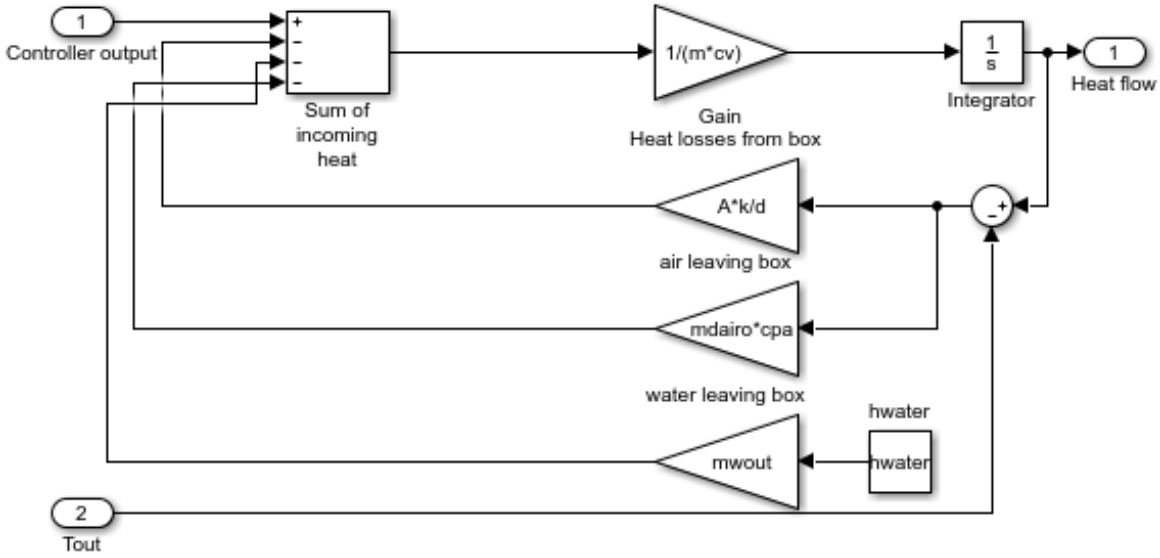

Figure 6.5 Inside subsystem Heat lost

6.3 Simulated system for humidity control

The Humidity has to be set based on the setpoint that has been defined. The system for obtaining controlled temperature can be seen in the figure 6.6 and is based on equation (3.21).

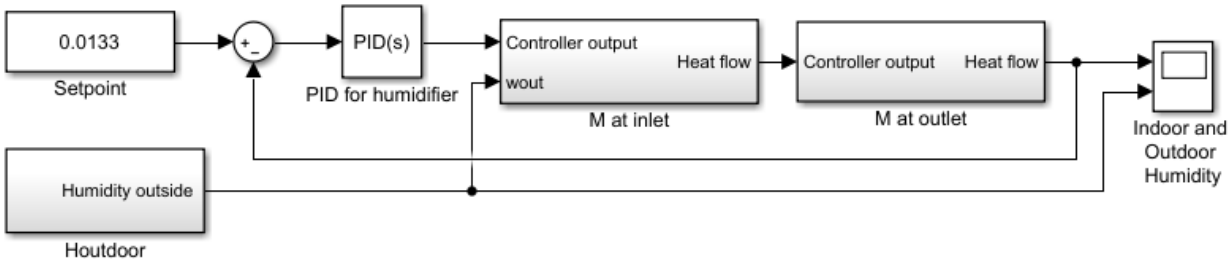

Figure 6.6 Simulated system for humidity control control

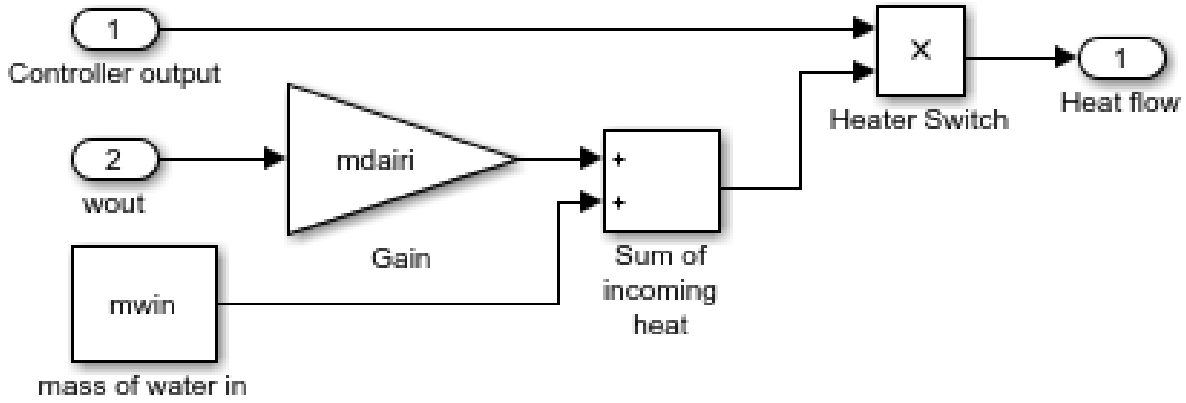

Figure 6.7 Inside subsytem M at inlet

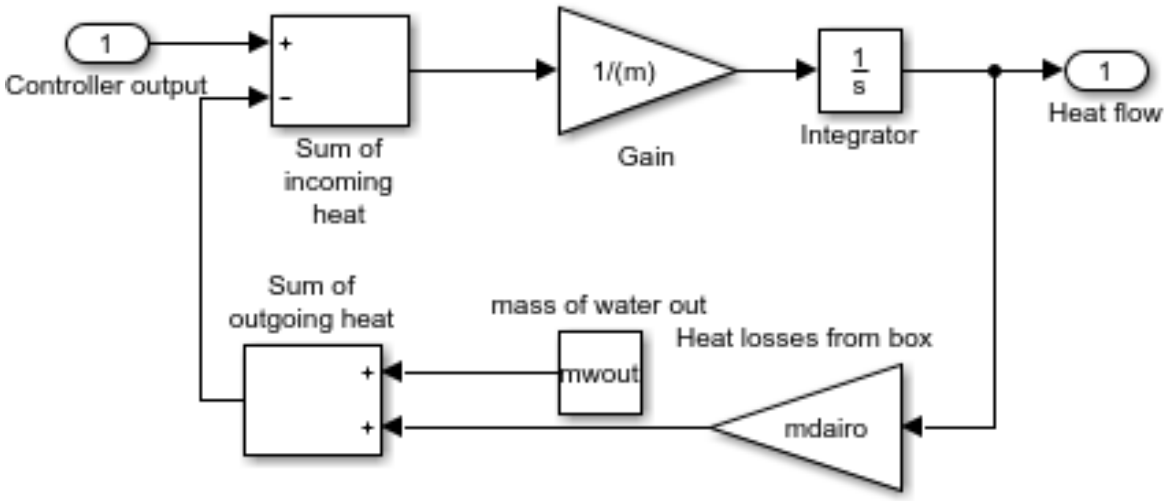

Figure 6.8 Inside subsytem M at outlet

6.4 MATLAB simulation parmeters

The values of parameters used for the MATLAB simulation of this task are obtained from different sources. The value of mdairi is obtained from the specification of fan [40]. The value of mwin is obtained from humidifier specification [43]. The value of A is calculated based on the dimensions of the box 2. The value of P is obtained heater specification [41]. The value of Twater, Tin and T_1 is assumed to be same as the setpoint while T2 is assumed to be same as the outside temperature. The remaining values are obtained from [7] [8] [10]. The simulation parameters used in MATLAB are as follows.

```
mdairi=0.0215;  %obtained from fan specification
cpa=1000;
Tout=25;
Tin=30;
mwin=0.000139;  %obtained from humidifier specification
cpw=4186;
Twater=30;
P=20;           %specification of heater 1
A=0.4166;       %calculated for the area of box2
k=0.03;         %thermal resistance for EPS
d=0.022;        %thickness of the insulator, box2
mdairo=0.0215;
mwout=0.000109;
hwater=2257000;
m=0.01;
cv=718;
```

6.5 Simulation results

The simulation for getting controlled temperature and humdity were initially checked without the use of PID controller. Then the system were subject to PID control and the indoor temperature and humidity inside the box were observed. The temperature and humidity were varied to see at what time the new value becomes close to the setpoint. The values of 30 ºC and 40 ºC are chosen for the setpoint of temperature and 50 % and 75 % for the relative humidity as an example to see the results.

To start with, the setpoint for temperature is initially set to 30 ºC. The outside temperature is supposed to be 25 ºC. The outside temperature is a sinusodial wave with 2 ºC change. PID control is not activated during this case and the results can be seen from the figure 6.9.

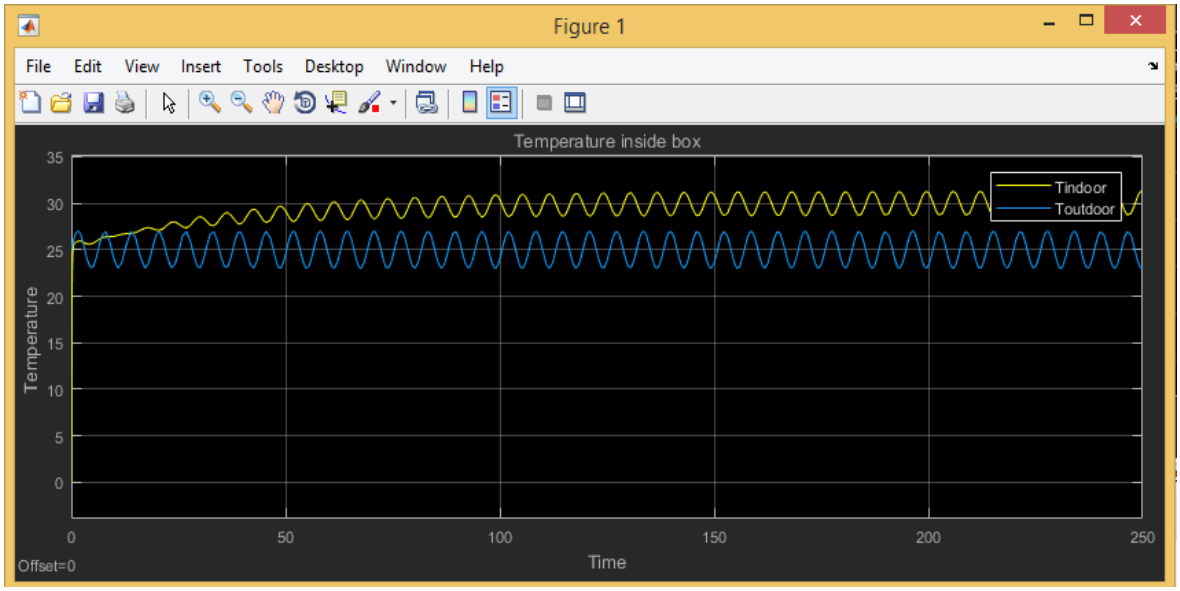

Figure 6.9 Indoor temperature and outdoor temperature without PID control

It is evident from the above result that the temperature reaches to the desired setpoint at around 60 to 70 s but is not able to be fixed around the desired temperature. The temperature fluctuates in the range of 1,5 ºC after this time with slight incement. This result indicate the the system produces around 5 % of error.

PID is introducted to the above system for outer fan, water heater and box heater. The values of PID can be seen in the table 6.1 which were obtained by tuning the PID control manually in the PID block for outer fan, water heater and box heater in the MATLAB software. The following values for the P, I and D parameters from figure 6.1 were selected from manual tuning because they produced minimum oscillations.

Table 6.1 Values of P, I and D for temperature control

	P	I	D
Outer fan	0,797	0,051	- 1,461
Water heater	0,856	0,121	- 1,671
Box heater	0,915	0,059	- 1,488

The setpoint for temperature is kept 30 ºC and the outdoor temperature is 25 ºC with results in the figure 6.10.

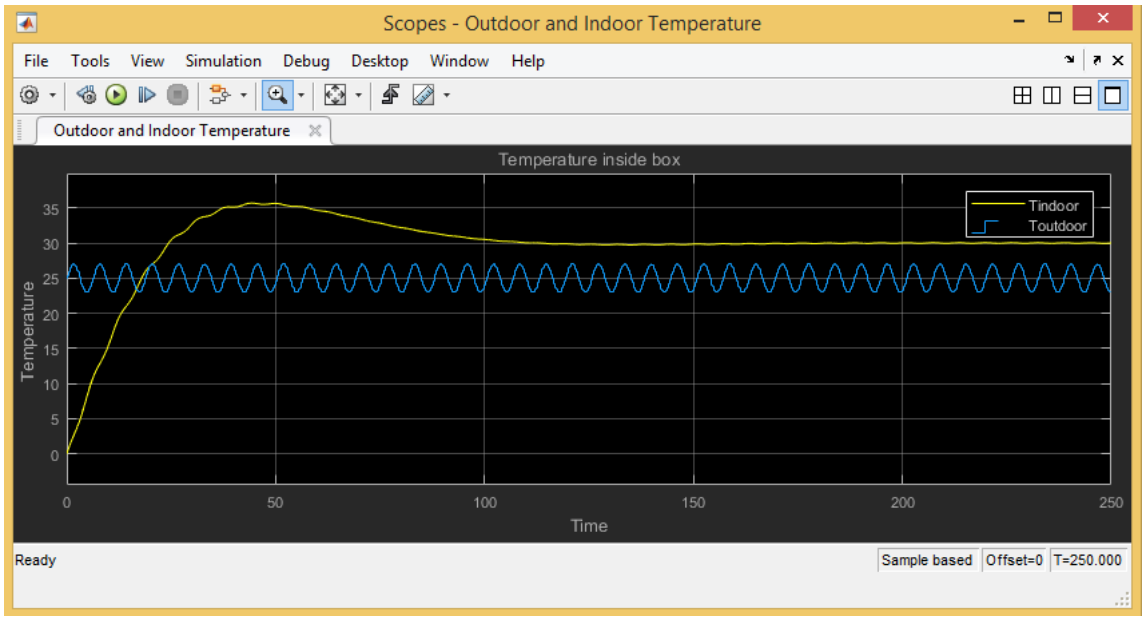

Figure 6.10 Indoor and outdoor temperature with PID control for 30 ºC setpoint

It is evident from the above result that the temperature reaches to the desired setpoint at around 105 s and remains around the desired temperature. The temperature fluctuates in the range of 0,05 ºC. This result indicate the the system produces around 0,17 % of error.

The setpoint for temperature is kept as 40 ºC and the outdoor temperature is 25 ºC. The values for P, I and D are same as mentioned in the table 6.1.

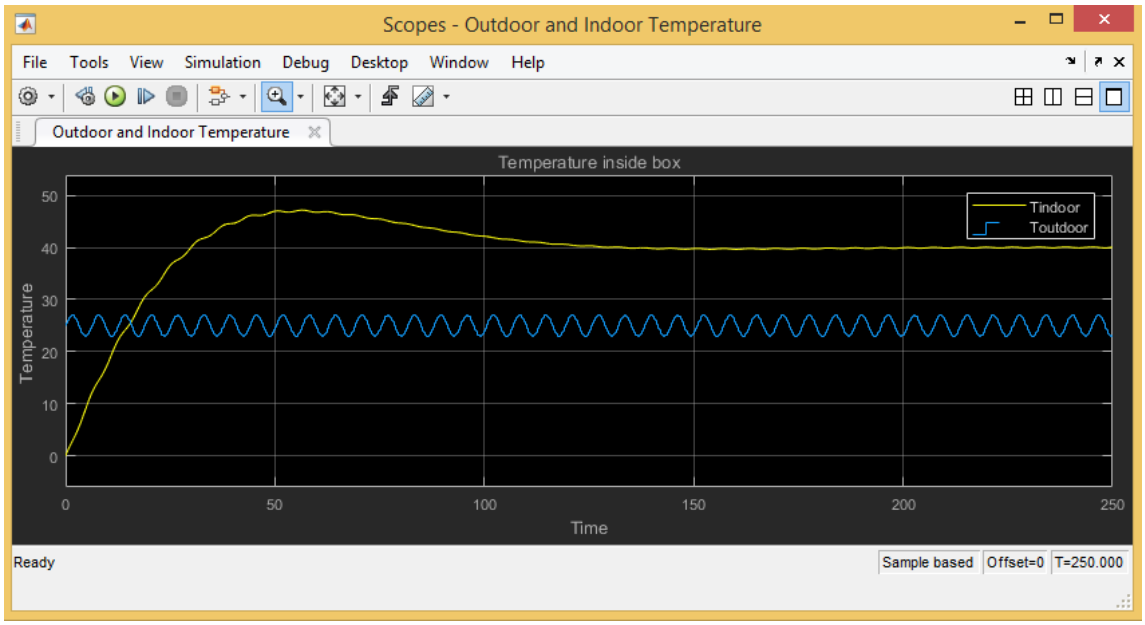

Figure 6.11 Indoor and outdoor temperature with PID control for 40 ºC setpoint

It is evident from the above result that the temperature reaches to the desired setpoint at around 125 s and remains around the desired temperature. The temperature fluctuates in the range of 0,06 ºC This result indicate the the system produces around 0,15 % of error.

To start with, the setpoint for humidity is initially set to 50 %. The outside humidity is supposed as 25 %. In the simulink section these values were expressed in kg $_{water}$/ kg $_{dry\ air}$ which is 0,0065 kg $_{water}$/ kg $_{dry\ air}$ for the 25 % relative humidity and 0,0133 kg $_{water}$/ kg $_{dry\ air}$ for 50 % at 30 ºC. The outside humidity is a sinusodial wave with ± 7 % change to the setpoint. PID control is not activated during this case and the results can be seen in the figure 6.12.

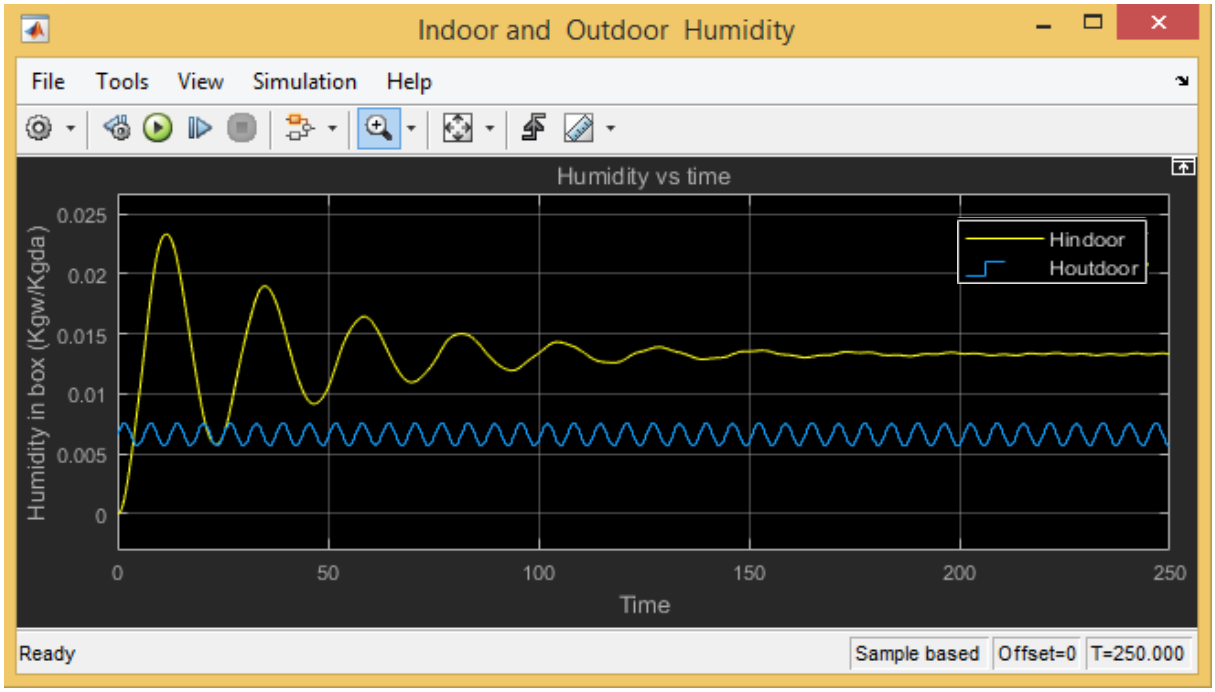

Figure 6.12 Indoor humidity and outdoor humidity without PID control

It is evident from the above result that the humidity reaches to the desired setpoint at around 170 s but has too large oscillations. The fluctuation remains for 170 s and remains around the setpoint. This later result indicate the the system produces around 3 % of error.

PID is introducted to the above system for humidifier. The values of P is 2,431, I is 0,181 and D is - 0,1655. The setpoint and the outdoor humidity remains same. The results can be seen in the figure 6.13.

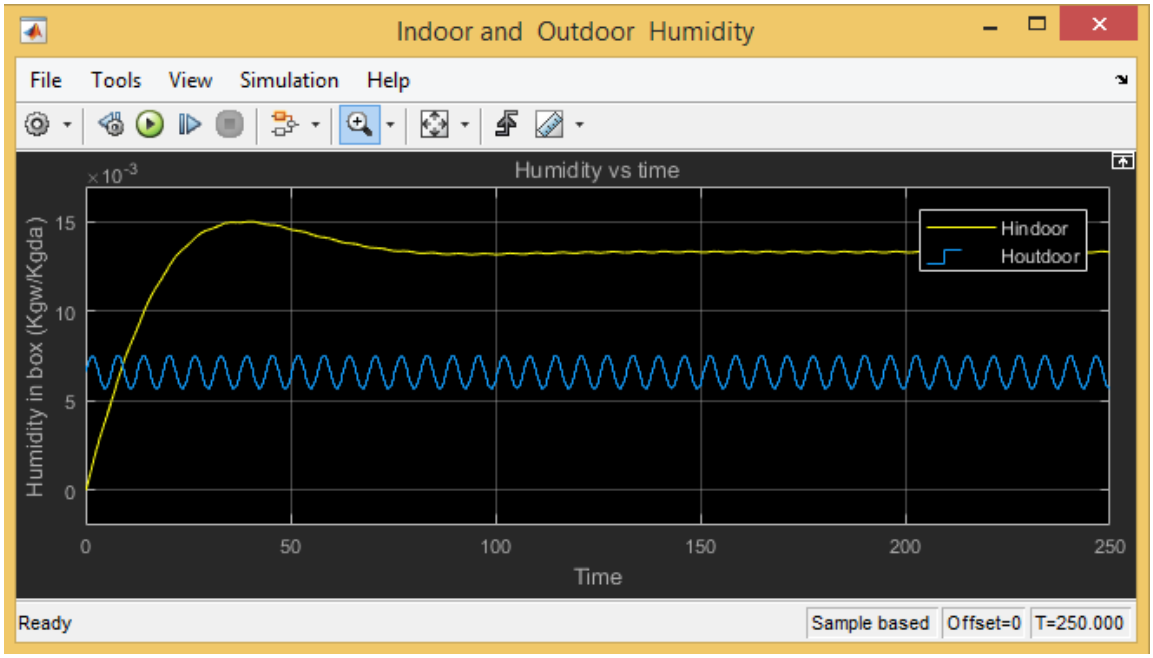

Figure 6.13 Indoor humidity and outdoor humidity with PID control for 50 % setpoint

It is evident from the above result that the humidity reaches to the desired setpoint at around 80 s but has no oscillations. The humidity increases more than the setpoint at the begining and remains around the setpoint later. This later result indicate the the system produces around 2 % of error.

The setpoint for humidity is kept as 75 % and the outdoor humidity is 25 %. The values for P, I and D are same as mentioned in the previous case of humidity.

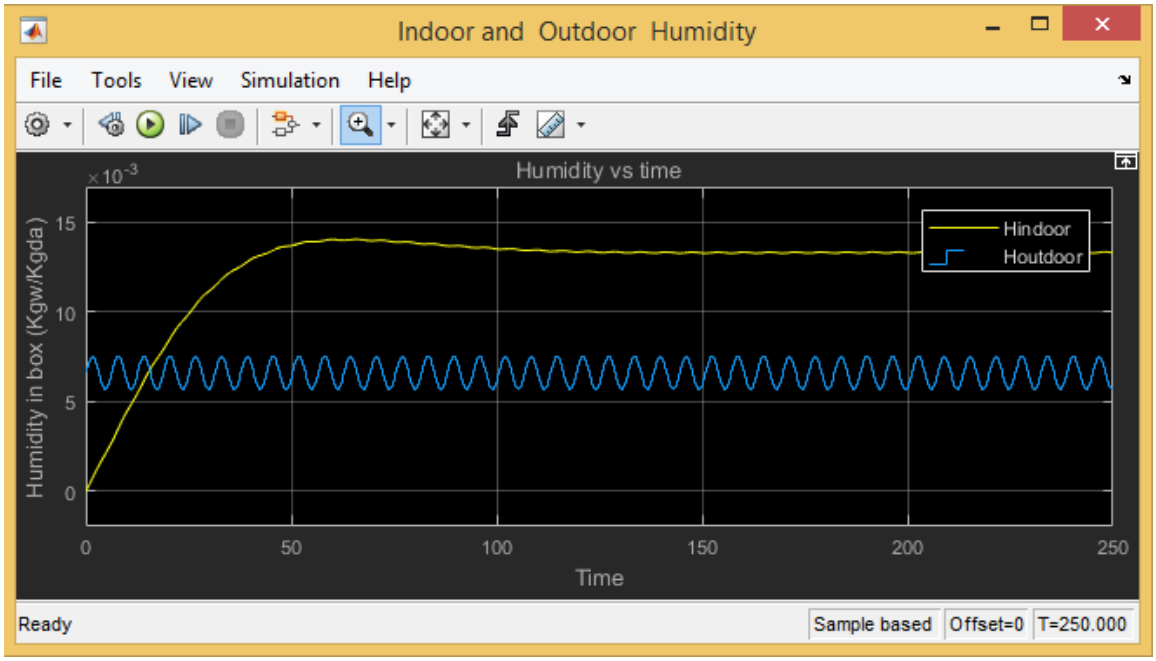

Figure 6.14 Indoor humidity and outdoor humidity with PID control for 75 % setpoint

It is evident from the above result that the humidity reaches to the desired setpoint at around 105 s but has no oscillations. The humidity increases more than the setpoint at the begining and remains around the setpoint later. This increase is slighly less than the previous case. This later result indicate the the system produces around 1,9 % of error.

6.6 Conclusion

It was observed that the system produced better results when PID control was introduced to the system. There were oscillations of higher amplitude when PID control was disable for the simulation. When PID was introduced to the system it yeilded better results with less oscillation. The PID enabled system produced better results with more stable temperature and humidity. It also fulfilled the requirements mentioned in chapter 2.6.

The values for various parameters for the modeling of the overall system were chosen based on the selected device's specificaiton. These selected values were used for the simulation. The results from the simulation indicated that the error produced are lower enough than the one mentioned in the requirements in chapter 2.6. Thus, it can be concluded that the selected components are suitable for this getting controlled temperature and humidity.

7 SUMMARY

7.1 Conclusion

Hipot testing is used in measuring the insulation and leakage current of the electrical and electronic device. The results of this test are likely to be affected by temperature and humidity which might lead to testing failures. Currently, there are no products available in the market which consists of Hipot tester calibration device along with temperature and humidity control. Therefore, the main objective of this thesis was the development of the golden sample for the Hipot tester with stabilized temperature and humidity for ABB drives and renewables factory in Juri, Estonia. Also, the created device could be useable universally in different Hipot tester, producing results with negligible deviations that are not affected by humidity or temperature.

The objective of selecting the golden sample, which has minimum self-heating (less than 5 ^{o}C), minimal loss of resistance (less than 1 % from TCR and VCR) from leakage current test and insulation resistance test was achieved with high accuracy. The golden sample tested at real test voltages showed significant results and the resistor MOX97021004FVE (resistance of 1 MΩ) was used as the golden sample for this project. It was selected because the results from short test and long term test showed it could be used for more than 3500 times for Hipot testing and the deviation in insulation resistance and leakage current after this amount of test was around 0,3 %.

The golden sample is to be maintained at fixed temperature and humidity, so modeling for obtaining the desired temperature and humidity was done. Various components were selected based on the model for designing the real system. Furthermore, CAD design was made for the insulating box and explaining the methods of placing components. The selected components and the mathematical model were further verified by developing simulations on MATLAB software. The results from the simulation showed that the selected components fulfill the requirements mentioned by ABB. The results after introducing PID control to the system showed that it is capable of stabilizing temperature and humidity in less than two and half minutes.

In short, the proposed system is robust and accurate for fulfilling the primary objective of obtaining the golden sample and maintaining it at fixed temperature and humidity for the development of golden sample for Hipot testers.

7.2 Recommendation and Future Work

The test results from the selected golden sample showed higher accuracy and fulfilled the requirements mentioned by ABB. However, the current tolerance for the golden sample is ± 1 % but resistors having up to ± 0,01 % of tolerance can give higher accuracy than the current one. Thus, it is recommended to test resistor of lower tolerance to see if it can be used as a better golden sample.

The current golden sample has a resistance of 1 MΩ, which itself is placed in lower end of measurement range of the measuring equipment used in ABB. Lowering the resistance value down 10 times gives more measurement precision, from 2,7 mA to 27 mA range at 2,7 kV supply voltage, but it needs to be balanced out by correct power rating of the component, which is 10 times more than the previous one.

The results of the simulation for obtaining desired temperature and humidity showed that the results are accurate and fulfill the requirements specified by ABB. The real prototype is currently under development. The comparative study of the results from the real design and simulation can help in determining the real accuracy of the device.

Currently, tuning is done manually for the PID control. However, use of auto-tune can be an optimal solution for the PID control. One of the optimal auto-tune methods like Ziegler-Nicholas method can be used and the results of manual tune and auto-tune of PID can be an exciting area for comparison of the results.

KOKKUVÕTE

Järeldus

Kõrgepinge testimine aitab mõõta isolatsiooni ning lekkevoolu elektri või elektroonikaseadmes. Testimise tulemused on suure tõenäosusega mõjutatud temperatuurist ja niiskusest, mis võib viia testi läbikukkumiseni. Hetkel ei ole müügil sellist toodet, mis seob omas kõrgepinge testri kalibreerimise seadet ja niiskuse ja temperatuuri kontrolli. Seepärast selle lõputöö primaarne eesmärk oli arendada etalon näidis stabiliseeritud niiskuse ja temperatuuri juhtimisega ABB ajamite ja taastuvenergia tehase jaoks, Jüris, Eestis. Lisaks võib seadet kasutada universaalelt erinevate kõrgepinge testrite juures, luues võrreldavaid testitulemusi tühise variatsiooniga ning seejuures ei ole mõjutatud niiskusest ega temperatuurist.

Eesmärgiks oli valida etalon näidis,mis valiti edukalt ning suure täpsusega ning täidab järgmisi spetsifikatsiooni eesmärke: minimaalne iseeneslik soojenemine (vähem kui 5 ^{o}C), minimaalne takistuse(vähem kui 1%TCR-i ja VCR-i mõjutusele) vähenemine lekke voolu testist. Etalon näidise testimine reaalsete pingete lõppes edukalt ja projekti näidiseks valiti takisti MOX97021004FVE (takistusega 1 MΩ). See takisti valiti, kuna seda saab kasutada rohkem kui 3500 testikorda ja variatsioon isolatsiooni takistuse ja lekkevoolus peale 3500 testimist oli umbes 0,3%.

Etalon näidist peab hoidma fikseeritud temperatuuril ja niiskusel, leidmaks parameetrid, mudeldati süsteem. Mudelile toetudes valiti reaalsesse süsteemi komponendid. Lisaks tehti CAD isoleeriva karbi jaoks ning seletati komponentide paigutus ja metoodika. Komponentide selektsioon ja matemaatiline mudel verifitseeriti MATLAB simulatsiooni tarkvara kasutades. Simulatsiooni tulemused näitasid, et valitud komponendid täidavad ABB spetsiifitseeritud nõudeid. Rakendades PID juhtimise meetodit näitasid tulemused, et süsteem stabiliseerib niiskuse ja temperatuuri vähem kui kahe ja poole minutiga.

Lühidalt, süsteem on robustne ja täpne täitmaks talle seatud primaarseid eesmärke, leida etalon näidis ja hoida seda fikseeritud niiskuse ja temperatuuri tasemel, milleks on stabiliseeritud etalon näidise arendus kõrgepinge testrite tarvis.

Soovitused ja edasine töö

Valitud etalon näidise testitulemused näitasid kõrget mõõtetäpsust ja täitsid ABB poolt ette pandud spetsifikatsiooni. Praeguse takisti tolerants on ± 1 %, kuid tolerantsiga ± 0,1 % oleks võimalik saavutada kõrgem täpsus. Tulevikus soovitatakse kasutada kõrgema toleratsiga takistit, mis oleks parem etalon näidisena.

Valitud etalon on 1MΩ takistusega, mis iseenesest on madalamas mõõteotsas, ABB mõõtemasinaid kasutades. Alandades takistus 10 korda, suurendaksime mõõteampluaa kasutust ja parendaksime mõõteresolutsiooni, Mõõdis suureneks 2,7 mA-lt 27 mA-le 2,7 kV toitepinge juures, aga see tähendab, et takisti võimsus näitajad on vaja hoolikalt valida, mis praegusel juhul tähendaks 10 kordset võimsuse tõusu võrreldes eelneva takistiga.

Simulatsiooni tulemused niiskuse ja temperatuuri saavutamisel näitasid, et tulemused on täpsed ja täidavad ABB poolt sätestatud eesmärke. Päris prototüüp on hetkel arendamisel. Võrdlus analüüs simuleeritud ja real süsteemi vahel aitaks tulevikus paremini ennustada süsteemi täpsust.

Hetkel teostatakse PID süsteemi peenhäälestamine manuaalselt. Automaat häälestamine võiks olla optimaalne lahendus PID juhtimise korral. Üheks optimaalseks automaathäälestuse meetodiks, mida kasutada, võib olla Ziegler-Nicholas meetod ja selle tulemusi võrrelda käsitsi ja automaatselt peenhäälestatud süsteemide puhul on huvitav võimalik tuleviku arendus suund.

REFERENCES

[1] J. M. Bruner, "Hazards of Electrical Apparatus," *Anesthesiology ,* vol. 28, pp. 396-425, March-April 1967.

[2] IEEE, "MEDICAL ELECTRICAL SAFETY TESTING UNDER ATTACK IN THE U.S.A.," IEEE Product Safety Engineering Newsletter, U.S.A., 2010, June.

[3] J. A. DeDad, "The Basics of Insulation Resistance testing," EC&M, 2000 August 01. [Online]. Available: http://www.ecmweb.com/ops-amp-maintenance/basics-insulation-resistance-testing. [Accessed 25 4 2018].

[4] Jiguparmar, "What is HIPOT Testing," Electrical Engineering Portal, 22 12 2011. [Online]. Available: http://electrical-engineering-portal.com/what-is-hipot-testing-dielectric-strength-test. [Accessed 25 4 2018].

[5] SEFELEC, "HIPOT TESTER," SEFELEC, [Online]. Available: https://www.sefelec.com/en/HIPOT-TESTER.php. [Accessed 25 4 2018].

[6] CIRRIS, "How Humidity Can Affect Testing," Cirris Systems, [Online]. Available: https://www.cirris.com/learning-center/general-testing/diagnosing-failures/218-how-humidity-can-affect-testing. [Accessed 25 4 2018].

[7] T.-M. L. C.-C. C. Jing-Nang Lee, "Modeling Validation and control Analysis for controlled Temperature and Humidity of Air conditioning system," *The scientific World Journal,* vol. 2014, 2014 August 07.

[8] M. A.Saleh, "Analysis of Control Strategies and simulation of Heating systems using simulink/MATLAB model," *Journal of Thermal Engineering,* vol. 2, no. 5, pp. 921-927, October 2016.

[9] MathWorks, "MATLAB overview," MathWorks, [Online]. Available: https://www.mathworks.com/products/matlab.html. [Accessed 12 4 2018].

[10] M. M. M. A.-R. Bourhan Tashtoush, "Dynamic model of HVAC system for control analysis," *Science Direct,* vol. Energy 30, no. 2005, pp. 1729-1745, 2004.

[11] T. Electronics, "5069- Insulation Tester Calibrator," [Online]. Available: https://www.timeelectronics.com/assets/upload/download_centre/documents/5069-datasheet.pdf. [Accessed 30 4 2018].

[12] CalCard, "NICEIC CalCard Calibration Checkbox," Tester, [Online]. Available: https://www.tester.co.uk/niceic-calcard-calibration-checkbox. [Accessed 30 4 2018].

[13] Megger, "Megger CB101 5KV Calibration Box Datasheet," [Online]. Available: https://content.megger.com/getattachment/94f4eabe-5aec-4b25-847e-175adbd5149b/CB101_DS_en_V02.pdf?_ga=2.251784586.248734065.1527083149-1649709431.1527083149. [Accessed 30 4 2018].

[14] N. B. N. J.G. ZIEGLER, "Optimum Settings for Automatic Controllers," *Transactions of the A.S.M.E,* vol. 64, pp. 759-765, 1942.

[15] E. Standards, "CSN EN 50178 (Electronic equipment for use in power installations)," 1997. [Online]. Available: https://www.en-standard.eu/csn-en-50178-electronic-equipment-for-use-in-power-installations/. [Accessed 7 5 2018].

[16] Ohmite, "Super MOX Resistor," [Online]. Available: http://www.farnell.com/datasheets/1928573.pdf?_ga=2.139261745.303018963.1521115718-311758823.1518785987&_gac=1.208792102.1520257850.EAIaIQobChMIy4ba4KnV2QIVAZ4bCh3ejAsqEAAYASAAEgIDw_D_BwE. [Accessed 18 3 2018].

[17] R. guide, "Thin and thick film resistor," Resistor guide, [Online]. Available: http://www.resistorguide.com/thin-and-thick-film/. [Accessed 3 5 2018].

[18] M. Adams, "Aluminum Oxide properties," Accuratus, 2013. [Online]. Available: http://accuratus.com/alumox.html. [Accessed 4 5 2018].

[19] "Technical data Aluminum Oxide," Kyocera, [Online]. Available: https://global.kyocera.com/prdct/fc/list/material/alumina/alumina.html. [Accessed 4 5 2018].

[20] G. I. a. M. M. cASALE, "Ruthenium oxide Glaze Resistors," *Platinum Metals Review,* vol. 11, no. 4, pp. 126-129, 1967.

[21] C. Wells, "How to calculate the effects of resistor self-heating," Texas Instruments, 3 May 2014. [Online]. Available: https://e2e.ti.com/blogs_/archives/b/precisionhub/archive/2014/03/14/how-to-calculate-the-effects-of-resistor-self-heating. [Accessed 12 3 2018].

[22] Ohmite, "Ohmite Slim-Mox Series," Ohmite, [Online]. Available: http://www.ohmite.com/assets/docs/res_slimmox.pdf. [Accessed 12 3 2018].

[23] S. Electric, "Determination of the overtemperature in appliance subject to cyclic overcurrents," Schneider Electric, Bergamo, Italy.

[24] B. T. I. Welwyn, "Medical Application note Resistors," 3 2017. [Online]. Available: http://www.ttelectronics.com/themes/ttelectronics/datasheets/resistors/literature/Medical.pdf. [Accessed 9 5 2018].

[25] J. S. Dr. Felix Zandman, "Non-Linearity of Resistance/Temperature Characteristic: Its Influence on Performance of Precision Resistors," Vishay Precision Group, 2013.

[26] G. H. MILLARD, "MEASUREMENTS OF NON-LINEARITY IN CRACKED-CARBON RESISTORS," *The Institution of Electrical Engineers,* pp. 31-34, 1959.

[27] R. P. Fynman, "Conservation of Energy," California Institute of Technology, 2013. [Online]. Available: http://www.feynmanlectures.caltech.edu/I_04.html. [Accessed 7 5 2018].

[28] M. A. B. Deakin, "The development of the Laplace transform," in *Archive for History of Exact Sciences*, Springer, 1981, pp. 343-390.

[29] FLIR, "FLIR T440 Thermal Imaging Camera," [Online]. Available: https://www.flir-direct.com/product/flir-t440-infrared-camera. [Accessed 21 3 2018].

[30] FLIR, "FLIR E40 Thermal Imaging Camera," [Online]. Available: https://www.flir-direct.com/product/flir-e40-infrared-camera. [Accessed 9 3 2018].

[31] "Kikusui T5050A Operation manual," [Online]. Available: http://www.kikusui.co.jp/kiku_manuals/T/TOS5000A_E91.pdf. [Accessed 21 3 2018].

[32] C. ARNOUX, "C.A 6547 technical specifications," [Online]. Available: https://eshop.micronix.cz/data/cz/att/002/7108-4380.pdf. [Accessed 21 03 2018].

[33] R. B. Northrop, Introduction to Instrumentation and Measurements, New York: Taylor and Francis, 2005.

[34] T. H. C. L. CRAIG, "INTERPRETATION OF INSULATION RESISTANCE MEASUREMENTS," *Electrical Insulation Conference Materials and Application,* no. 1962 EI, pp. 127-132, Feb. 1962.

[35] H. H. Skilling, Electric Transmission Lines, McGraw-Hill, 1951.

[36] "Detailed information for: PM564," ABB, [Online]. Available: http://new.abb.com/products/1SAP120900R0071/pm564-tp-ethac500-prog-logic-controller-128kb-6di-6do-t-2ai-1ao-24vdc-1xrs485. [Accessed 12 3 2018].

[37] "Detailed information for: DA501," ABB, [Online]. Available: http://new.abb.com/products/1SAP250700R0001/da501s500-digital-analog-input-output-module16di-4ai-2ao-8dc-24vdc-di24vdcdo. [Accessed 12 3 2018].

[38] ABB, "Detailed information for: CP607," ABB, [Online]. Available: http://new.abb.com/products/1SAP507100R0001/cp607cp600-eco-control-panel-tft-grafic-display-touchscreen-7-800x480-pixe. [Accessed 16 3 2018].

[39] T. H. o. Hydro, "1 Disc mist maker," The House of Hydro, [Online]. Available: https://thehouseofhydro.com/store/p98/%28230v%29_1_Disc_Mist_Maker.html. [Accessed 14 3 2018].

[40] Farnell, "614NGH - Axial Fan," Farnell, [Online]. Available: http://ee.farnell.com/ebm-papst/614ngh/fan-60mm-24vdc/dp/9600353?ost=614NGH&scope=partnumberlookahead&exaMfpn=true&searchref=searchlookahead&ddkey=http%3Aet-EE%2FElement14_Estonia%2Fw%2Fsearch. [Accessed 14 3 2018].

[41] Farnell, "PTC touch safe heater," Farnell, [Online]. Available: http://ee.farnell.com/stego/06030-0-00/heater-120-240v-ac-dc-20w-t-safe/dp/1870823?MER=bn_level5_5NP_EngagementRecSingleItem_1. [Accessed 17 3 2018].

[42] Farnell, "LC-R127R2PG - Rechargeable Battery," Farnell, [Online]. Available: http://ee.farnell.com/panasonic-electronic-components/lc-r127r2pg/battery-vrla-12v-7-2ah-187-faston/dp/1769779?st=12%20V%20battery. [Accessed 15 3 2018].

[43] Farnell, "T9602-3-D-1 -HUMIDITY/TEMP SENSOR," Farnell, [Online]. Available: http://ee.farnell.com/amphenol-advanced-sensors/t9602-3-d-1/humidity-temp-sensor-0-100-rh/dp/2506110?ost=T9602-3-D-1&scope=partnumberlookahead&exaMfpn=true&searchref=searchlookahead&ddkey=http%3Aet-EE%2FElement14_Estonia%2Fw%2Fsearch. [Accessed 16 3 2018].

[44] Farnell, "PJ14126RTW - ENCLOSURE, JUNCTION BOX," Farnell, [Online]. Available: http://ee.farnell.com/hammond/pj14126rtw/enclosure-junction-box-pet-grey/dp/2786246. [Accessed 16 3 2018].

[45] Farnell, "Panel heater HP05-1/10-24," Farnell, [Online]. Available: http://ee.farnell.com/dbk/hp05-1-10-24/heater-ptc-f-plate-50w/dp/4408391?st=PTC%20heater. [Accessed 15 3 2018].

[46] Sparkfun, "Aqua Valves," Aqua Tech Trading Corp. Ltd, [Online]. Available: https://www.sparkfun.com/datasheets/Robotics/Aqua%20Tech%20Solenoid%20Valves.pdf. [Accessed 16 3 2018].

[47] R. E. Bellman, Adaptive Control Processes: A Guided Tour, Princeton University Press, December 8, 2015.

[48] E. Optics, "Fundamental parameters of an Imaging System," [Online]. Available: https://www.edmundoptics.eu/resources/application-notes/imaging/6-fundamental-parameters-of-an-imaging-system/. [Accessed 20 03 2018].

[49] Codesys, "Codesys," [Online]. Available: https://www.codesys.com/the-system.html. [Accessed 20 3 2018].

[50] ABB, "Automation Builder software," ABB, [Online]. Available: http://new.abb.com/plc/automationbuilder/platform/software. [Accessed 23 3 2018].

[51] ABB, "CP600 - Software," ABB, [Online]. Available: http://new.abb.com/plc/control-panels/cp600/software. [Accessed 24 3 2018].

APPENDIX A

A.1 Specifications for C.A 6547

The specifications for the device C.A 6547 is in table A. 1 [32].

Table A. 1 Specifications for C.A. 6547 [32]

Insulation	Pre-set test voltage: 500 / 1000 / 2500 / 5000 Adjustable test voltage: 40 V to 5100 V by increments of 10 or 100 V Range: 10 kΩ to 10 TΩ
Voltage	from 1 to 5100 V (15 Hz to 500 Hz or DC)
Capacitance	0,005 to 49,99 µF
Leakage current	0,000 nA to 3000 µA
Accuracy for resistance measurement	± (5 %)
Accuracy for current measurement	± (10 %)

Figure A. 1 CA6547 [32]

A.2 Specifications for Kikusui TOS5050a

The specifications for the device Kikusui TOS5050a is in table A. 2 [31].

Table A. 2 Specifications for Kikusui TOS5050a [31]

Output rating	500 VA/ 5 kV, 100 mA (with nominal line voltage)
Analog Voltmeters	5 kV AC, ± 5 % accuracy
Digital Voltmeters	2,5 kV/ 5kV, ± 1,5 % accuracy
Digital ammeter	± (5 % + 20 µA) of upper cutoff current
Timer	Range: 0,5 to 999 s

Figure A. 2 Kikusui TOS5050a [31]

A.3 Specification for FLIR T440

The specifications for the device FLIR T440 is in table A.3 [29].

Table A. 3 Specifications for FLIR T440 [30]

IR resolution (array size)	320 x 240
Thermal sensitivity	< 0,045°C
Field of view	25° H x 19° V
Temperature range	-20 to 1200°C (- 4 to 2192 °F)
Accuracy	± (2 % ± 2 °C)
Focal length	17 mm

Figure A. 3 FLIR T440 [29]

A.4 Specification for FLIR E40

The specifications for the device FLIR E40 is in table A. 4 [30].

Table A. 4 Specification for FLIR E40 [30]

IR resolution (array size)	19,200 (160 x 120)
Thermal sensitivity	< 0,07 °C
Field of view	25 °H x 19 °V
Temperature range	-20 to 650 °C
Accuracy	± (2 % ± 2 °C)
Focal length	17 mm

Figure A. 4 FLIR E40 [30]

APPENDIX B

B.1 Theory for image setup

The temperature of the resistor has to be monitored continuously over time and it is subject to higher voltage (2,7 kV AC and 1000 DC). For safety, it is must to have a measurement device which monitors the temperature wirelessly and precisely because if a sensor is kept in contact to the resistor it might lead to short circuit or might damage the sensor and if it the sensor is not kept in contact then it might not give proper readings so, IR camera were used to get precise and accurate measurements taking safety into consideration.

Use of proper IR camera, lens, lighting conditions and other optical instruments are critical steps in image application. Making necessary setup in the imaging environment even plays a vital role in the data acquisition. There could be lot of saving of time in case the system has been setup properly so it requires less time during processing time at the run time. Fundamental parameters of an imaging system are the crucial factors that must be taken into consideration before selecting the camera and lens. Five fundamental parameters comprise an imaging system: resolution, field of view, working distance, sensor size and depth of field [48].

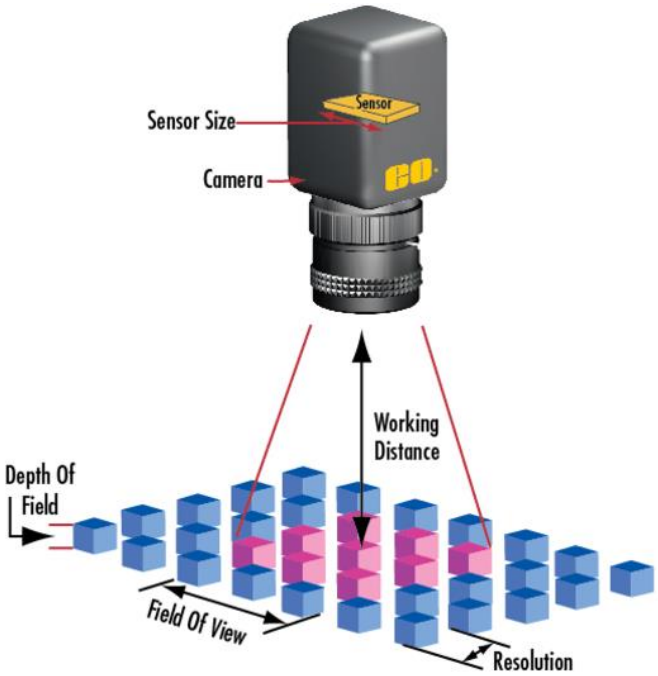

Figure B. 1 Description of fundamental parameters for image setup [48]

- Resolution: the smallest feature size on your object that the imaging system can distinguish
- Field of view (FOV): the area of inspection that the camera can acquire
- Working distance (WD): the distance from the front of the camera lens to the object under inspection
- Sensor size: the size of a sensor's active area
- Depth of field: the maximum object depth that remains in focus

B.2 Image setup for SM102031005FE

The calculation of fundamental parameters for image setup are as follows.

- **Object Resolution:** The object resolution in our case is size of the resistor we want to detect. The dimensions we want to measure is about 14,7 mm x 2,5 mm.
- **Field of view and focal length:** The object resolution in our case is of dimensions 14,7 mm x 2,5 mm. We could consider the field of view to be 200 x 150 mm for this case. Since the measured object is not small so we could consider the focal length of around 17 mm.
- **Sensor resolution:** If we consider the Field of View as 200 x 150 mm then the sensor resolution is given by

  Horizontal Sensor resolution = (FOV/resolution) x 2

  = 400/14,7
  = 27,16 pixels per side
  Vertical Sensor resolution = (FOV/resolution) x 2
  = 300/2,5
  = 118,11 pixels per side

- **Working distance and expected resolution:** Let us consider standard sensor that has more than 27,16 x 118,11 pixel per side be of 160x120, with its ½ inch sensor dimensions: 6,4 mm x 4,8 mm. The expected working distance will be

  Focal length = sensor size x working distance / FOV
  Working distance = Focal Length* field of view/ sensor size

  = (17*200)/6,4

  = 531,3 mm

  And the expected resolution given actual 160 per side will be 2*200 / 160
  = 2,5 mm.

  And the expected resolution given actual 120 per side will be 2*150 / 120
  = 2,5 mm.

The cameras E40 and T440 were selected for the project having focal length of 17 mm for both. They have focal lengths, sensor resolution which is suitable for current application. It was observed that the camera could regularly monitor the temperature of the resistor even if kept on normal position so no special arrangements were made for the placement of camera.

The geometry of the imaging setup could be seen in the figure B. 2.

Figure B. 2 Image for DC testing using E40

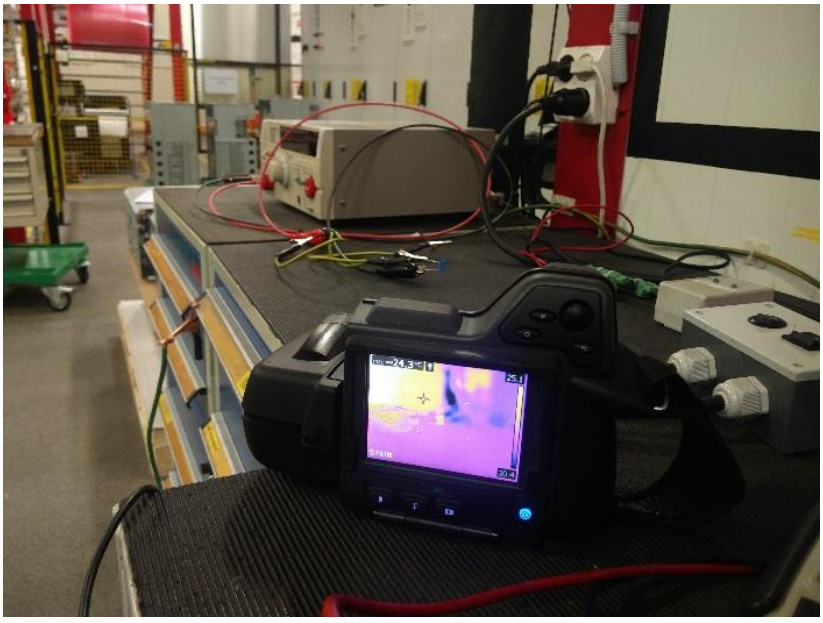

Figure B. 3 Image for AC testing using T440

The thermal IR camera selected for current application has automatic hot spot detection algorithm which detects the hottest spot inside the screen and this algorithm was used to detect the temperature of the resistor. Some of the examples of the image for detection of the temperature could be seen from figure B. 4.

Figure B. 4 Resistor SM102031005FE initially when starting to heat

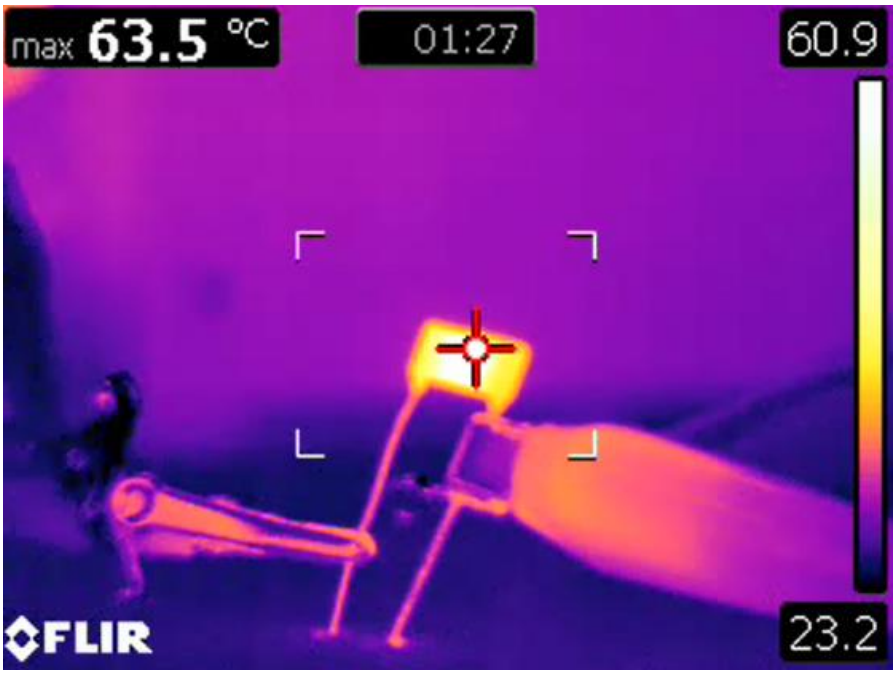

Figure B. 5 Resistor SM102031005FE while heating

B.3 Image setup for MOX97021004FVE

The calculation of fundamental parameters for image setup are as follows.

- **Object Resolution:** The object resolution in our case is size of the resistor we want to detect. The dimensions we want to measure is about 153,7 mm x 8,2 mm.
- **Field of view and focal length:** The object resolution in our case is of dimensions 153,7 mm x 8,2 mm. We could consider the field of view to be 200 x 150 mm for this case. Since the measured object is not small so we could consider the focal length of around 17 mm.
- **Sensor resolution:** If we consider the Field of View as 200 x 150 mm then the sensor resolution is given by

  Horizontal Sensor resolution = (FOV/resolution) x 2
  = 400/153,7

  = 2,6 pixels per side

  Vertical Sensor resolution

  = (FOV/resolution) x 2

  = 300/8,2

  = 36,58 pixels per side

- **Working distance and expected resolution:** Let us consider standard sensor that has more than 2,6 x 36,58 pixels per side be of 160 x 120, with its ½ inch sensor dimensions: 6,4 mm x 4,8 mm. The expected working distance will be

  Working distance = Focal Length* field of view/ sensor size

  = (17*200)/6,4

  = 531,3 mm

  And the expected resolution given actual 160 per side will be 2*200 / 160
  = 2,5 mm.

  And the expected resolution given actual 120 per side will be 2*150 / 120
  = 2,5 mm.

The cameras E40 and T440 were selected for the project having focal length of 17 mm for both. They have focal lengths, sensor resolution which is suitable for our application. It was observed that the camera could regularly monitor the temperature of the resistor even if kept on normal position so no special arrangements were made for the placement of camera.

The geometry of the imaging setup could be seen in the figure B. 6.

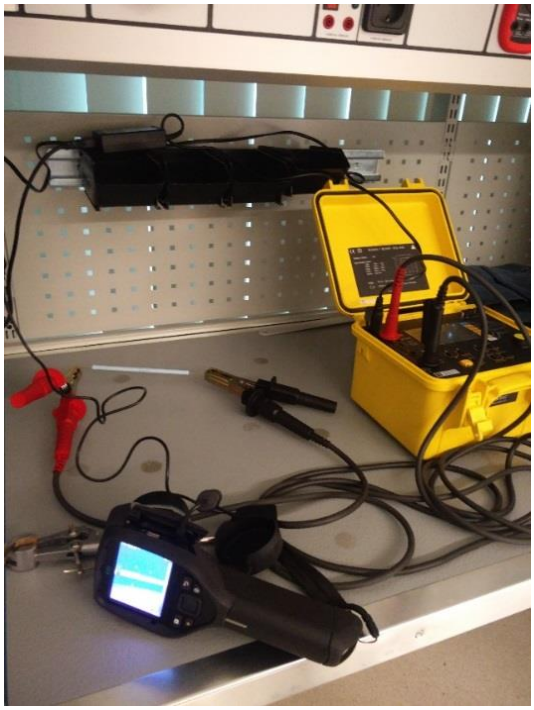

Figure B. 6 Image for DC testing using E40

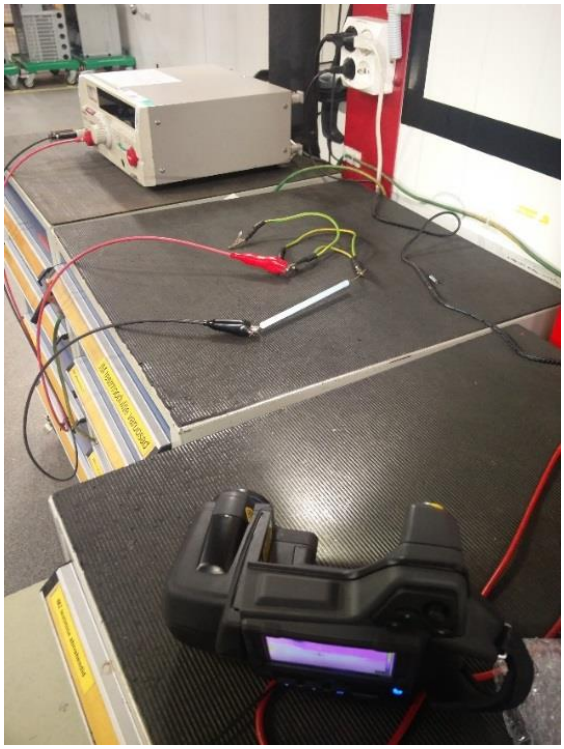

Figure B. 7 Image for AC testing using T440

The thermal IR camera selected for current application has automatic hot spot detection algorithm which detects the hottest spot inside the screen and this algorithm was used to detect the temperature of the resistor. Some of the examples of the image for detection of the temperature could be seen from figure B. 8.

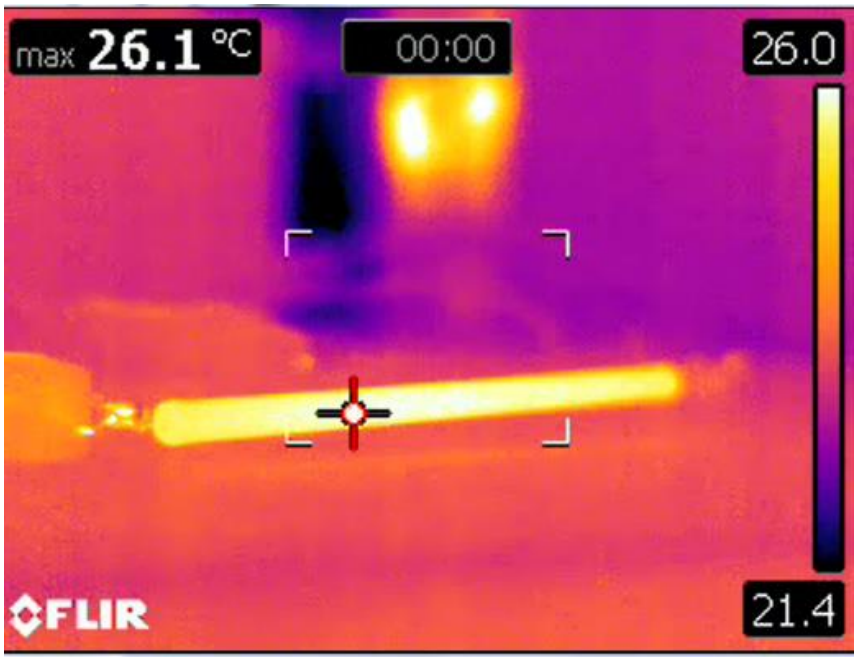

Figure B. 8 Resistor MOX97021004FVE initially when starting to heat

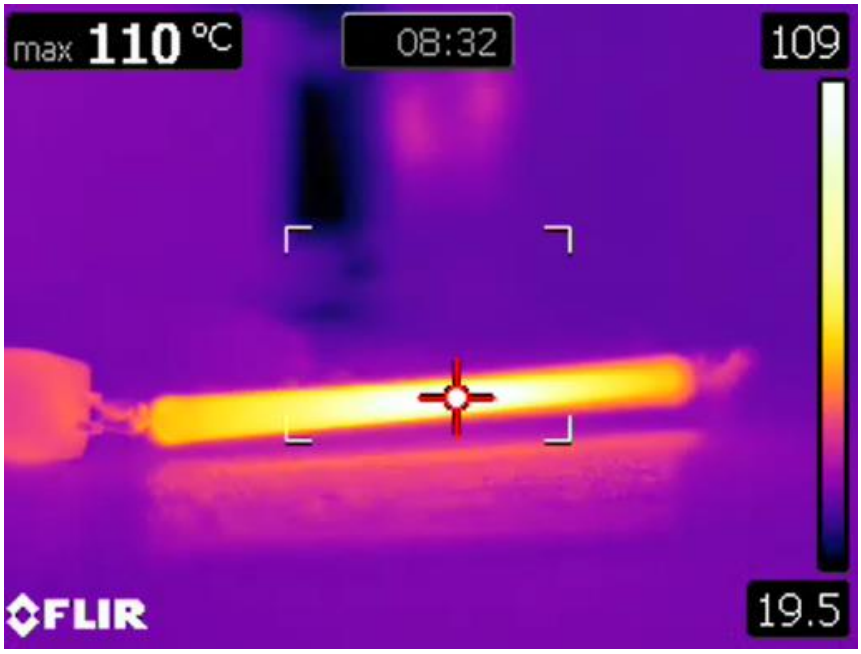

Figure B. 9 Resistor MOX97021004FVE while heating

APPENDIX C

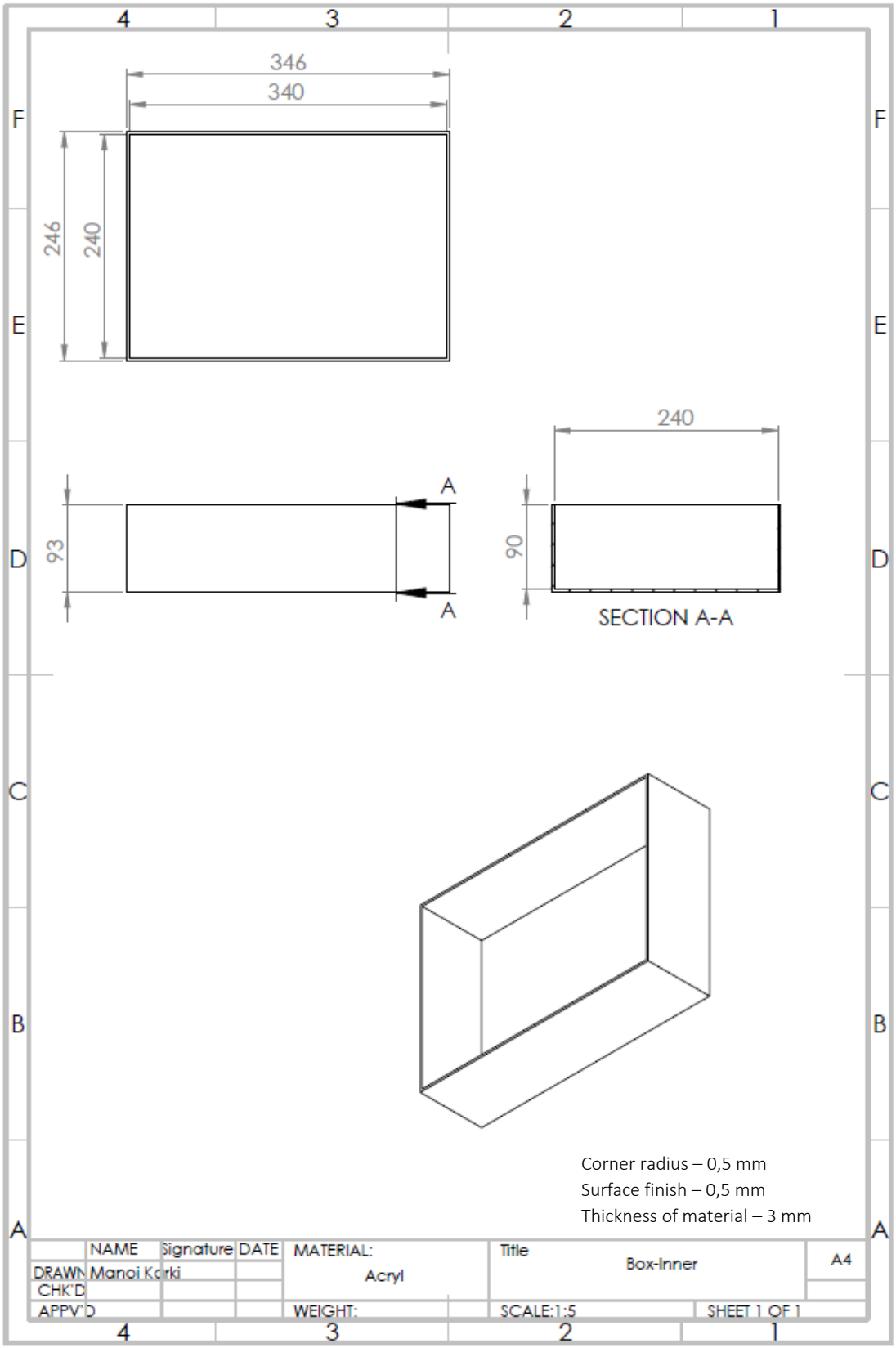
346
340
246
240
93
A
A
240
90
SECTION A-A
Corner radius – 0,5 mm
Surface finish – 0,5 mm
Thickness of material – 3 mm
NAME
Signature
DATE
DRAWN
Manoi Korki
CHK'D
APPV'D
MATERIAL:
Acryl
WEIGHT:
Title
Box-Inner
A4
SCALE:1:5
SHEET 1 OF 1

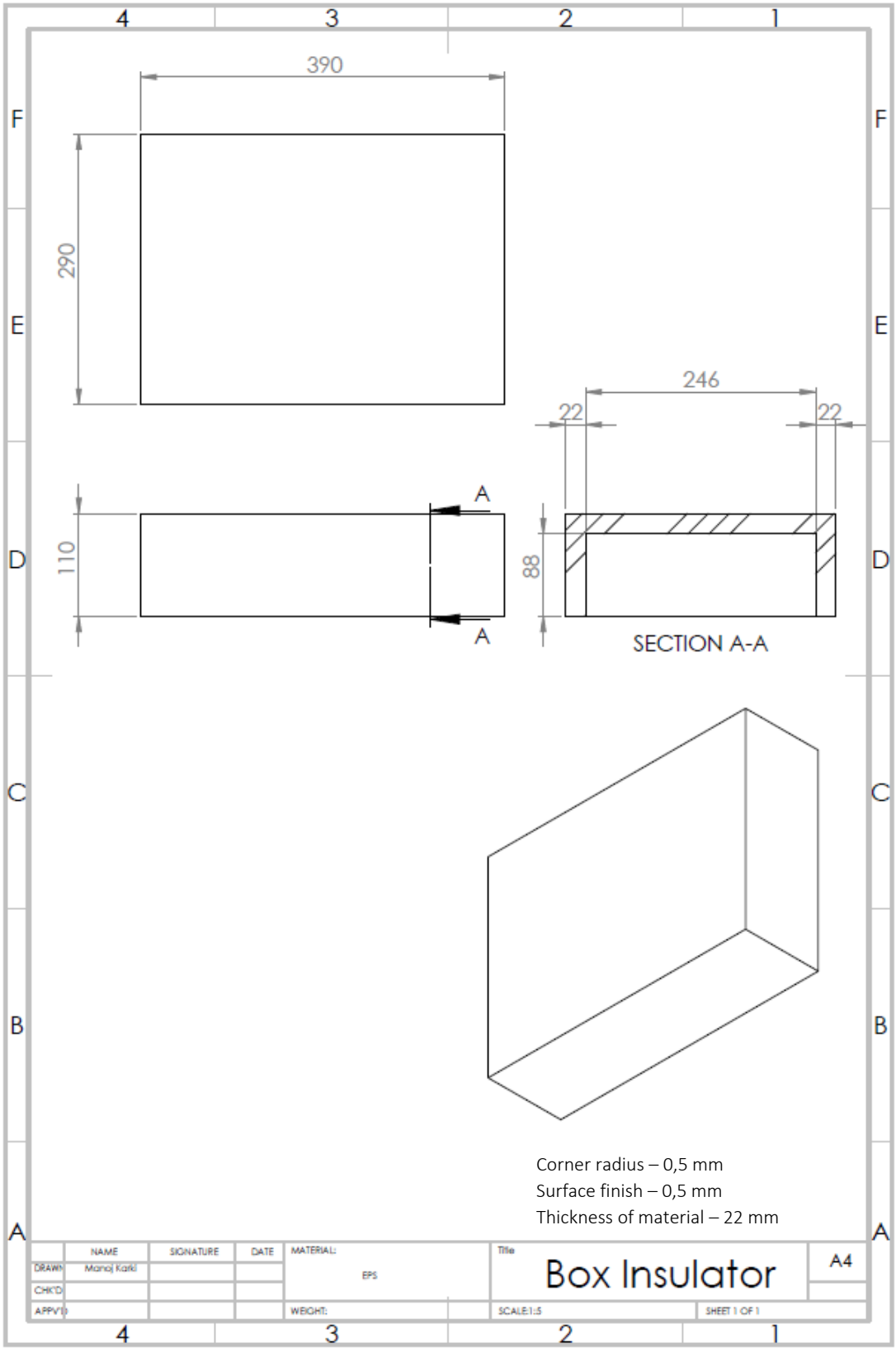
390
290
110
A
A
246
22
22
88
SECTION A-A
Corner radius – 0,5 mm
Surface finish – 0,5 mm
Thickness of material – 22 mm
NAME
SIGNATURE
DATE
DRAWN
Manoj Karki
CHK'D
APPV'D
MATERIAL:
EPS
WEIGHT:
Title
Box Insulator
A4
SCALE:1:5
SHEET 1 OF 1

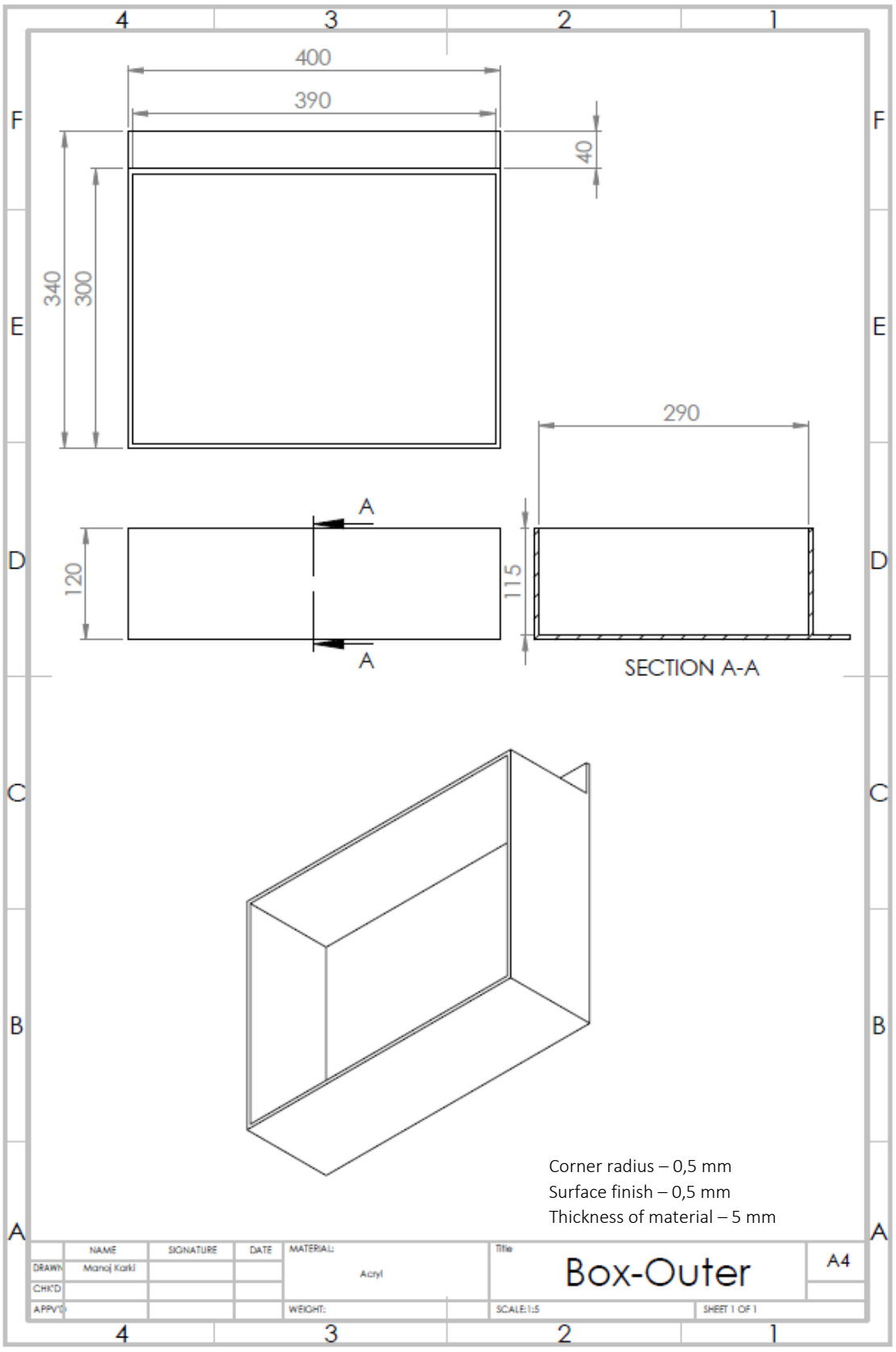

Corner radius – 0,5 mm
Surface finish – 0,5 mm
Thickness of material – 5 mm

	NAME	SIGNATURE	DATE	MATERIAL:	Title	
DRAWN	Manoj Karki			Acryl	Box-Outer	A4
CHK'D						
APPV'D				WEIGHT:	SCALE:1:5	SHEET 1 OF 1

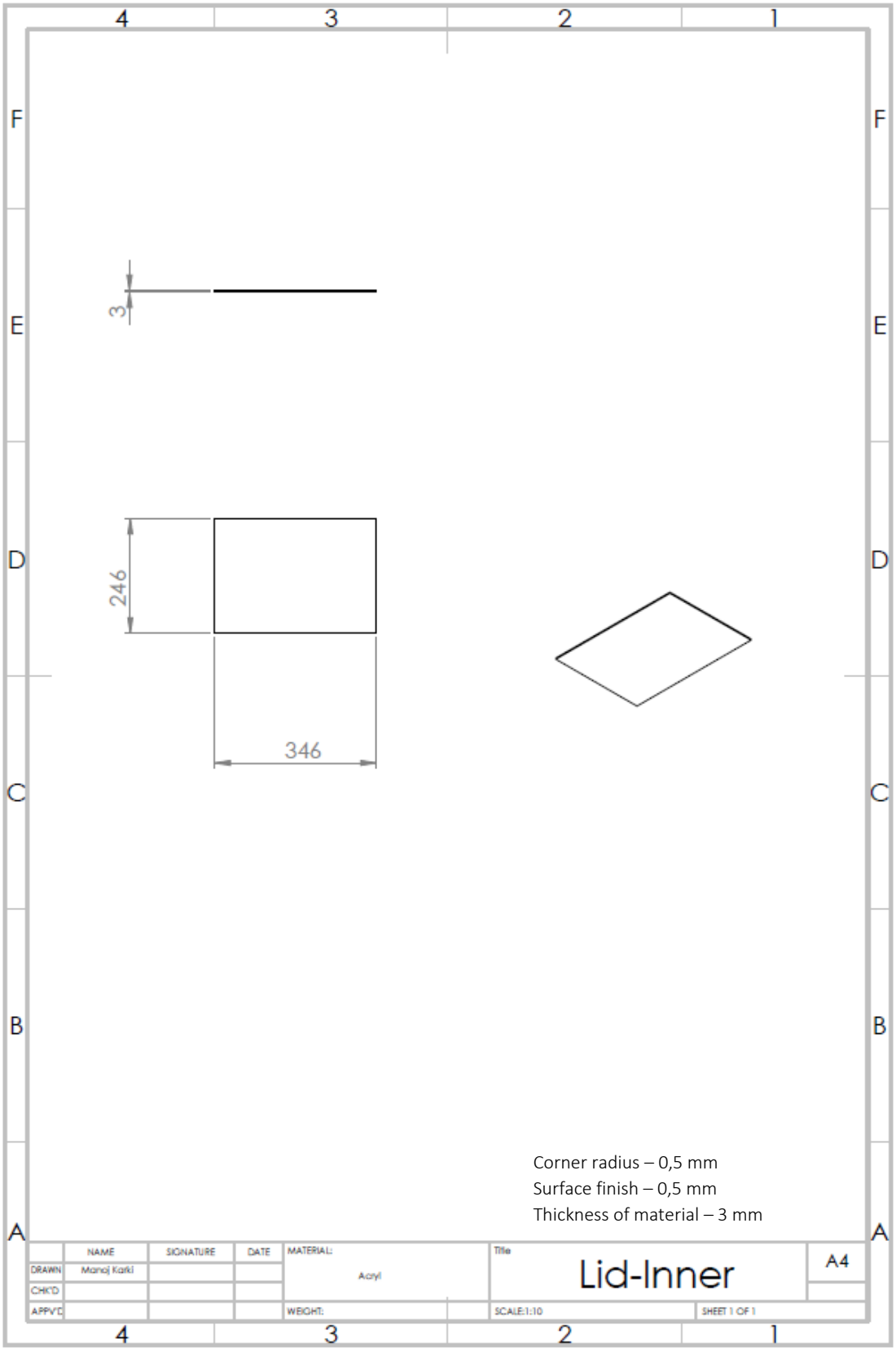
4
3
2
1
F
E
D
C
B
A
3
246
346
Corner radius – 0,5 mm
Surface finish – 0,5 mm
Thickness of material – 3 mm
NAME
SIGNATURE
DATE
MATERIAL:
Acryl
DRAWN
Manoj Karki
CHK'D
APPV'D
WEIGHT:
Title
Lid-Inner
A4
SCALE:1:10
SHEET 1 OF 1

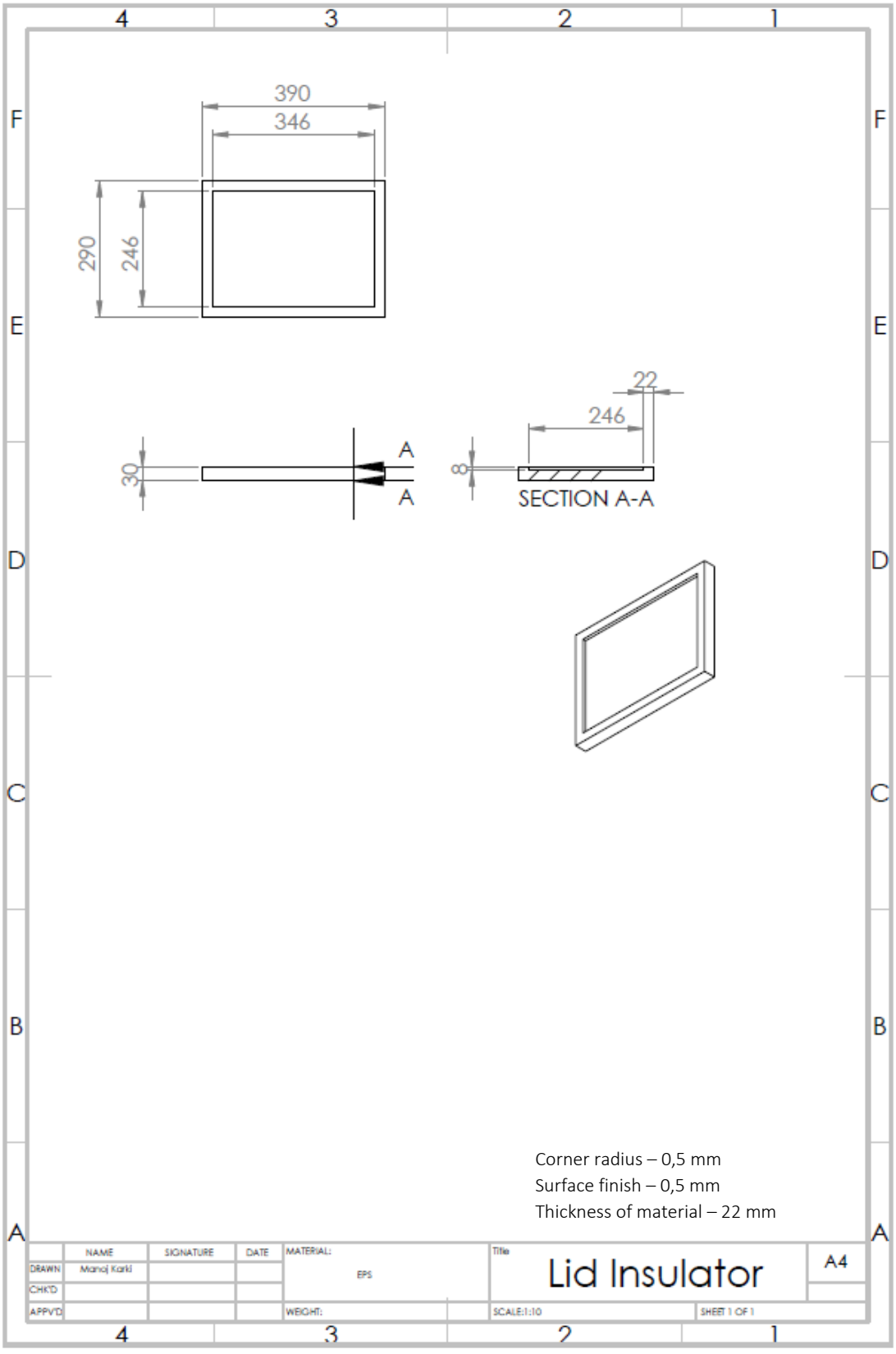

Corner radius – 0,5 mm
Surface finish – 0,5 mm
Thickness of material – 22 mm

	NAME	SIGNATURE	DATE	MATERIAL:	Title	
DRAWN	Manoj Karki			EPS	Lid Insulator	A4
CHK'D						
APPV'D				WEIGHT:	SCALE:1:10	SHEET 1 OF 1

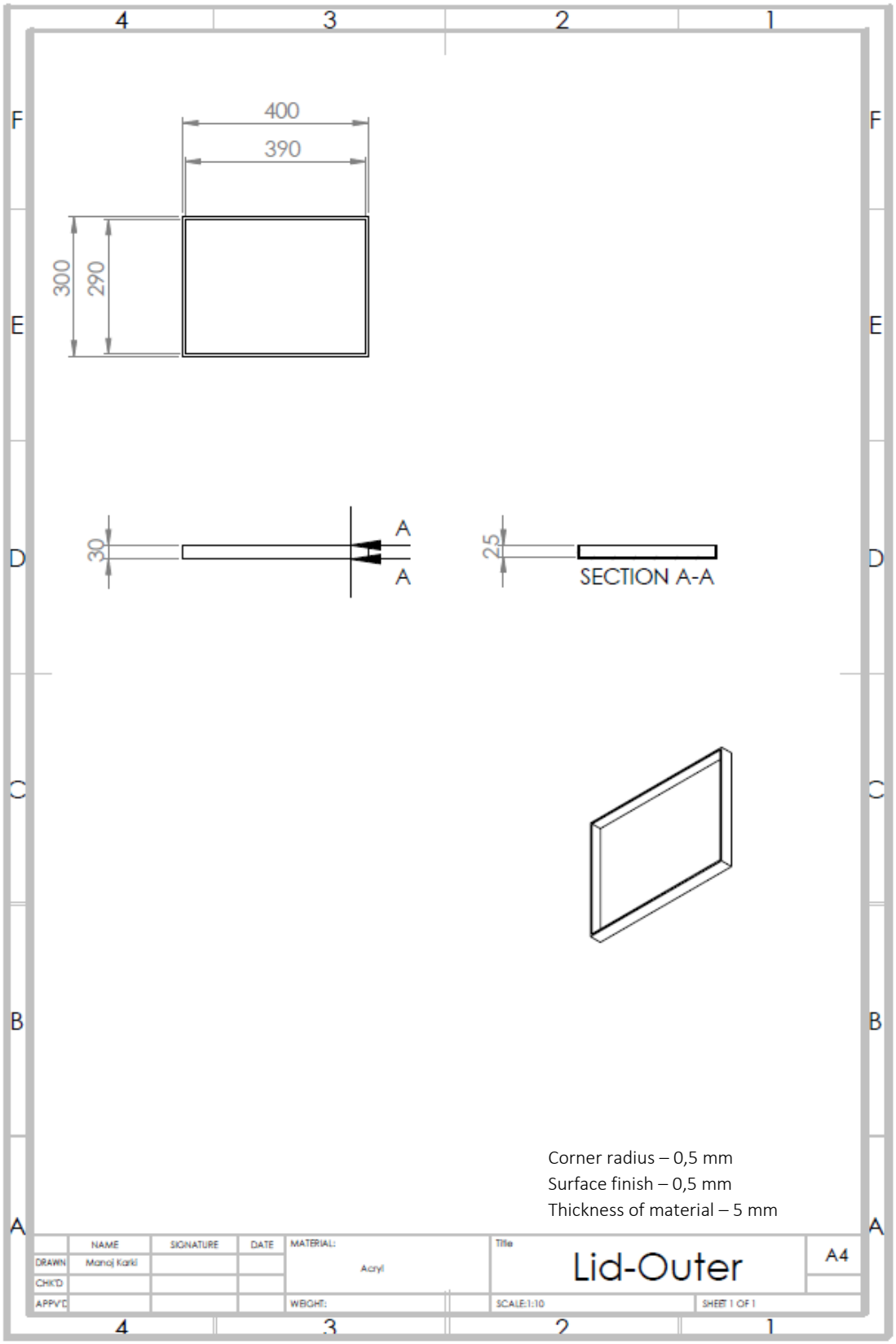
4
3
2
1
F
E
D
C
B
A
400
390
300
290
30
A
A
25
SECTION A-A
Corner radius – 0,5 mm
Surface finish – 0,5 mm
Thickness of material – 5 mm
NAME
SIGNATURE
DATE
DRAWN
Manoj Karki
CHK'D
APPV'D
MATERIAL:
Acryl
WEIGHT:
Title
Lid-Outer
A4
SCALE:1:10
SHEET 1 OF 1